Rozprawa doktorska pt.

Organizacja mitochondrialnego kompleksu importowego TOB/SAM u śluzowca Dictyostelium discoideum w procesie tworzenia wczesnych struktur wielokomórkowych

(ang. Organisation of the mitochondrial import complex TOB/SAM of the slime mold Dictyostelium discoideum in the process of forming of early multicellular structures)

Monika Mazur

Promotor:

Prof. UAM dr hab. Małgorzata Wojtkowska

Instytut Biologii Molekularnej i Biotechnologii, Wydział Biologii

Uniwersytet im. Adama Mickiewicza w Poznaniu

Poznań, 2022

Składam serdeczne podziękowania

Pani Promotor prof. UAM dr hab. Małgorzacie Wojtkowskiej

za pomoc udzieloną w trakcie przygotowywania pracy doktorskiej, oraz za cierpliwość i wsparcie, zwłaszcza w najtrudniejszych momentach

Pani prof. dr hab. Hannie Kmicie

za zaangażowanie, wyrozumiałość dla moich ograniczeń i pomoc, a szczególne za wiarę w moje możliwości

Pracownikom, Doktorantom, Koleżankom i Kolegom z Zakładu Bioenergetyki

w szczególności

dr Darii Wojciechowskiej – za pomoc i przyjaźń, która uciszała niejedną burzę

dr Annie Kicińskiej – za cenne rady w wielu kwestiach naukowych i bezcenny uśmiech

dr. Andonisowi Karachitosowi – za wszystkie radosne dyskusje naukowe, pomoc i ratunek - zwłaszcza w sprawach nagłych i niespodziewanych, oraz za zarażanie niesłabnącą pasją do pracy naukowej,

prof. UAM dr hab. Ninie Antos-Krzemińskiej – za nauczenie mnie kreatywności i skuteczności w modyfikowaniu protokołów – tej umiejętności niniejsza praca doktorska zawdzięcza wiele

Wiolettcie Nobik – za okazane serce i optymizm, który rozchmurza najcięższe troski

Pracownikom, Doktorantom, Koleżankom i Kolegom z Instytutu Biologii Molekularnej i Biotechnologii

w szczególności

prof. UAM dr. hab. Michałowi Rurkowi

za otrzymaną pomoc, cenne porady i zwracanie mojej uwagi na dbałość o szczegóły przeprowadzanego eksperymentu

Dr Annie Rugowskiej

za przypominanie mi w najtrudniejszych momentach o radości z pracy naukowej, za cieszenie się ze mną w chwilach sukcesów i za entuzjastyczną wiarę we mnie w chwilach kiedy nic się nie udawało.

Moim rodzicom i mojemu mężowi.

Bez Waszego wsparcia i miłości ta praca by nie powstała.

SPIS TREŚCI

FINANSOWANIE

Niniejsza praca powstała przy finansowym udziale:

1. Narodowego Centrum Nauki:
    - Grant 2012/05/N/NZ3/00293, Kierownik: Monika Mazur
2. Ministerstwa Nauki i Szkolnictwa Wyższego:
    - Grant NN303 143937, Kierownik: Małgorzata Wojtkowska
3. Krajowego Naukowego Ośrodka Wiodącego – KNOW Poznańskie Konsorcjum RNA

LISTA PUBLIKACJI WCHODZĄCYCH W SKŁAD ROZPRAWY DOKTORSKIEJ

1. **Mazur**, **M**., Wojtkowska, M., Skalski, M., Slocinska, M., Kmita, H. The TOB/SAM complex composition in mitochondria of *Dictyostelium discoideum* during progression from unicellularity to multicellularity. Acta Biochim Pol, 12;66(4):551-557 (2019). doi: 10.18388/abp.2019_2791. IF 2.149, MNiSW 70.
2. **Mazur**, **M**., Wojciechowska, D., Sitkiewicz, E., Malinowska, A., Swiderska, B., Kmita, H., Wojtkowska, M. Mitochondrial Processes during Early Development of *Dictyostelium discoideum*: From Bioenergetic to Proteomic Studies. Genes (Basel), 12(5): 638 (2021). doi: 10.3390/genes12050638. IF 4,096, MNiSW 100.
3. **Mazur**, **M**., Kmita, H., Wojtkowska, M. The Diversity of the Mitochondrial Outer Membrane Protein Import Channels: Emerging Targets for Modulation. Molecules, 26(13): 4087 (2021). doi: 10.3390/molecules26134087. IF 4,412, MNiSW 140.

LISTA PUBLIKACJI DOKTORANTKI NIEWCHODZĄCYCH W SKŁAD ROZPRAWY DOKTORSKIEJ

1. Wojtkowska, M., Buczek, D., Stobienia, O., Karachitos, A., **Antoniewicz, M.**, Slocinska, M., Makalowski, W., Kmita, H. The TOM Complex of Amoebozoans: the Cases of the Amoeba *Acanthamoeba castellanii* and the Slime Mold *Dictyostelium discoideum*. Protist, 166(3):349-62 (2015). doi: 10.1016/j.protis.2015.05.005. IF 2,566, MNiSW 100.
2. Buczek, D., Wojtkowska, M., Suzuki, Y., Sonobe, S., Nishigami, Y., **Antoniewicz, M.**, Kmita, H., Makalowski, W. Protein import complexes in the mitochondrial outer membrane of Amoebozoa representatives. BMC Genomics. 6;17:99 (2016). doi: 10.1186/s12864-016-2402-2. IF 3,969, MNiSW 140.
3. Karachitos, A., Grobys, D., **Antoniewicz, M.**, Jedut, S., Jordan, J., Kmita, H. Human VDAC isoforms differ in their capability to interact with minocycline and to contribute to its cytoprotective activity. Mitochondrion, 28:38-48 (2016). doi: 10.1016/j.mito.2016.03.004. IF 4,16, MNiSW 100.

STRESZCZENIE

Głównym celem mojej rozprawy doktorskiej była weryfikacja hipotezy zakładającej występowanie różnych form kompleksu TOB/SAM u organizmów wielokomórkowych i ustalenie składu podjednostkowego tych form na etapie tworzenia wczesnych struktur wielokomórkowych. Kompleks TOB/SAM (ang. Topogenesis of the mitochondrial outer membrane β-barrel proteins/Sorting and assembly machinery), zlokalizowany jest w zewnętrznej błonie mitochondrialnej, gdzie odpowiada za wbudowywanie białek o strukturze beczułki β. Badania przeprowadziłam przy użyciu organizmu modelowego, tj. śluzowca *Dictyostelium discoideum*, posiadającego charakterystyczny cykl życiowy, w którym wyróżnić można zarówno fazę jednokomórkową - występującą w sprzyjających warunkach środowiska, jak i fazy wielokomórkowe, które tworzą się w warunkach niekorzystnych i poprzedzają wytworzenie spor, umożliwiających przetrwanie tych warunków. Badanie kompleksu TOB/SAM u *D. discoideum* wykonałam wykorzystując komórki z fazy jednokomórkowej oraz dwóch wczesnych faz wielokomórkowych; tj. fazy agregacji i fazy strumieni. W badaniach wykorzystałam elektroforezę BN-PAGE, immunodetekcję, spektrometrię mas typu LC-MS/MS, analizy bioinformatyczne oraz pomiary oksygraficzne. Dzięki temu wykazałam, że: (1) mitochondria śluzowca zawierają dwie formy kompleksu TOB/SAM: o masie cząsteczkowej 160 kDa i 600 kDa, różniące się składem podjednostkowym; (2) podjednostki kompleksu TOB/SAM to: Tob55/Sam50 - wskazana w obu formach kompleksu i metaksyna (Mtx) – wskazana tylko w mniejszej formie (160 kDa); (3) wraz z wymienionymi podjednostkami wykryłam również białka współwystępujące, pochodzące z kompleksów współpracujących z TOB/SAM: Tom40 – w większej formie kompleksu (600 kDa), Mdm10 - w mniejszej formie kompleksu (160 kDa) oraz mitofilinę - w obu formach kompleksu (Tob55/Sam50, Mtx, Mdm10 oraz mitofilinę zidentyfikowałam w mitochondriach *D. discoideum* na poziomie białkowym po raz pierwszy); (4) wymienione wyżej białka zidentyfikowałam we wszystkich badanych fazach cyklu życiowego, za wyjątkiem mitofiliny, którą wskazałam tylko dla fazy jednokomórkowej; (5) proteomiczne analizy porównawcze przeprowadzone przeze mnie na mitochondriach badanych faz (badania ilościowe i jakościowe) wykazały zmiany

metaboliczne umożliwiające uruchomienie glukoneogenezy w odpowiedzi na stres (brak pożywienia), które zachodzą u *D. discoideum* podczas tworzenia wczesnych struktur wielokomórkowych, jednakże zmiany te nie obejmują istotnych statystycznie ilościowych różnic dla wymienionych podjednostek kompleksu TOB/SAM, oraz białek z nim związanych; (6) zaobserwowałam różnice w wyznaczonych wartościach parametrów bioenergetycznych: wydajności sprzężenia (coupling efficiency), pojemności sprzężenia (coupling capacity) i rezerwowej pojemności oddechowej (spare respiratory capacity) między mitochondriami pochodzącymi z komórek z badanych faz cyklu życiowego *D. discoideum* – zmiany te mogą być związane z procesami adaptacji komórek do warunków głodu. Wyniki te mają istotne znaczenie w dalszych badaniach nad rolą mitochondriów w procesach metabolicznego reprogramowania komórek oraz w badaniach nad biologią rozwoju.

SUMMARY

The main goal of my doctoral dissertation was to verify the hypothesis assuming the presence of various forms of the TOB/SAM complex in multicellular organisms and to determine the subunit composition of these forms in the process of forming of early multicellular structures. The TOB/SAM complex (Topogenesis of the mitochondrial outer membrane β-barrel proteins/Sorting and assembly machinery) is located in the mitochondrial outer membrane, where it is responsible for the insertion of β-barrel proteins. I conducted the research with the use of a model organism, i.e., slime mold *Dictyostelium discoideum*, which has a characteristic life cycle, in which can be distinguish both the unicellular phase - occurring under favorable environmental conditions, and the multicellular phases, which are formed under unfavorable conditions and precede the formation of spores, enabling surviving these conditions. I tested the TOB/SAM complex in *D. discoideum* using cells from the unicellular stage and two early multicellular stages, i.e., the aggregation stage and the streams stage. In the research I used BN-PAGE electrophoresis, immunodetection, LC-MS/MS mass spectrometry, bioinformatic analysis and oxygraphic measurements. As a result, I showed that: (1) slime mold mitochondria contain two forms of the TOB/SAM complex: with a molecular weight of 160 kDa and 600 kDa, differing in their subunit composition; (2) the subunits of the TOB/SAM complex are: Tob55/Sam50 - indicated in both complex forms and metaxin (Mtx) - indicated only in a smaller form (160 kDa); (3) together with the mentioned subunits, I also detected co-occurring proteins derived from complexes cooperating with TOB/SAM: Tom40 - in the larger form of the complex (600 kDa), Mdm10 - in the smaller form of the complex (160 kDa) and mitofilin - in both forms of the complex (I identified Tob55/Sam50, Mtx, Mdm10 and mitofilin in *D. discoideum* mitochondria at the protein level for the first time); (4) I identified the above-mentioned proteins in all studied life cycle stages, except for mitofilin, which I indicated only for the unicellular stage; (5) comparative proteomic analysis carried out by me on the mitochondria of the studied stages (quantitative and qualitative studies) showed metabolic changes enabling the activation of gluconeogenesis in response to stress (lack of food) that occur in *D. discoideum* during the formation of early multicellular structures, however, these changes do not cover statistically significant

quantitative differences for the mentioned TOB/SAM complex subunits and associated proteins; (6) I observed differences in the determined values of bioenergetic parameters: coupling efficiency, coupling capacity and spare respiratory capacity, between mitochondria derived from cells from the studied stages of the *D. discoideum* life cycle - these changes may be associated with processes of cell adaptation to starvation conditions. These results are important in further research on the role of mitochondria in metabolic cell reprogramming and in research of developmental biology.

WPROWADZENIE

Kompleks TOB/SAM (ang. Topogenesis of the mitochondrial outer membrane β-barrel proteins/Sorting and assembly machinery) zlokalizowany jest w zewnętrznej błonie mitochondrialnej. Jego podstawowym zadaniem jest translokacja i wbudowywanie białek o strukturze beczułki β, które odgrywają kluczową rolę w funkcjonowaniu mitochondriów. Ponadto, kompleks TOB/SAM, wraz z kompleksem TOM (ang. Translocase of the mitochondrial outer membrane), współtworzy szlaki importu białek do mitochondriów (Sokol i in., 2014; Wiedemann i in., 2017) oraz bierze udział w transporcie metabolitów (Galganska i in. 2008; 2010). Dotychczasowe badania nad kompleksem TOB/SAM prowadzone są głównie przy wykorzystaniu modelu drożdżowego, tj. komórek *Saccharomyces cerevisiae*, w mitochondriach których kompleks ten składa się z trzech podjednostek. Jedna z nich tworzy kanał (białko Tob55/Sam50), a dwie pozostałe pełnią funkcję receptorów (Tob38/Sam35 (Tom38) i Tob37/Sam37 (Tom37, Mas37)) (Wiedemann i in. 2003; Waizenegger i in., 2004; Klein i in., 2012; Diederichs i in., 2020).

Opis importu białek przez zewnętrzną błonę mitochondrialną oraz budowę kompleksu TOB/SAM przedstawiłam w pracy przeglądowej „The Diversity of the Mitochondrial Outer Membrane Protein Import Channels: Emerging Targets for Modulation", opublikowanej w Molecules.

ZRÓŻNICOWANIE FORM KOMPLEKSU TOB/SAM ŚLUZOWCA *Dictyostelium discoideum* WE WCZESNYCH ETAPACH TWORZENIA STRUKTUR WIELOKOMÓRKOWYCH

Punktem wyjścia moich badań były dane wskazujące, że kompleks TOB/SAM może różnić się masą cząsteczkową i składem podjednostkowym w przypadku organizmów eukariotycznych reprezentujących różne linie filogenetyczne. Tob55/Sam50 jest białkiem konserwatywnym, natomiast białka o funkcji receptorów są zróżnicowane. Różnice w składzie kompleksu TOB/SAM w porównaniu z organizmem modelowym *S. cerevisiae* wykazano dla grzybów: *Neurospora crassa*; zwierząt: *Drosophila melanogaster*, *Ceanorhabditis elegans,* dla komórek ludzkich, mysich i

szczurzych; oraz roślin: *Oryza sativa*, *Solanum tuberosum* i *Arabidopsis thaliana* (Paschen i in., 2003; Dolezal i in., 2006; Bredemeier i in., 2007; Carrie i in., 2010; Zhao i in., 2021). Co więcej, u organizmów wielokomórkowych stwierdzono obecność różnych form kompleksu TOB/SAM (Waizenegger i in., 2004; Xie i in., 2007; Kozjak-Pavlovic i in., 2007; Yamano i in., 2010; Lackey i in., 2011; Klein i in., 2012; Ott i in., 2012). Dlatego postanowiłam sprawdzić, czy istnieje związek między organizacją kompleksu TOB/SAM i wielokomórkowością.

Więcej informacji na temat form kompleksu TOB/SAM u różnych organizmów zebrałam w pracy eksperymentalnej „The TOB/SAM complex composition in mitochondria of Dictyostelium discoideum during progression from unicellularity to multicellularity", opublikowanej w Acta Biochimica Polonica.

Hipotezę zakładającą istnienie związku między wielokomórkowością i organizacją kompleksu TOB/SAM postanowiłam zweryfikować przy wykorzystaniu śluzowca *Dictyostelium discoideum*. Organizm ten, według obowiązującego podziału systematycznego, należy do supergrupy Amoebozoa (Adl i in., 2005) i charakteryzuje się złożonym cyklem życiowym, obejmującym zarówno etap jednokomórkowy, jak i etapy wielokomórkowe (Schilde i in., 2013). W sprzyjających warunkach środowiska i stałym dostępnie do pożywienia, jego komórki dzielą się cyklicznie w wyniku mitozy (faza nazwana w rozprawie fazą jednokomórkową, ang. *unicellular* - por. Rys.1). Natomiast w warunkach stresu głodowego następuje przełączenie z fazy intensywnych podziałów do fazy różnicowania, która ma na celu wytworzenie form przetrwalnikowych w postaci spor. W tym procesie komórki *D. discoideum* wydzielają do środowiska sygnał chemiczny w postaci cAMP, rozpoznawany przez inne komórki. Pod jego wpływem komórki migrują do miejsca największego stężenia cAMP, tworząc początkowo grupy komórek, co rozpoczyna proces powstawania wczesnych struktur wielokomórkowych (faza nazwana w rozprawie fazą agregacji, ang. *aggregation*). Następnie, ruch komórek staje się bardziej uporządkowany i przypomina strumienie zbiegające się spiralnie w jednym wspólnym punkcie (faza nazwana w rozprawie fazą strumieni, ang. *streams*). W trakcie tych wczesnych etapów rozpoczyna się proces różnicowania komórek na te, które zostaną przekształcone w spory oraz na te, których przeznaczeniem jest budowa tzw. łodygi, która unosi na 1-2 mm w górę kulę

wypełnioną sporami (tzw. ciałko owocujące – por. Rys.1) (Dormann i in., 2001; Maeda 2011; Du i in., 2015; Kawabe i in., 2019).

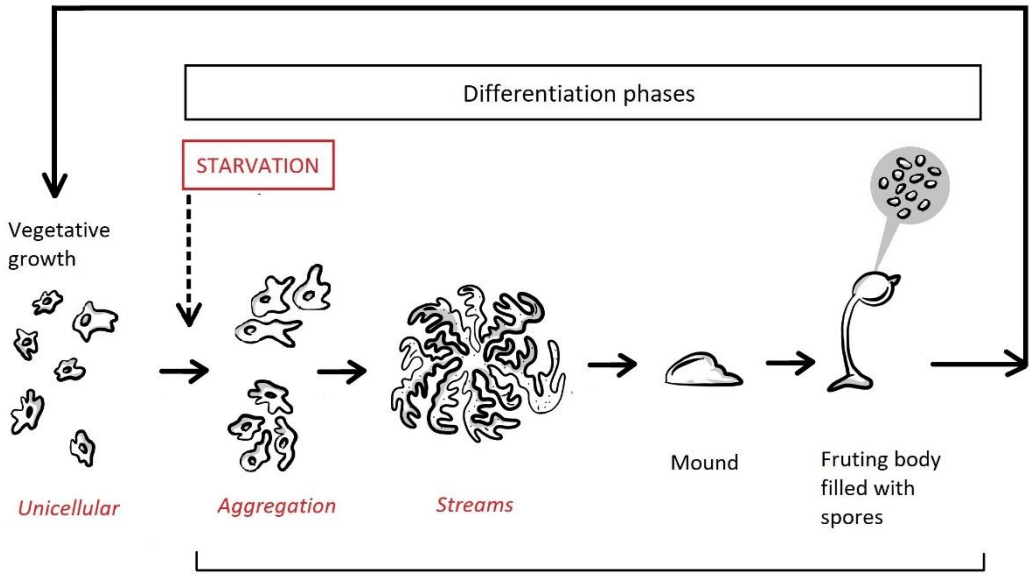

Rysunek 1. Cykl życiowy śluzowca *D. discoideum* (opis zawarty w tekście). Rozmnażanie wegetatywne *D. discoideum* poprzez podział mitotyczny komórek – ang. Vegetative growth; warunki głodu – ang. Starvation; fazy cyklu w których następuje różnicowane się komórek – ang. Differentiation phases; faza jednokomórkowa – ang. Unicellular; faza agregacji – ang. Aggregation; faza strumieni – ang. Streams; forma poprzedzająca wytworzenie ciałka owocującego – ang. Mound; tzw. ciałko owocujące, wypełnione sporami – ang. Fruting body filled with spores. [Na podstawie rysunku w pracy pt.: *The TOB/SAM complex composition in mitochondria of Dictyostelium discoideum during progression from unicellularity to multicellularity,* opublikowanej w czasopiśmie Acta Biochimica Polonica].

W celu określenia składu podjednostkowego kompleksu TOB/SAM śluzowca *D. discoideum*, zidentyfikowałam sekwencję genu kodującego białko Tob55/Sam50 oraz ortolog białka receptorowego o nazwie metaksyna, które występuje również w składzie kompleksu TOB/SAM mitochondriów ssaków i roślin (Wojtkowska i in., 2012; Buczek i in., 2016). Następnie wyizolowałam mitochondria z komórek pochodzących z trzech faz cyklu życiowego śluzowca (jednokomórkowej, agregacji i strumieni), rozdzieliłam białka metodą elektroforezy natywnej typu BN-PAGE i za pomocą immunodetekcji z wykorzystaniem przeciwciał skierowanych przeciwko: Tob55/Sam50 śluzowca (zaprojektowane przeze mnie przeciwciało otrzymałam w

wyniku syntezy peptydu i oczyszczenia uzyskanego serum na specyficznym złożu chromatograficznym) oraz ludzkiej metaksynie (przeciwciało dostępne komercyjnie), zidentyfikowałam formy kompleksu TOB/SAM. Tym sposobem stwierdziłam występowanie Tob55/Sam50 i metaksyny w mitochondriach komórek w każdej z badanych faz cyklu życiowego. Ponadto, wskazałam na obecność w tych mitochondriach, niezależnie od badanej fazy cyklu życiowego, dwóch form kompleksu TOB/SAM, tj. o masie cząsteczkowej 160 kDa i 600 kDa. Następnie, dla każdej z badanych faz, zidentyfikowane metodą immunodetekcji dwie formy kompleksu TOB/SAM poddałam analizie metodą spektrometrii mas (LC-MS/MS) w Środowiskowym Laboratorium Spektrometrii Mas Instytutu Biochemii i Biofizyki Polskiej Akademii Nauk w Warszawie. Uzyskane wyniki przedstawiłam schematycznie na Rys. 2. Niezależnie od badanej fazy cyklu życiowego, obecność białka Tob55/Sam50 stwierdziłam w obu formach kompleksu TOB/SAM, natomiast metaksyny tylko w większej formie kompleksu (600 kDa). Ponadto, w badanych próbach stwierdziłam obecność białek Tom40 i Mdm10 (sekwencja Mdm10 *D. discoideum* została przedstawiona po raz pierwszy w pracy Buczek i in., 2016, a na poziomie białkowym potwierdziłam ją w moich badaniach) oraz mitofiliny (Mic60; zidentyfikowanej z wykorzystaniem Blastp oraz modelu Pfam oraz na poziomie białkowym po raz pierwszy w ramach niniejszych badań). Obecność białka Tom40 wykazałam w większej formie kompleksu (600 kDa), a Mdm10 w mniejszej formie (160 kDa), jednakże oba białka były obecne we wszystkich badanych fazach cyklu życiowego. Obecność mitofiliny wykazałam w obu formach kompleksu, ale tylko w przypadku fazy jednokomórkowej.

Białko Tom40 jest główną podjednostką kompleksu TOM, którego zadaniem jest rozpoznanie, wprowadzenie i segregacja większości białek kierowanych do mitochondriów, w tym również podjednostek kompleksu TOB/SAM. Z drugiej zaś strony, kompleks TOB/SAM jest odpowiedzialny za wbudowywanie białek o strukturze beczułki β w zewnętrzną błonę mitochondrialną, a do tej grupy białek zalicza się właśnie białko Tom40 (Qiu i in., 2013; Wenz i in., 2015; Wiedemann i in., 2017). Wykazana przeze mnie obecność białka Tom40 w większej formie kompleksu (600 kDa) potwierdza funkcjonalne powiązanie kompleksu TOB/SAM z kompleksem TOM, które ma miejsce podczas insercji w błonę białka Tom40, a do czego niezbędny jest udział

kompleksu TOB/SAM (Qiu i in., 2013; Wenz i in., 2015). Białko Mdm10 (ang. Mitochondrial distribution and morphology protein 10) uważa się za podjednostkę współdzieloną przez kompleks TOB/SAM i kompleks ERMES (ang. Endoplasmic reticulum-mitochondria encounter structure), uczestniczący w oddziaływaniu między retikulum endoplazmatycznym i mitochondriami (Meisinger i in., 2004; Yamano i in., 2010; Thornton i in., 2010; Ellenrieder i in., 2016; Takeda i in., 2021). Białko to uczestniczy wraz z kompleksem TOB/SAM w prawidłowym wbudowaniu białek w zewnętrzną błonę, w tym we wbudowywaniu białka Tom40 (Meisinger i in., 2004; Yamano i in., 2010; Thornton i in., 2010; Ellenrieder i in., 2016; Takeda i in., 2021). Obecność Mdm10 wykazałam w mniejszej formie kompleksu TOB/SAM (160 kDa), a więc nie w tej samej formie, w której obecne jest białko Tom40 (600 kDa). Może to sugerować występowanie Tob55/Sam50 w postaci izoform, różniących się możliwością oddziaływania z białkami Tom40 i Mdm10, które zostało stwierdzone u *N. crassa* (Hoppins i in., 2007; Klein i in. 2012), i co u śluzowca wymaga dalszych badań. Z kolei obecność mitofiliny stwierdziłam tylko w fazie jednokomórkowej, ale w obu formach kompleksu TOB/SAM. Białko to zaliczane jest do kompleksu MICOS (ang. Mitochondrial contact site and cristae organizing system), a więc systemu białek odpowiedzialnych za utrzymanie struktury grzebieni mitochondrialnych (Harner i in., 2011; von der Malsburg i in., 2011; Eydt i in., 2017). Obecność mitofiliny może sugerować, że w fazie jednokomórkowej dochodzi do oddziaływania kompleksu TOB/SAM z kompleksem MICOS (Ott i in., 2012) oraz kompleksu MICOS z kompleksem TOM (von der Malsburg i in., 2011).

Wyniki dotyczące form kompleksu TOB/SAM i analizy tych form metodą spektrometrii mas zostały przedstawione w pracy eksperymentalnej „The TOB/SAM complex composition in mitochondria of Dictyostelium discoideum during progression from unicellularity to multicellularity", opublikowanej w czasopiśmie Acta Biochimica Polonica.

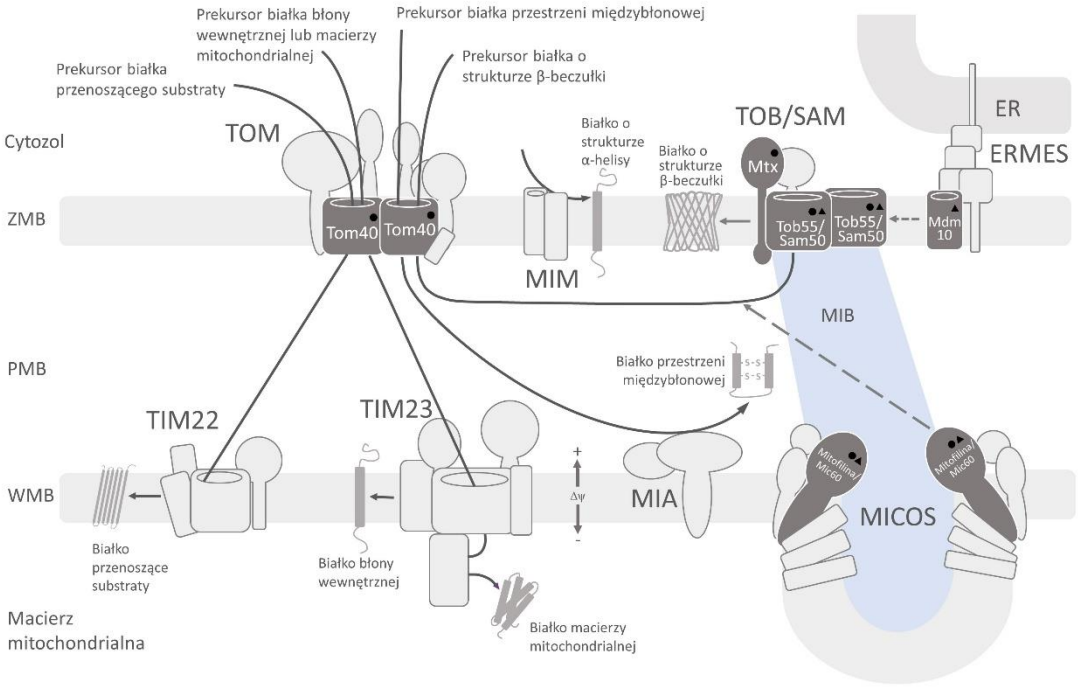

Rysunek 2. Uproszczony model importu białek do mitochondrium. Kolorem ciemnoszarym zostały oznaczone podjednostki kompleksu TOB/SAM oraz białka z nimi współwystępujące, zidentyfikowane w mitochondriach każdej z badanych faz cyklu życiowego śluzowca *D. discoideum* (z wyjątkiem mitofiliny zidentyfikowanej tylko w fazie jednokomórkowej) w ramach niniejszej rozprawy doktorskiej: ● - podjednostki zidentyfikowane w kompleksie TOB/SAM o masie cząsteczkowej 600 kDa; ▲ - podjednostki zidentyfikowane w kompleksie TOB/SAM o masie cząsteczkowej 160 kDa (dane przedstawione w pracy *The TOB/SAM complex composition in mitochondria of Dictyostelium discoideum during progression from unicellularity to multicellularity*, opublikowanej w czasopiśmie Acta Biochimica Polonica). ZMB – zewnętrzna błona mitochondrialna; PMB – przestrzeń międzybłonowa; WMB – wewnętrzna błona mitochondrialna. Szczegółowe informacje dotyczące importu białek do mitochondriów zawarłam w publikacji *The Diversity of the Mitochondrial Outer Membrane Protein Import Channels: Emerging Targets for Modulation*, opublikowanej w Molecules [Na podstawie rysunku z ww. publikacji].

STAN METABOLICZNY KOMÓREK ŚLUZOWCA *Dictyostelium discoideum* WE WCZESNYCH ETAPACH TWORZENIA STRUKTUR WIELOKOMÓRKOWYCH: PROTEOMIKA PORÓWNAWCZA

Aby lepiej zrozumieć obserwowane różnice w organizacji kompleksu TOB/SAM wykonałam porównawczą analizę proteomiczną mitochondriów z wykorzystaniem spektrometrii mas LC-MS/MS (współpraca z dr Ewą Sitkiewicz z Instytutu Biochemii i Biofizyki PAN w Warszawie). Wyodrębniłam 294 białka mitochondrialne, które na podstawie dostępnych danych zawartych w bazie danych śluzowca (dictybase.org) oraz GenBank, zaklasyfikowałam do 9 funkcjonalnych grup: metabolizm białek, sygnalizacja, import białek, transport, ekspresja genów mitochondrialnych, cykl Krebsa, OXPHOS, inne poznane procesy (do tej grupy zostały przypisane białka związane z reakcjami redoks i metabolizmem kwasów tłuszczowych) oraz białka niescharakteryzowane. Liczby białek przypisanych do wymienionych grup funkcyjnych były porównywalne dla mitochondriów z badanych faz. Najliczniej reprezentowane były białka przyporządkowane do grupy metabolizm białek, następnie OXPHOS i kolejno grupa inne poznane procesy. Mniej licznymi grupami były transport, import białek, cykl Krebsa i białka niescharakteryzowane. Najmniej białek przypisano do grup: sygnalizacja i ekspresja genów mitochondrialnych.

Zatem, pod względem jakościowym, uzyskane dane proteomiczne dla badanych wczesnych stadiów rozwojowych były porównywalne. Dlatego wykonałam ilościową analizę porównawczą uzyskanych danych proteomicznych. Analizę różnicową wykonałam dla następujących porównań izolowanych mitochondriów: faza agregacji/faza jednokomórkowa, faza strumieni/faza jednokomórkowa oraz faza agregacji/faza strumieni. Uzyskane wyniki nie wykazały różnic na poziomie istotności statystycznej dla białek kompleksu TOB/SAM: Tob55/Sam50, metaksyny oraz białek współwystępujących: Mdm10, Tom40 i mitofiliny, a także białek wchodzących w skład innych kompleksów importowych. Jednakże wykazałam, że białka mitochondrialne, których poziom rośnie w miarę jak komórki przechodzą od fazy jednokomórkowej do fazy strumieni, należą do grupy import białek i są to następujące białka: mitochondrialne białko Q z rodziny białek przenoszących substraty i mtHsp70. Ponadto analogiczną zmianę ilościową zaobserwowałam dla następujących grup: cykl Krebsa (ligaza

bursztynianowo-CoA i karboksykinaza fosfoenolopirogronianowa, PCK2); metabolizm białek (kinaza acetyloglutaminianowa, transaminaza kwasu γ-aminomasłowego i Hsp70); z grupy białek niescharakteryzowanych (mitochondrialna transferaza caf17 i dehydrogenaza kwasu 1-pirolino-5-karboksylowego) oraz z grupy inne poznane procesy: reakcje redoks (dysmutaza ponadtlenkowa SOD2) i metabolizm kwasów tłuszczowych (podjednostka α i podjednostka β flawoproteiny związanej z przenoszeniem elektronów). Natomiast wyraźną tendencję spadkową przy przejściu od fazy jednokomórkowej do fazy strumieni zaobserwowałam dla białek przypisanych do następujących grup: metabolizm białek (aminotransferaza aminokwasów rozgałęzionych); OXPHOS (podjednostka IV oksydazy cytochromu c); cykl Krebsa (syntaza cytrynianowa; dehydrogenaza izocytrynianowa (NAD+) i transferaza 3-oksokwasu CoA) oraz do grupy inne poznane procesy: metabolizm kwasów tłuszczowych (oksydaza acylo-CoA A i C-acetylotransferaza acetylo-CoA).

Uzyskane w proteomicznych analizach porównawczych ustalenia mogą wskazywać na adaptację metaboliczną komórek do stanu głodu, umożliwiającą uruchomienie glukoneogenezy. Znanym czynnikiem stymulującym glukoneogenezę w warunkach głodu jest acetylo-CoA (Kaleta i in., 2011), jednak wykazane obniżenie ilości enzymów zaangażowanych w proces β-oksydacji (oksydaza acylo-CoA A i C--acetylotransferaza acetylo-CoA), może w konsekwencji powodować, że to nie acetylo--CoA jest źródłem energii. Ciekawa jest natomiast podwyższona w fazie strumieni ilość białka PCK2, którego gen na poziomie transkrypcji podlega pozytywnej regulacji przez cAMP, który jest równocześnie sygnałem w procesie agregacji komórek. Z kolei podwyższona ilość białka mtHsp70 w fazie strumieni, może wskazywać na rosnące zapotrzebowanie na biogenezę centrów żelazowo-siarkowych, które stanowią grupy prostetyczne licznych istotnych białek komórkowych i mitochondrialnych (Stehling i in., 2014; Shan i Cortopassi, 2016; Dutkiewicz i Nowak, 2018) w tym PCK2. Ponadto, obniżenie ilości enzymów cyklu Krebsa sugeruje obniżenie jego aktywności, a tendencja spadkowa zaobserwowana dla grupy funkcjonalnej metabolizm białek może wskazywać na wykorzystywanie przez komórki śluzowca aminokwasów jako źródła węgla do uruchomienia glukoneogenezy.

Wyniki tej części badań zostały przedstawione w pracy „Mitochondrial Processes during Early Development of Dictyostelium discoideum: From Bioenergetic to Proteomic Studies", opublikowanej w czasopiśmie Genes.

STAN METABOLICZNY KOMÓREK ŚLUZOWCA *Dictyostelium discoideum* WE WCZESNYCH ETAPACH TWORZENIA STRUKTUR WIELOKOMÓRKOWYCH: ANALIZA FUNKCJONALNA MITOCHONDRIÓW

Jak pokazują badania, mitochondria śluzowca *D. discoideum* na różnych etapach jego cyklu życiowego są zaangażowane m.in. w procesy różnicowania i ruchu komórek, tj. chemotaksji (Barth i in., 2007). Dlatego za interesujące uznałam określenie ogólnej kondycji mitochondriów w nienaruszonych komórkach podczas tworzenia przez *D. discoideum* wczesnych struktur wielokomórkowych, tj. przeprowadziłam pomiary zużycia tlenu przez komórki pochodzące z fazy jednokomórkowej, agregacji i strumieni, w obecności związków oddziałujących na procesy przekształceń energetycznych zachodzących w mitochondriach (inhibitor syntazy ATP i tzw. rozprzęgacz). Pomiary te przeprowadziłam przy użyciu elektrody tlenowej Clarka, która mierzy zawartość tlenu w płynie, co umożliwia wyznaczenie wartości podstawowych parametrów określających funkcjonowanie mitochondriów. Są to: wydajność sprzężenia (ang. *coupling efficiency*), pojemność sprzężenia (ang. *coupling capacity*) i rezerwowa pojemność oddechowa (ang. *spare respiratory capacity*) (Brand i Nicholls, 2011; Karachitos i in, 2012; 2016). Na podstawie porównania wartości wydajności sprzężenia stwierdziłam, że w mitochondriach komórek z fazy jednokomórkowej synteza ATP zachodziła na wyższym poziomie, niż w mitochondriach komórek z fazy agregacji i strumieni, w których poziom ten był zbliżony. Jednak mitochondria te wykazywały różnicę dotyczącą pojemności sprzężenia, tj. była ona niższa w przypadku fazy strumieni. Pozostaje to w związku z obserwowaną różnicą w rezerwowej pojemności oddechowej, która w przypadku mitochondriów komórek z fazy strumieni była niższa, niż w przypadku mitochondriów komórek z fazy agregacji. Co ciekawe, wartość tego parametru w przypadku mitochondriów komórek z fazy jednokomórkowej była niższa niż w przypadku mitochondriów komórek z fazy agregacji. Jednym ze znanych czynników wpływających na rezerwową pojemność oddechową

mitochondriów jest dostępność substratów oddechowych, która wymaga ich dostępności do cyklu Krebsa, który z kolei jest zsynchronizowany z transportem elektronów w łańcuchu oddechowym (Brand i Nicholls, 2011). Obniżenie wartości rezerwowej pojemności oddechowej w fazie strumieni w porównaniu z fazą jednokomórkową oraz podwyższenie wartości tego parametru w fazie agregacji w porównaniu z fazą jednokomórkową, może wskazywać na zachodzącą adaptację do głodu, obejmującą metaboliczne przeprogramowanie komórek.

Wyniki tej części badań zostały przedstawione w pracy „Mitochondrial Processes during Early Development of Dictyostelium discoideum: From Bioenergetic to Proteomic Studies", opublikowanej w czasopiśmie Genes.

PODSUMOWANIE

Przeprowadzone badania wskazały, że w procesie tworzenia wczesnych struktur wielokomórkowych w odpowiedzi na stres głodu, w komórkach śluzowca *D. discoideum* może dochodzić do zmian w oddziaływaniu kompleksu TOB/SAM z innymi białkami mitochondrialnymi. Jednak organizacja kompleksu TOB/SAM, jak i poziom ekspresji jego zidentyfikowanych podjednostek nie ulegają zmianie. Zmiany te dotyczą jednak białek, które funkcjonalnie łączone są z możliwością uruchomienia glukoneogenezy oraz stanu funkcjonalnego mitochondriów. Łącznie stanowić mogą one istotny element odpowiedzi komórek śluzowca na brak pożywienia i konieczność wykorzystania alternatywnego źródła węgla.

Interesującym wydaje się przeprowadzenie analogicznych analiz proteomicznych i funkcjonalnych mitochondriów dla komórek śluzowca *D. discoideum* wchodzących w dalsze fazy cyklu życiowego, które prowadzą do formowania kolejnych struktur wielokomórkowych. Umożliwiłoby to z pewnością uzyskanie jeszcze pełniejszego obrazu organizacji i oddziaływań kompleksu TOB/SAM. Ze względu na wykorzystanie *D. discoideum* jako organizmu modelowego, poszerzone w ten sposób wyniki z niniejszej pracy mogłyby mieć istotne znaczenie w badaniach nad rolą mitochondriów w procesach związanych z metabolicznym reprogramowaniem komórek, oraz w badaniach z obszaru biologii rozwoju.

LITERATURA

1. Adl, S.M., Simpson, A.G., Farmer, M.A., Andersen, R.A., Anderson, O.R., Barta, J.R., Bowser, S.S., Brugerolle, G., Fensome, R.A., Fredericq, S., James, T.Y., Karpov, S., Kugrens, P., Krug, J., Lane, C.E., Lewis, L.A., Lodge, J., Lynn, D.H., Mann, D.G., McCourt, R.M., Mendoza, L., Moestrup, O., Mozley-Standridge, S.E., Nerad, T.A., Shearer, C.A., Smirnov, A.V., Spiegel, F.W., Taylor, M.F. The new higher level classification of eukaryotes with emphasis on the taxonomy of protists. *J Eukaryot Microbiol* **52**(5):399-451 (2005).
2. Barth, C., Le, P., Fisher, P.R. Mitochondrial biology and disease in Dictyostelium. *Int Rev Cytol* **263**, 207–252 (2007).
3. Brand, M.D., Nicholls, D.G. Assessing mitochondrial dysfunction in cells. *Biochem J* **435**, 297–312 (2011).
4. Bredemeier, R., Schlegel, T., Ertel, F., Vojta, A., Borissenko, L., Bohnsack, M.T., Groll, M., von Haeseler, A., Schleiff E. Functional and phylogenetic properties of the pore-forming β-barrel transporters of the Omp85 family. *J Biol Chem* **282**(3):1882-90 (2007).
5. Buczek, D., Wojtkowska, M., Suzuki, Y., Sonobe, S., Nishigami, Y., Antoniewicz, M., Kmita, H., Makałowski, W. Protein import complexes in the mitochondrial outer membrane of Amoebozoa representatives. *BMC Genom* **17**, 99 (2016).
6. Carrie, C., Murcha, M.W., Whelan, J. An in silico analysis of the mitochondrial protein import apparatus of plants. *BMC Plant Biol* **10**:243 (2010).
7. Diederichs, K.A., Ni, X., Rollauer, S.E., Botos, I., Tan, X., King, M.S., Kunji, E.R.S., Jiang, J., Buchanan, S.K. Structural insight into mitochondrial β-barrel outer membrane protein biogenesis. *Nat Commun* **11**, 3290 (2020).
8. Dolezal, P., Likic, V., Tachezy, J., Lithgow, T. Evolution of the molecular machines for protein import into mitochondria. *Science* **313**, 314–318 (2006).
9. Dormann, D., Kim, J.Y., Devreotes, P.N., Weijer, C.J. cAMP receptor affinity controls wave dynamics, geometry and morphogenesis in Dictyostelium. *J Cell Sci* **114**, 2513–2523 (2001).

10. Du, Q., Kawabe, Y., Schilde, C., Zhi-Hui, C., Schaap, P. The evolution of aggregative multicellularity and cell-cell communication in the Dictyostelia. *J Mol Biol* **427**, 3722–3733 (2015).
11. Dutkiewicz, R., Nowak, M. Molecular chaperones involved in mitochondrial iron-sulfur protein biogenesis. *J Biol Inorg Chem* **23**(4):569-579 (2018).
12. Ellenrieder, L., Opalinski, L., Becker, L., Kruger, V., Mirus, O., Straub, S.P., Ebell, K., Flinner, N., Stiller, S.B., Guiard, B., Meisinger, Ch., Wiedemann, N., Schleiff, E., Wagner, R., Pfanner, N., Becker, T. Separating mitochondrial protein assembly and endoplasmic reticulum tethering by selective coupling of Mdm10. *Nat Commun* **7**,13021 (2016).
13. Eydt, K., Davies, K.M., Behrendt, C., Wittig, I., Reichert, A.S. Cristae architecture is determined by an interplay of the MICOS complex and the F1F0 ATP synthase via Mic27 and Mic10. *Microb Cell* **4**: 259–272 (2017).
14. Galganska, H., Budzinska, M., Wojtkowska, M., Kmita, H. Redox regulation of protein expression in *Saccharomyces cerevisiae* mitochondria: Possible role of VDAC. *Arch Biochem Biophys* **479**, 39–45 (2008).
15. Galganska, H., Karachitos, A., Wojtkowska, M., Stobienia, O., Budzinska, M., Kmita, H. Communication between mitochondria and nucleus: Putative role for VDAC in reduction/oxidation mechanism. *Biochim Biophys Acta* **1797**, 1276–1280 (2010).
16. Harner, M., Korner, C., Walther, D., Mokranjac, D., Kaesmacher, J., Welsch, U., Griffith, J., Mann, M., Reggiori, F., Neupert, W. The mitochondrial contact site complex, a determinant of mitochondrial architecture. *EMBO J* **30**: 4356–4370 (2011).
17. Hoppins, S.C., Go, N.E., Klein, A., Schmitt, S., Neupert, W., Rapaport, D., Nargang, F.E. Alternative splicing gives rise to different isoforms of the *Neurospora crassa* Tob55 protein that vary in their ability to insert beta-barrel proteins into the outer mitochondrial membrane. *Genetics* **177**(1):137-49 (2007).
18. Kaleta, C., de Figueiredo, L.F., Werner, S., Guthke, R., Ristow, M., Schuster, S. In silico evidence for gluconeogenesis from fatty acids in humans. *PLoS Comput Biol* **7**(7):e1002116 (2011).

19. Karachitos, A., Jordan, J., Kmita, H. Cytoprotective activity of minocycline includes improvement of mitochondrial coupling: The importance of minocycline concentration and the presence of VDAC. *J Bioenerg Biomembr* **44**, 297–307 (2012).
20. Karachitos, A., Grobys, D., Antoniewicz, M., Jedut, S., Jordan, J., Kmita, H. Human VDAC isoforms differ in their capability to interact with minocycline and to contribute to its cytoprotective activity. *Mitochondrion* **28**, 38–48 (2016).
21. Kawabe, Y., Du, Q., Schilde, C., Schaap, P. Evolution of multicellularity in Dictyostelia. *Int J Dev Biol* **63**, 359–369 (2019).
22. Klein, A., Israel, L., Lackey, S.W.K., Nargang, F.E., Imhof, A., Baumeister, W., Neupert, W., Thomas, D.R. Characterization of the insertase for β-barrel proteins of the outer mitochondrial membrane. *J Cell Biol* **199**: 599–611(2012).
23. Kozjak-Pavlovic, V., Ross, K., Benlasfer, N., Kimming, S., Karlas, A., Rudel, T. Conserved roles of Sam50 and metaxins in VDAC biogenesis. *EMBO Rep* **8**: 576–582 (2007).
24. Lackey, S.W., Wideman, J.G., Kennedy, E.K., Go, N.E., Nargang, F.E. The *Neurospora crassa* TOB complex: analysis of the topology and function of Tob38 and Tob37. *PLoS One* **6**: e25650 (2011).
25. Maeda, Y. Cell-cycle checkpoint for transition from cell division to differentiation. *Dev Growth Differ* **53**, 463–481 (2011).
26. von der Malsburg, K., Muller, J.M., Bohnert, M., Oeljeklaus, S., Kwiatkowska, P., Becker, T., Loniewska-Lwowska, A., Wiese, S., Rao, S., Milenkovic, D., Hutu, D.P., Zerbes, R.M., Schulze-Specking, A., Meyer, H.E., Martinou, J.C., Rospert, S., Rehling, P., Meisinger, C., Veenhuis, M., Warscheid, B., van der Klei, I.J., Pfanner, N., Chacinska, A., van der Laan, M. Dual role of mitofilin in mitochondrial membrane organization and protein biogenesis. *Dev Cell* **21**: 694–707 (2011).
27. Meisinger, C., Rissler, M., Chacinska, A., Szklarz, L.K., Milenkovic, D., Kozjak, V., Schonfisch, B., Lohaus, C., Meyer, H.E., Yaffe, M.P., Guiard, B., Wiedemann, N., Pfanner, N. The Mitochondrial Morphology Protein Mdm10 Functions in Assembly of the Preprotein Translocase of the Outer Membrane. *Dev Cell* **7**, 61–71 (2004).

28. Ott, C., Ross, K., Straub, S., Thiede, B., Gotz, M., Goosmann, C., Krischke, M., Mueller, M.J., Krohne, G., Rudel, T., Kozjak-Pavlovic, V. Sam50 functions in mitochondrial intermembrane space bridging and biogenesis of respiratory complexes. *Mol Cell Biol* **32**: 1173–1188 (2012).
29. Paschen, S.A., Waizenegger, T., Stan, T., Preuss, M., Cyrklaff, M., Hell, K., Rapaport, D., Neupert, W. Evolutionary conservation of biogenesis of β-barrel membrane proteins. *Nature* **426**(6968):862-6 (2003).
30. Qiu, J., Wenz, L.S., Zerbes, R.M., Oeljeklaus, S., Bohnert, M., Stroud, D.A., Wirth, Ch., Ellenrieder, L., Thornton, N., Kutik, S., Wiese, S., Schulze-Specking, A., Zufall, N, Chacinska, A., Guiard, B., Hunte, C., Warscheid, B., van der Laan, M., Pfanner, N., Wiedemann, N., Becker, T. Coupling of mitochondrial import and export translocases by receptor-mediated supercomplex formation. *Cell* **154**, 596–608 (2013).
31. Schilde, C., Schaap, P. The Amoebozoa. *Methods Mol Biol* **983**, 1–15 (2013).
32. Shan, Y., Cortopassi, G. Mitochondrial Hspa9/Mortalin regulates erythroid differentiation via iron-sulfur cluster assembly. *Mitochondrion* **26**, 94–103 (2016).
33. Sokol, A.M., Sztolsztener, M.E., Wasilewski, M., Heinz, E., Chacinska, A. Mitochondrial protein translocases for survival and wellbeing. *FEBS Lett* **1**;588(15):2484-95 (2014).
34. Stehling, O., Wilbrecht, C., Lill, R. Mitochondrial iron–sulfur protein biogenesis and human disease. *Biochimie* **100**, 61–77 (2014).
35. Takeda, H., Tsutsumi, A., Nishizawa, T., Lindau, C., Busto, J.V., Wenz, L.S., Ellenrieder, L., Imai, K., Straub, S.P., Mossmann, W., Qiu, J., Yamamori, Y., Tomii, K., Suzuki, J., Murata, T., Ogasawara, S., Nureki, O., Becker, T., Pfanner, N., Wiedemann, N., Kikkawa, M., Endo T. Mitochondrial sorting and assembly machinery operates by β-barrel switching. *Nature* **590**(7844):163-169 (2021).
36. Thornton, N., Stroud, D.A., Milenkovic, D., Guiard, B., Pfanner, N., Becker, T. Two modular forms of the mitochondrial sorting and assembly machinery are involved in biogenesis of alpha-helical outer membrane proteins. *J Mol Biol* **396**, 540–549 (2010).

37. Waizenegger, T., Habib, S.J., Lech, M., Mokranjac, D., Paschen, S.A., Hell, K., Neupert, W., Rapaport, D. Tob38, a novel essential component in the biogenesis of beta-barrel proteins of mitochondria. *EMBO Rep* **5**, 704709 (2004).
38. Wenz, L.S., Ellenrieder, L., Qiu, J., Bohnert, M., Zufall, N., van der Laan, M., Pfanner, N., Wiedemann, N., Becker, T. Sam37 is crucial for formation of the mitochondrial TOM–SAM supercomplex, thereby promoting β-barrel biogenesis. *J Cell Biol* **210**, 1047–1054 (2015).
39. Wiedemann, N., Kozjak, V., Chacinska, A., Schonfisch, B., Rospert, S., Ryan, M.T., Pfanner, N., Meisinger, Ch. Machinery for protein sorting and assembly in the mitochondrial outer membrane. *Nature* **31**;424(6948):565-71 (2003).
40. Wiedemann, N., Pfanner, N. Mitochondrial machineries for protein import and assembly. *Annu Rev Biochem* **86**, 685–714 (2017).
41. Wojtkowska, M., Jakalski, M., Pienkowska, J.R., Stobienia, O., Karachitos, A., Przytycka, T.M., Weiner, J., Kmita, H., Makalowski, W. Phylogenetic Analysis of Mitochondrial Outer Membrane β-Barrel Channels. *Genome Biol Evol* **4**(2): 110–125 (2012).
42. Xie, J., Marusich, M.F., Souda, P., Whitelegge, J., Capaldi, R.A. The mitochondrial inner membrane protein Mitofilin exists as a complex with SAM50, metaxins 1 and 2, coiled-coil-helix domain-containing protein 3 and 6 and DnaJC11. *FEBS Lett* **581**: 3545–3549 (2007).
43. Yamano, K., Tanaka-Yamano, S., Endo, T. Mdm10 as a dynamic constituent of the TOB/SAM complex directs coordinated assembly of Tom40. *EMBO Rep* **11**: 187–193 (2010).
44. Zhao, Y., Song, E., Wang, W., Hsieh, Ch.H., Wang, X., Feng, W., Wang, X., Shen, K. Metaxins are core components of mitochondrial transport adaptor complexes. *Nat Commun* **12**(1):83 (2021).

OŚWIADCZENIA DOKTORANTA

Poznań, 27.02.2022 r.

Monika Mazur
Uniwersytet im. Adama Mickiewicza, Poznań
Wydział Biologii
Zakład Bioenergetyki
ul. Uniwersytetu Poznańskiego 6
61-614 Poznań
e-mail: monika.a@amu.edu.pl

Oświadczenie o zmianie nazwiska

Niniejszym oświadczam, że wraz ze wstąpieniem w związek małżeński dnia 12.09.2015r. zmieniłam nazwisko z nazwiska panieńskiego: Antoniewicz, na nazwisko męża: Mazur. Tak więc na publikacjach z moim udziałem do roku 2015 znajduje się nazwisko Monika Antoniewicz, a na publikacjach od 2016 r. nazwisko Monika Mazur.

Monika Mazur

.....

Monika Mazur

Poznań, 25.02.2022 r.

Monika Mazur
Uniwersytet im. Adama Mickiewicza, Poznań
Wydział Biologii
Zakład Bioenergetyki
ul. Uniwersytetu Poznańskiego 6
61-614 Poznań
e-mail: monika.a@amu.edu.pl

Oświadczenie określające wkład w powstanie artykułu

Niniejszym oświadczam, że mój wkład w powstanie poniższego artykułu: **Mazur M.**, Wojtkowska M., Skalski M., Słocińska M., Kmita H. 2019. The TOB/SAM complex composition in mitochondria of *Dictyostelium discoideum* during progression from unicellularity to multicellularity. *Acta Biochim Pol*, 12;66(4):551-557, polegał na planowaniu eksperymentów, prowadzeniu hodowli komórek śluzowca *Dictyostelium discoideum*, izolacji mitochondriów badanego organizmu, optymalizacji i wykonaniu techniki natywnego rozdziału elektroforetycznego białek (BN-PAGE), wykonaniu immunodetekcji metodą Western blot, wykonaniu zdjęć komórek *D. discoideum* spod mikroskopu świetlnego, opracowaniu wyników uzyskanych dzięki analizie spektrometrii mas LC-MS/MS. Przygotowałam opis materiałów i metod do przeprowadzonych przez mnie eksperymentów, opracowałam graficznie figury zamieszczone w publikacji, brałam udział w dyskusji naukowej i redagowaniu manuskryptu. W tym artykule jestem pierwszym autorem.

Mój całkowity wkład w pracę wynosi 60%.

Z wyrazami szacunku,

Monika Mazur

Poznań, 25.02.2022 r.

Monika Mazur
Uniwersytet im. Adama Mickiewicza, Poznań
Wydział Biologii
Zakład Bioenergetyki
ul. Uniwersytetu Poznańskiego 6
61-614 Poznań
e-mail: monika.a@amu.edu.pl

Oświadczenie określające wkład w powstanie artykułu

Niniejszym oświadczam, że mój wkład w powstanie poniższego artykułu: **Mazur M.,** Wojciechowska D., Sitkiewicz E., Malinowska A., Świderska B., Kmita H., Wojtkowska M., 2021. Mitochondrial Processes during Early Development of *Dictyostelium discoideum*: From Bioenergetic to Proteomic Studies. *Genes (Basel),* 12(5): 638, polegał na planowaniu eksperymentów, prowadzeniu hodowli komórek śluzowca *Dictyostelium discoideum*, izolacji mitochondriów, uczestniczeniu w pracach związanych z pomiarem zużycia tlenu przez komórki śluzowca oraz wykonaniu części pomiarów oksygraficznych przy użyciu elektrody tlenowej Clarka; opracowaniu wyników uzyskanych dzięki analizie spektrometrii mas LC-MS/MS (segregacja danych, przypisanie białkom kategorii, zestawienie wyników w formie graficznej). Brałam również udział w interpretacji uzyskanych wyników proteomicznych, przygotowałam opis materiałów i metod do przeprowadzonych przeze mnie eksperymentów, opracowałam graficznie figury i tabele zamieszczone w publikacji, uczestniczyłam w dyskusji wyników oraz redagowaniu manuskryptu. W tym artykule jestem pierwszym autorem.

Mój całkowity wkład w pracę wynosi 40%.

Z wyrazami szacunku,

Monika Mazur

Poznań, 25.02.2022 r.

Monika Mazur
Uniwersytet im. Adama Mickiewicza, Poznań
Wydział Biologii
Zakład Bioenergetyki
ul. Uniwersytetu Poznańskiego 6
61-614 Poznań
e-mail: monika.a@amu.edu.pl

Oświadczenie określające wkład w powstanie artykułu

Niniejszym oświadczam, że mój wkład w powstanie poniższego artykułu: **Mazur M.,** Kmita H., Wojtkowska M., 2021. The Diversity of the Mitochondrial Outer Membrane Protein Import Channels: Emerging Targets for Modulation. *Molecules,* 26(13): 4087, polegał na pisaniu manuskryptu – w szczególności rozdziału: „Overview of the Mitochondrial Protein Import Machinery", podrozdziałów: „Tob55/Sam50 Channel", „Mdm10 Channel", „Mim1 Channel", przygotowaniu tabeli i rysunków oraz redagowaniu manuskryptu. W tym artykule jestem pierwszym autorem.

Mój całkowity wkład w pracę wynosi 50%.

Z wyrazami szacunku,

Monika Mazur

OŚWIADCZENIA WSPÓŁAUTORÓW

Poznań, 02.02.2022 r.

Prof. UAM dr hab. Małgorzata Wojtkowska
Uniwersytet im. Adama Mickiewicza, Poznań
Wydział Biologii
Zakład Bioenergetyki
ul. Uniwersytetu Poznańskiego 6
61-614 Poznań
e-mail:

Oświadczenie określające wkład w powstanie artykułu

Niniejszym oświadczam, że mój wkład w powstanie poniższego artykułu: **Mazur M.**, Wojtkowska M., Skalski M., Słocińska M., Kmita H. 2019. The TOB/SAM complex composition in mitochondria of *Dictyostelium discoideum* during progression from unicellularity to multicellularity. *Acta Biochim Pol*, 12;66(4):551-557, polegał na uczestniczeniu w planowaniu eksperymentów, analizie i interpretacji danych, dyskusji wyników i pisaniu manuskryptu.

Swój całkowity wkład w pracę oceniam na 20%.

Małgorzata Wojtkowska

Poznań, 19.11.2021 r.

Mgr Marcin Skalski
ul. gen. Stanisława Maczka 18/96
60-651 Poznań
e-mail: marcinskalski1993@gmail.com

Oświadczenie określające wkład w powstanie artykułu

Niniejszym oświadczam, że mój wkład w powstanie poniższego artykułu: **Mazur M.**, Wojtkowska M., Skalski M., Słocińska M., Kmita H. 2019. The TOB/SAM complex composition in mitochondria of *Dictyostelium discoideum* during progression from unicellularity to multicellularity. *Acta Biochim Pol*, 12;66(4):551-557, polegał na pomocy przy: hodowli komórek śluzowca *Dictyostelium discoideum*, natywnej elektroforezie białek (BN-PAGE), oraz immunodetekcji metodą Western blot.

Swój całkowity wkład w pracę oceniam 1%.

Z wyrazami szacunku,

Skalski Marcin

Poznań, 14.01.022 r.

Prof. UAM dr hab. Małgorzata Słocińska
Uniwersytet im. Adama Mickiewicza w Poznaniu
Wydział Biologii
Zakład Fizjologii i Biologii Rozwoju Zwierząt
ul. Uniwersytetu Poznańskiego 6
61-614 Poznań
e-mail: malgorzata.slocinska@amu.edu.pl

Oświadczenie określające wkład w powstanie artykułu

Niniejszym oświadczam, że mój wkład w powstanie poniższego artykułu: **Mazur M.**, Wojtkowska M., Skalski M., Słocińska M., Kmita H. 2019. The TOB/SAM complex composition in mitochondria of *Dictyostelium discoideum* during progression from unicellularity to multicellularity. *Acta Biochim Pol*, 12;66(4):551-557, polegał na wykonaniu znakowania białka Tob55/Sam50 w komórkach śluzowca *Dictysotelium discoideum,* przy wykorzystaniu immunofluorescencji: użycie MitoTracker Red FM oraz przeciwciała ze znacznikiem fluorescencyjnym (FITC); a następnie na wykonaniu zdjęć spod mikroskopu fluorescencyjnego w celu prezentacji wyników zawartych w suplemencie.

Swój całkowity wkład w pracę oceniam na 4%.

Z wyrazami szacunku,

M. Słocińska

Poznań, 13.01.2022 r.

Prof. dr hab. Hanna Kmita
Uniwersytet im. Adama Mickiewicza, Poznań
Wydział Biologii
Zakład Bioenergetyki
ul. Uniwersytetu Poznańskiego 6
61-614 Poznań
e-mail: hanna.kmita@amu.edu.pl

Oświadczenie określające wkład w powstanie artykułu

Niniejszym oświadczam, że mój wkład w powstanie poniższego artykułu: **Mazur M.**, Wojtkowska M., Skalski M., Słocińska M., Kmita H. 2019. The TOB/SAM complex composition in mitochondria of *Dictyostelium discoideum* during progression from unicellularity to multicellularity. *Acta Biochim Pol*, 12;66(4):551-557, polegał na uczestniczeniu w analizie i interpretacji danych, dyskusji naukowej oraz współtworzeniu tekstu manuskryptu.

Swój całkowity wkład w pracę oceniam na 15%.

Hanna Kmita

Z wyrazami szacunku,

Poznań, 13.01.2022 r.

Dr Daria Wojciechowska
Uniwersytet im. Adama Mickiewicza w Poznaniu
Wydział Fizyki
Zakład Fizyki Biomedycznej
ul. Uniwersytetu Poznańskiego 2
61-614 Poznań
e-mail: grobys.d@amu.edu.pl

Oświadczenie określające wkład w powstanie artykułu

Niniejszym oświadczam, że mój wkład w powstanie poniższego artykułu: **Mazur M.,** Wojciechowska D., Sitkiewicz E., Malinowska A., Świderska B., Kmita H., Wojtkowska M., 2021. Mitochondrial Processes during Early Development of *Dictyostelium discoideum*: From Bioenergetic to Proteomic Studies. *Genes (Basel),* 12(5): 638, polegał na nadzorowaniu i wykonaniu większości pomiarów oksygraficznych przy użyciu elektrody tlenowej Clarka, udziale w interpretacji uzyskanych danych oraz w opracowaniu wyników tego eksperymentu w formie liczbowej i graficznej.

Swój całkowity wkład w pracę oceniam na 20%.

Z wyrazami szacunku,

Daria Wojciechowska

Poznań, 20.01.2022 r.

Dr Ewa Sitkiewicz
Instytut Biochemii i Biofizyki Polskiej Akademii Nauk
ul. Pawińskiego 5a
02-106 Warszawa
e-mail: ewa@ibb.waw.pl

Oświadczenie określające wkład w powstanie artykułu

Niniejszym oświadczam, że mój wkład w powstanie poniższego artykułu: **Mazur M.,** Wojciechowska D., Sitkiewicz E., Malinowska A., Świderska B., Kmita H., Wojtkowska M., 2021. Mitochondrial Processes during Early Development of Dictyostelium discoideum: From Bioenergetic to Proteomic Studies. *Genes (Basel),* 12(5): 638, polegał na analizie prób zawierających białka mitochondrialne, wyizolowane z komórek pochodzących z różnych faz cyklu życiowego śluzowca *D. discoideum*: analiza jakościowa oraz ilościowa peptydów/białek mitochondrialnych z wykorzystaniem odpowiednich oprogramowania (MASCOT, MScan), analiza statystyczna uzyskanych wyników, identyfikacja białek obecnych w próbce oraz białek różniących się w sposób istotny statystycznie pomiędzy badanymi grupami (DiffProt).

Swój całkowity wkład w pracę oceniam na 10%.

Z wyrazami szacunku,

Ewa Sitkiewicz

Warszawa, 22.03.2022 r.

Dr Agata Malinowska
Instytut Biochemii i Biofizyki Polskiej Akademii Nauk
ul. Pawińskiego 5a
02-106 Warszawa
e-mail: esme@ibb.waw.pl

Oświadczenie określające wkład w powstanie artykułu

Niniejszym oświadczam, że mój wkład w powstanie poniższego artykułu: **Mazur M.,** Wojciechowska D., Sitkiewicz E., Malinowska A., Świderska B., Kmita H., Wojtkowska M., 2021. Mitochondrial Processes during Early Development of Dictyostelium discoideum: From Bioenergetic to Proteomic Studies. *Genes (Basel)*, 12(5): 638, polegał na wykonaniu histogramów klasyfikacji białek w poszczególnych grupach próbek.

Swój całkowity wkład w pracę oceniam na 2%.

Z wyrazami szacunku,

Warszawa, 22.03.2022 r.

Mgr Bianka Świderska
Instytut Biochemii i Biofizyki Polskiej Akademii Nauk
ul. Pawińskiego 5a
02-106 Warszawa
e-mail: bianka.swiderska@gmail.com

Oświadczenie określające wkład w powstanie artykułu

Niniejszym oświadczam, że mój wkład w powstanie poniższego artykułu: **Mazur M.,** Wojciechowska D., Sitkiewicz E., Malinowska A., Świderska B., Kmita H., Wojtkowska M., 2021. Mitochondrial Processes during Early Development of Dictyostelium discoideum: From Bioenergetic to Proteomic Studies. *Genes (Basel),* 12(5): 638, polegał na przygotowaniu próbek do analizy proteomicznej i przeprowadzeniu pomiarów LC-MS/MS.

Swój całkowity wkład w pracę oceniam na 3%.

Z wyrazami szacunku,

Bianka Świderska

Poznań, 13.01.2022 r.

Prof. dr hab. Hanna Kmita
Uniwersytet im. Adama Mickiewicza, Poznań
Wydział Biologii
Zakład Bioenergetyki
ul. Uniwersytetu Poznańskiego 6
61-614 Poznań
e-mail: hanna.kmita@amu.edu.pl

Oświadczenie określające wkład w powstanie artykułu

Niniejszym oświadczam, że mój wkład w powstanie poniższego artykułu: **Mazur M.,** Wojciechowska D., Sitkiewicz E., Malinowska A., Świderska B., Kmita H., Wojtkowska M., 2021. Mitochondrial Processes during Early Development of Dictyostelium discoideum: From Bioenergetic to Proteomic Studies. *Genes (Basel),* 12(5): 638, polegał na uczestniczeniu w analizie i interpretacji danych, dyskusji wyników oraz współtworzeniu tekstu manuskryptu.

Swój całkowity wkład w pracę oceniam na 10%.

Hanna Kmita

Z wyrazami szacunku,

Poznań, 02.02.2022 r.

Prof. UAM dr hab. Małgorzata Wojtkowska
Uniwersytet im. Adama Mickiewicza, Poznań
Wydział Biologii
Zakład Bioenergetyki
ul. Uniwersytetu Poznańskiego 6
61-614 Poznań
e-mail:

Oświadczenie określające wkład w powstanie artykułu

Niniejszym oświadczam, że mój wkład w powstanie poniższego artykułu: **Mazur M.,** Wojciechowska D., Sitkiewicz E., Malinowska A., Świderska B., Kmita H., Wojtkowska M., 2021. Mitochondrial Processes during Early Development of Dictyostelium discoideum: From Bioenergetic to Proteomic Studies. *Genes (Basel),* 12(5): 638, polegał na uczestniczeniu w planowaniu eksperymentów, analizie i interpretacji danych, współtworzeniu tekstu manuskryptu.

Swój całkowity wkład w pracę oceniam na 15%.

Małgorzata Wojtkowska

Poznań, 13.01.2022 r.

Prof. dr hab. Hanna Kmita
Uniwersytet im. Adama Mickiewicza, Poznań
Wydział Biologii
Zakład Bioenergetyki
ul. Uniwersytetu Poznańskiego 6
61-614 Poznań
e-mail: hanna.kmita@amu.edu.pl

Oświadczenie określające wkład w powstanie artykułu

Niniejszym oświadczam, że mój wkład w powstanie poniższego artykułu: **Mazur M.,** Kmita H., Wojtkowska M., 2021. The Diversity of the Mitochondrial Outer Membrane Protein Import Channels: Emerging Targets for Modulation. *Molecules,* 26(13): 4087, polegał na pisaniu manuskryptu – w szczególności podrozdziałów: „Transport of RNA" i „Transport of Metabolites" oraz na dyskusji wyników.

Swój całkowity wkład w pracę oceniam na 20%.

Hanna Kmita

Z wyrazami szacunku,

Poznań, 02.02.2022 r.

Prof. UAM dr hab. Małgorzata Wojtkowska
Uniwersytet im. Adama Mickiewicza, Poznań
Wydział Biologii
Zakład Bioenergetyki
ul. Uniwersytetu Poznańskiego 6
61-614 Poznań
e-mail:

Oświadczenie określające wkład w powstanie artykułu

Niniejszym oświadczam, że mój wkład w powstanie poniższego artykułu: **Mazur M.,** Kmita H., Wojtkowska M., 2021. The Diversity of the Mitochondrial Outer Membrane Protein Import Channels: Emerging Targets for Modulation. *Molecules,* 26(13): 4087, polegał na pisaniu manuskryptu – w szczególności części: "Abstract", "Introduction", "Tom40 Channel", "Mitochondrial Apoptosis-Induced Channel (MAC)", "Ayr1 and OMC7 and OMC8: Mitochondrial Outer Membrane Channels for Unknown Molecules", "Conclusions and Perspectives", oraz na dyskusji naukowej i nadzorze merytorycznym całości tekstu.

Swój całkowity wkład w pracę oceniam na 30%.

Małgorzata Wojtkowska

PUBLIKACJE STANOWIĄCE PODSTAWĘ ROZPRAWY DOKTORSKIEJ

ACTA ABP BIOCHIMICA POLONICA

THE 44th FEBS CONGRESS 6-11 JULY 2019 Krakow, Poland

Vol. 66, No 4/2019
551–557
https://doi.org/10.18388/abp.2019_2791

Regular paper

The TOB/SAM complex composition in mitochondria of *Dictyostelium discoideum* during progression from unicellularity to multicellularity*

Monika Mazur[1], Małgorzata Wojtkowska[1], Marcin Skalski[1], Małgorzata Słocińska[2] and Hanna Kmita[1]✉

[1]Institute of Molecular Biology and Biotechnology, Department of Bioenergetics, Faculty of Biology, Adam Mickiewicz University, Poznań, Poland; [2]Department of Animal Physiology, Faculty of Biology, Adam Mickiewicz University, Poznań, Poland

Despite its complex life cycle including unicellular and multicellular stages, the slime mold *Dictyostelium discoideum*, a well-known model in biomedical research, has not been used as a model organism in studies on mitochondrial import, including its significance in cellular processes. Moreover, data concerning mitochondrial protein import machinery in *D. discoideum* mitochondria is limited and nothing is known about the impact of that machinery on slime mold life cycle. Here, we focused on the TOB/SAM (topogenesis of the mitochondrial outer membrane β-barrel proteins/sorting and assembly machinery) complex. This complex is localized in the mitochondrial outer membrane and is indispensable for the formation of metabolite exchange and protein import pathways in the membrane, and substantially contributes to the regulation of mitochondrial morphology and distribution. Furthermore, the available data suggests that the TOB/SAM complex variants differ between mitochondria of multicellular and unicellular eukaryotes. Therefore, we decided to determine these variants of the TOB/SAM in mitochondria of *D. discoideum* progressing from single cells to early multicellular stages, when the cells stream together to form a multicellular organism. The results revealed two complex variants of the TOB/SAM complex of about 160 and 600 kDa molecular weight, present in mitochondria of *D. discoideum* cells at the studied stages. The discussed complex variants resemble the ones that have been already detected for the yeast *Saccharomyces cerevisiae,* fungus *Neurospora crassa* and human cells, and one of investigated variants differentiates unicellular and initial multicellular stages of the *D. discoideum* life cycle.

Key words: mitochondria, protein import, TOB/SAM complex, *Dictyostelium discoideum*

Received: 14 March, 2019; revised: 17 July, 2019; accepted: 16 September, 2019; available on-line: 12 November, 2019

✉e-mail: kmita@amu.edu.pl

***Acknowledgements of financial support:**
The costs of the article published as a part of the 44th FEBS Congress Kraków 2019 – From molecules to living systems block are financed by the Ministry of Science and Higher Education of the Republic of Poland (Contract 805/P-DUN/2019).
This project was supported by the National Science Centre (Poland) project (grant no. 2012/05/N/NZ3/00293), and the "KNOW RNA Research Centre in Poznan" (grant no. 01/KNOW2/2014).

Abbreviations: MICOS, mitochondrial contact site and cristae-organizing system; TOB/SAM, topogenesis of the mitochondrial outer membrane β-barrel proteins/sorting and assembly machinery; TOM, translocase of the outer membrane; XP_641975.1, Mdm10; XP_642798.1, Tom40; XP_642848.1, metaxin; XP_646058.1, Tob55/Sam50; XP_646782.1, mitofilin/Mic60

INTRODUCTION

The slime mold *Dictyostelium discoideum* is recognized by the National Institute of Health (NIH) as a model of particular value in biomedical research, including mitochondrial diseases (www.nih.gov/science/models). The reason is high homology of *D. discoideum* protein sequences to human proteins (e.g. Eichinger *et al.*, 2005) and its complex life cycle (see Fig. 1). The latter includes different unicellular and multicellular stages which provides a possibility to study cellular processes at intracellular and intercellular levels. This also applies to the mitochondrial protein import process being crucial for the mitochondrial biogenesis and functioning. Most of the mitochondrial proteins are synthesized in the cytosol and therefore have to be imported into various mitochondrial subcompartments.

The mitochondrial outer membrane contains two main import complexes, i.e. the TOM complex (translocase of the outer membrane) and the TOB/SAM complex (topogenesis of the mitochondrial outer membrane β-barrel proteins/sorting and assembly machinery). The TOM complex recognizes, sorts and translocates most of the mitochondrial precursor proteins from the cytosol, whereas the TOB/SAM complex participates in the TOM complex assembly and inserts β-barrel proteins into the outer membrane after translocation of these

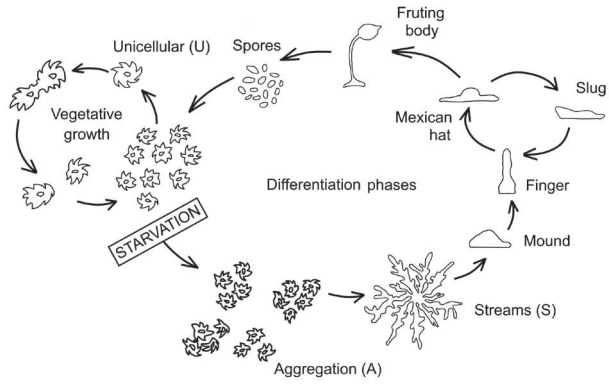

Figure 1. Life cycle of *D. discoideum*.
The vegetative phase (U, unicellular) ceases when food is depleted (bacteria in the soil). Single cells enter differentiation phase, also termed a social phase. After passing the early multicellular stages (A, aggregation; S, streams) cells aggregate and form a motile slug, which ultimately develops into a fruiting body dispersing spores to new feeding sites.

proteins into the intermembrane space by the TOM complex (reviewed by Endo & Yamano, 2010; Neupert, 2015; Höhr *et al*., 2018; Pfanner *et al*., 2019). The proteins are exemplified by mitochondrial porin required for metabolite transport, as well as channel forming subunits of the TOM and TOB/SAM complexes, Tom40 and Tob55/Sam50, respectively (Höhr *et al*., 2018). Thus, the TOB/SAM complex is essential for formation of the metabolite exchange and protein import pathways in the mitochondrial outer membrane and substantially contributes to regulation of mitochondrial functioning.

In studies on the function and interplay of mitochondrial protein import complexes, the yeast *Saccharomyces cerevisiae* is mainly applied as a model organism (e.g. Sokol *et al*., 2014; Neupert, 2015). The *S. cerevisiae* TOB/SAM complex is proposed to consist of three main subunits, i.e. Tob55/Sam50, Tob38/Sam35 (Tom38), and Tob37/Sam37 (Tom37, Mas37). However, in the case of other eukaryotes, smaller or bigger differences in the complex subunits have been reported. For example, the animal TOB/SAM complex contains metaxin-2 as a counterpart of Tob38/Sam35, as well as metaxin-1 and metaxin-3 as counterparts of Mas37/Sam37 (Sokol *et al*., 2014), whereas the subunits predicted for the complex of the slime mold *D. discoideum* include Tob55/Sam50 and metaxin as a sole receptor subunit (Buczek *et al*., 2016; Wojtkowska *et al*., 2017). It is assumed that the monomeric form of the TOB/SAM complex, composed of the main subunits, has molecular weight of 160–250 kDa, depending on the studied organism (e.g. Kozjak-Pavlovic *et al*., 2007; Yamano *et al*., 2010; Ott *et al*., 2012; Neupert, 2015), although other forms of the complex are also detected due to complex interaction with proteins that are also subunits of other complexes, including the TOM complex (Qiu *et al*., 2013; Wenz *et al*., 2015),endoplasmic reticulum-mitochondria encounter structure complex (Kornmann *et al*., 2009; Yamano *et al*., 2010; Flinner *et al*., 2013) and the MICOS (mitochondrial contact site and cristae-organizing system) complex (e.g. Rampelt *et al*., 2017). The available data indicate that detected forms of the TOB/SAM complex may differ between multicellular organisms, represented by human cells (Kozjak-Pavlovic *et al*., 2007; Xie *et al*., 2007; Ott *et al*., 2012), *Neurospora crassa* (Klein *et al*., 2012; Lackey *et al*., 2011) and unicellular ones, e.g. *S. cerevisiae* (Waizenegger *et al*., 2004; Yamano *et al*., 2010). This may imply a correlation between the TOB/SAM complex and multicellularity. Here, we present verification of this assumption by analysis of the TOB/SAM complex forms in mitochondria of *D. discoideum* progressing from single cells to early multicellular stages when the cells aggregate and then stream together to form a multicellular organism.

MATERIALS AND METHODS

***Dictyostelium discoideum* growth conditions and the studied life cycle stages**. *D. discoideum* is a social amoeba whose life cycle consists of vegetative growth and a differentiation phase (Flowers *et al*., 2010; Czarna *et al*., 2010). The unusual differentiation process starts from aggregation of single cells, which is triggered by nutrient depletion. Then, the developing multicellularity reaches the stage of streams formed by the aggregating cells and followed by a slug formation that culminates as a fruiting body (top of the stalk) consisting of spores (Fig. 1).

The axenic strain AX2 of *D. discoideum* was kindly provided by Prof. Michael Schleicher from Ludwig Maximilian University of Munich, Germany. *D. discoideum* cells were cultured in axenic growth medium containing 1% w/v proteose peptone, 0.5% w/v yeast extract, 0.45% w/v D-glucose, 0.09% w/v Na_2HPO_4 and 0.23% w/v KH_2PO_4. Cell culture was propagated in 850 ml of the axenic growth medium at 19°C, on a Certomat MO rotary shaker at 90 rpm. Cells were cultured exponentially till the density of approximately 2.0-3.0×10^6 cells/ml (the doubling time of 10–11 h). These cells constituted the unicellular (U) stage. Cells at aggregation (A) and stream (S) stages were obtained by placing U stage cells into Petri dishes (1.7×10^6 cells/cm^2) with a solid starvation medium called Development Buffer (DB) and containing 5 mM Na_2HPO_4, 5 mM KH_2PO_4, 1 mM $CaCl_2$, 2 mM $MgCl_2$, pH 6.5 and 1.25% w/v agar (Fey *et al*. 2007). The cells were harvested after ~23h for A stage, and ~25 h for S stage. The presence of U, A and S stages was confirmed by Nikon Eclipse TE 2000-U microscope. The images were obtained by Nikon DS-1QM camera, and processed by the NIS Elements A 3.10 software.

Immunofluorescent staining. Intact cells were incubated with 200 nM MitoTracker™ Red FM (Invitrogen), a red-fluorescent dye, which stains mitochondria due to accumulation dependent upon the inner membrane potential, for 1 h at 37°C. Cells were then washed in PBS and fixed in 4% paraformaldehyde solution (in PBS) for 20 min at room temperature, seeded on poly L-lysine slides and allowed to dry completely. The cells were subsequently fixed with ice cold methanol and permeabilized with cold acetone for 5 min. Subsequently, the fixed cells were blocked in 5% BSA at room temperature for 1 h and afterwards incubated for 1 h with antibodies raised against Tob55/Sam50 at a dilution of 1:100 in PBS buffer with 5% BSA, at room temperature. Next, the cells were washed in phosphate buffered saline (PBS), and incubated for 1 h at room temperature with goat-anti-rabbit IgG conjugated to fluorescein isothiocyanate (FITC) (Santa Cruz Biotechnology) at a dilution of 1:100 (Slocinska *et al*., 2011). Finally, samples were analyzed under Nikon Eclipse TE 2000-U fluorescence microscope. The images were obtained with a Nikon DS-1QM camera, and processed by the NIS Elements A 3.10 software.

Mitochondria isolation. Cells from U, A and S stages were centrifuged at 600×*g* for 5 min and then washed twice in phosphate medium A (14.5 mM KH_2PO_4, 5 mM Na_2HPO_4, pH 6) by centrifugation at 600×*g* for 5 min. Next, the cells were homogenized in medium B (0.38 M sucrose, 20 mM Tris-Cl, 0.5 mM EDTA, 1% defatted bovine serum albumin [BSA], pH 7.5) using glass/Teflon homogenizer and centrifuged at 860×*g* for 5 min. Supernatant was centrifuged at 10 000×*g* for 15 min. The obtained pellet was suspended in medium C (0.38 M sucrose, 20 mM Tris-Cl, 0.5 mM EDTA, 0.6% defatted BSA, pH 7.2) and centrifuged at 860×*g* for 5 min to remove remaining cells. Supernatant was centrifuged at 10 000×*g* for 10 min, mitochondrial pellet was suspended in medium D (0.38 M sucrose; 20 mM, Tris-Cl, pH 7.2) and centrifuged at 10 000×*g* for 15 min. After this step, the mitochondrial pellet was suspended in medium D and used for further analysis. Efficiency of the mitochondria isolation procedure varied depending on the stage, from 1.5 mg of mitochondrial proteins per 1 g of cells at A and S stages, to 4.5 mg of mitochondrial proteins per 1 g of cells at the U stage. All media used for mitochondria isolation were ice cold and centrifugation procedures were carried out at 4°C.

Protein electrophoresis. Blue Native Polyacrylamide Gel Electrophoresis (BN-PAGE) was performed accord-

ing to Witting and others (Witting *et al.*, 2012). Mitochondria (100 μg) were solubilized in a buffer containing 0.1 M EDTA, 50 mM NaCl, 10% glycerol, 20 mM Tris, 1 mM PMSF, pH 7.4 and 1.25% digitonin (Sigma-Aldrich) for 20 min at 4°C, and centrifuged for 50 min at 14000 × g and 4°C. Aliquots of solubilized mitochondria were mixed with Serva Sample Buffer for Blue Native (2× conc.) and loaded on the 6–13% native gradient gel (prepared in 1.5 M ε-amino-n-caproic acid and 0.15 M Bis-Tris, pH 7). Sodium Dodecyl Sulfate Polyacryl mide Gel Electrophoresis (SDS-PAGE) was performed according to Laemmli (Laemmli, 1970). SDS-PAGE and BN-PAGE gels were stained with Serva Coomassie Brilliant Blue G-250. To perform Western blot immunodecoration proteins separated by BN-PAGE were transferred to PolyVinylidene DifFluoride (PVDF) membrane (Millipore) and by SDS-PAGE to nitrocellulose membrane. After immunodecoration proteins were visualized by the Lumi-Light Western Blotting Substrate (Roche).

Mass spectrometry. Protein bands indicated by Western immunoassays were analyzed by liquid chromatography coupled to tandem mass spectrometry (LC-MS/MS) performed in the Mass Spectrometry Laboratory (Institute of Biochemistry and Biophysics, Polish Academy of Sciences Warsaw, Poland). The gel bands were subjected to digestion by a standard procedure where trypsin was used (Promega, Madison, WI, USA). Peptide mixtures were separated by LC-MS/MS prior to molecular mass measurements using LTQ-FTICR on Orbitrap Velos mass. The RP-18 precolumn and nano-HPLC RP-18 column was used for separation of peptides obtained by digestion. Raw data was processed by the Mascot search against the NCBI database (www.ncbi.nig.gov) restricted to Eukaryota and *D. discoideum* AX2 strain. Peptide mass tolerance was ±20 ppm.

Other methods. Protein concentration was measured by Bradford method, with BSA as a standard (Bradford, 1976). Amino acid sequence of mitofilin/Mic60 was predicted using the blastp algorithm (https://blast.ncbi.nlm.nih.gov) and the Pfam model (http://pfam.xfam.org).

Antibodies. The antibody against *D. discoideum* Tob55/Sam50 protein, supplied by the Pineda company (Berlin, Germany), was directed against the 20 amino acid N-terminal sequence (NH_2-DDDDIKIKFVNIKSENVFLC-$CONH_2$). The delivered serum was purified using the modified sulfhydrylagarose (Pierce). The first step of purification was binding of the peptide used for immunization with the SulfoLink Coupling Resin. This was done in coupling medium (50 mM Tris, 5 mM EDTA-Na; pH 8.5), using 1 ml of peptide per 1 ml of the resin, for 30 min at room temperature. The coupling efficiency was determined by spectrophotometrical (λ=280nm) estimation of peptide non-coupled fraction concentration. Next, the nonspecific binding sites on the resin were blocked by adding 1 ml of 50 mM cysteine solution to the column at room temperature for 15 minutes with shaking and without mixing for an additional 30 minutes. Afterwards, the column was washed by six resin-bed volumes of 1 M NaCl and stored in the PBS medium. For purification of the antibody against Tob55/Sam50, the column was incubated with 2 ml of serum overnight at 4°C and then washed with PBS. Finally, samples were eluted using 100 mM glycine (pH 3.0) and immediately neutralized by adding 50 μL of neutralization buffer (1 M Tris-Cl, pH 8.8). The elution efficiency was estimated spectrophotometrically (λ=280nm). Samples of interest were desalted in the presence of PBS and stored at –20°C. The antibody against human metaxin-1 protein was purchased from Sigma-Aldrich.

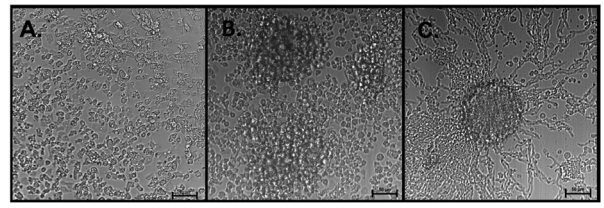

Figure 2. The early multicellular stages of the *D. discoideum* life cycle.
Samples were analyzed with a Nikon Eclipse TE 2000-U light microscope. The images were obtained with a Nikon DS-1QM camera. U, unicellular stage; A, aggregation stage; S, streams.

RESULTS

The early multicellular stages of the *D. discoideum* life cycle

To monitor changes of the TOB/SAM complex variants during transition from unicellularity to multicellularity, three stages: unicellular (U), aggregation (A) and streams (S) were selected. The occurrence of those stages in the *D. discoideum* life cycle is depicted in Fig. 1 and was confirmed by light microscopy as shown in Fig. 2. The starvation of U stage cells resulted in the A stage (Fig. 2B), characterized by the presence of irregular clusters of various amounts of cells. Further starvation of cells has led to the S stage (Fig. 2C), formed by cells in an aggregation process, and followed by mound formation (Fig. 1). As shown in Fig. 2C, cells at the S stage gathered by migrating in organized streams, finally producing a structure similar to a star or a flower.

Detection of the TOB/SAM complex main subunits in mitochondria of unicellular and early multicellular stages

As we had previously predicted the main subunits of the *D. discoideum* TOB/SAM complex using available genomic and transcriptomic sequences (Wojtkowska *et al.*, 2012; Buczek *et al.*, 2016), we decided to confirm the presence of the Tob55/Sam50 and metaxin subunits at a protein level. The designed polyclonal antibody against Tob55/Sam50 (Materials and Methods) was used to confirm the presence of Tob55/Sam50 in mitochondria of intact cells at the studied stages (Fig. 3A), as well as in mitochondria isolated from these cells (Fig. 3B). As shown in Fig. 3A, staining of mitochondria with MitoTracker™ Red FM (Fig. 3A.1) and subsequent incubation with the antibody against Tob55/Sam50 (Fig. 3A.2) co-localized in the merged image (Fig. 3A.3), indicating the presence of Tob55/Sam50. The protein was also detected in separated mitochondrial proteins by Western immunoassays (band ca. 45 kDa; Fig. 3B). Moreover, signals obtained with the antibody against Tob55/Sam50 for mitochondria isolated from cells at the studied stages were confirmed by LC-MS/MS using the corresponding band in SDS-PAGE gels (Table S1 at https://ojs.ptbioch.edu.pl/).The presence of metaxin was also confirmed in mitochondria isolated from cells at the studied stages by application of a commercially available human metaxin-1 antibody (Fig. 3B), as well as by LC-MS/MS using t he corresponding band in SDS-PAGE gels (Table

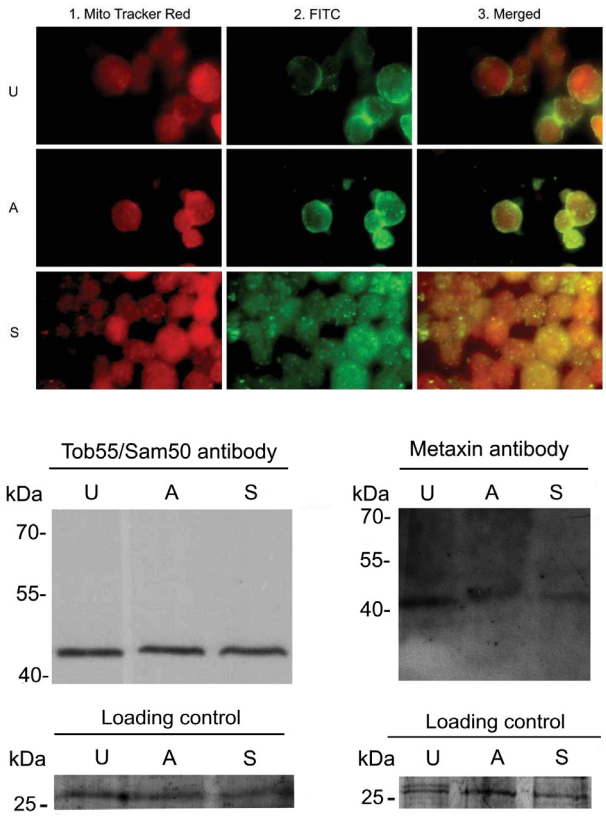

Figure 3. Detection of the *D. discoideum* TOB/SAM complex main subunits at a protein level.
(**A**) Immunofluorescence localization of Tob55/Sam50. The localization was performed for single cells (**U**), as well as cells from the early developmental stages (**U, A** and **S**). **Panel 1**, staining with MitoTracker™ Red FM (Invitrogen) to visualize mitochondria; **Panel 2**, incubation with goat anti-rabbit IgG recognizing the antibody against Tob55/Sam50 protein and conjugated to fluorescein isothiocyanate (FITC); **Panel 3**, the merged image. Specimens were analyzed with a Nikon Eclipse TE 2000-U fluorescence microscope. Images were obtained with a Nikon DS-1QM camera. (**B**) Immunodetection of Tob55/Sam50 and metaxin among mitochondrial proteins isolated from the cells described in (**A**), separated by 12% SDS-PAGE and immunodecorated by respective antibodies after Western blotting. The results shown in (**A**) and (**B**) are typical for 3 independent experiments. Loading control – a 25 kDa protein band shown on part of a Coomassie stained gel.

S1 https://ojs.ptbioch.edu.pl/). The molecular weight of this protein was estimated to be at about 46 kDa.

Estimation of the TOB/SAM complex variants in mitochondria of unicellular and early multicellular stages

The application of western immunoassay on BN blots with antibodies against Tob55/Sam50 and human metaxin-1 to detect possible variants of the TOB/SAM complex in mitochondria isolated from cells at U, A and S stages, indicated the presence of two distinct forms of the complex independently of the studied stage (Table 1). Their molecular weights were estimated to be at about 600 and 160 kDa. Importantly, metaxin was detected in the larger complex only. Other putative partners or subunits of the TOB/SAM complex variants could not be detected by immunoassays due to the lack of specific antibodies. Therefore, we applied LC-MS/MS to identify them. As a result, additional proteins were identified. In the 600 kDa complex, Tom40 (Wojtkowska *et al.*, 2012) and mitofilin/Mic60 were found (Table 2), the latter for the first time in this study (Table S2 at https://ojs.ptbioch.edu.pl/). Importantly, mitofilin/Mic60 was detected only at the U stage. A putative nucleotide sequence of mitofilin/Mic60 was found by blastp and Pfam model (Fig. S1 at https://ojs.ptbioch.edu.pl/), and used to detect the mitofilin domain (Yang *et al.*, 2012; Ott *et al.*, 2015) in a putative sequence obtained by LC-MS/MS. Interestingly, in the 160 kDa complex, we detected Mdm10, but not the Tom40 protein (Table 1). Notably, Mdm10 had been previously predicted in *D. discoideum* by bioinformatics analysis (Buczek *et al.*, 2016) but at a protein level it was confirmed for the first time in this study (Table S2 at https://ojs.ptbioch.edu.pl/).

Table 1. Components of the TOB/SAM complex variants from the U, A and S developmental stages in *D. discoideum* mitochondria

	Subunits detected by	
app. molecular weight	immunodetection	LC-MS/MS
600 kDa	Tob55/Sam50; metaxin	Tom40; mitofilin
160 kDa	Tob55/Sam50	Mdm10; mitofilin

DISCUSSION

The available data on different variants of the TOB/SAM complex detected for unicellular (*S. cerevisiae*) and multicellular (*N. crassa* and human cells) organisms suggests a correlation between this complex and the level of organism organization (Table 3). *D. discoideum* cells progressing from the single cell (U) stage to early multicellular (A and S) stages, when single cells aggregate and then stream together forming a multicellular structure, constitute a useful model to study a shift between unicellularity and multicellularity. However, the assumed relationship is not confirmed by the obtained results as they indicate that the TOB/SAM complex variants do not differ between the stages. Namely, the same two variants of the complex of molecular weight of about 600 and 160 kDa are present in mitochondria isolated from cells at these stages (Fig. 4).

Table 2. The TOB/SAM complex subunits identified at the protein level in mitochondria of *D. discoideum* cells progressing from unicellularity to early multicellularity

Identified protein	Accession number	Proteins identified at	
		the genome/transcriptome level	the protein level
Tob55/Sam50	XP_646058.1	Wojtkowska *et al.*, 2012	this study
Tom40	XP_642798.1	Wojtkowska *et al.*, 2012	Wojtkowska *et al.*, 2015
metaxin	XP_642848.1	Buczek *et al.*, 2016	this study
Mdm10	XP_641975.1	Buczek *et al.*, 2016	this study
mitofilin/Mic60	XP_646782.1	this study	this study

Table 3. Variants of the TOB/SAM complex of *S. cerevisiae*, *N. crassa*, human and *D. discoideum* mitochondria

S. cerevisiae (Qiu *et al*., 2013)	*N. crassa* (Klein *et al*., 2012)	Human (Ott *et al*., 2012)	*D. discoideum* this study
650 kDa supercomplex TOB/SAM: Tob55/Sam50; Sam37, Sam35; TOM: Tom40, Tom22, Tom20, Tom70, Tom6, Tom7, Tom5 **440 kDa** TOB/SAM: Tob55/Sam50; Sam37, Sam35; Mdm10 **200 kDa** TOB/SAM: Tob55/Sam50; Sam37, Sam35	**> 600 kDa** TOB/SAM: Tob55/Sam50; Sam37, Sam35 **200 kDa** TOB/SAM: Tob55/Sam50; Sam37, Sam35; Mdm10 **140 kDa** TOB/SAM: Tob55/Sam50; Sam37, Sam35	**> 700 kDa** **TOB/SAM**: Tob55/Sam50; Sam37, Sam35; mitofilin **250 kDa** **TOB/SAM**: Tob55/Sam50; Sam37, Sam35	**> 650kDa** TOB/SAM: Tob55/Sam50; Sam37, Sam35; Tom40; mitofilin* **160 kDa** Tob55/Sam50; Mdm10; mitofilin*

The detected variants of the *D. discoideum* TOB/SAM complex correspond to the monomeric variant of the complex composed of the main subunits (160 kDa) and the form interacting with other proteins (600 kDa). A monomeric variant of comparable size has been reported for *S. cerevisiae* (Waizenegger *et al*., 2004; Yamano *et al*., 2010; Qiu *et al*., 2013), *N. crassa* (Lackey *et al*., 2011; Klein *et al*., 2012) and human cells (Kozjak-Pavlovic et al., 2007; Ott *et al*., 2012) (Table 3). Importantly, the variant of the *D. discoideum* complex does not contain metaxin. As the protein is detected by anti-metaxin-1 antibody (Fig. 3), it might be assumed that this form is missing a counterpart of Tob37/Sam37 (Sokol *et al*., 2014), although may contain subunits still not detected. Tob37/Sam37 has been shown to be not essential and to act at the late stages of β-barrel assembly by assisting protein release from the complex (Chan & Lithgow, 2008; Dukanovic *et al*., 2009). Accordingly, in *S. cerevisiae* and *N. crassa,* mitochondria variants missing the Tob37/Sam37 protein have been also detected (Waizenegger *et al*., 2004; Lackey *et al*., 2011). Furthermore, it has been reported that in the human mitochondria, Tob55/Sam50 and metaxins seemed to be present in different complexes (Kozjak-Pavlovic *et al*., 2007). On the other hand, the *D. discoideum* form contains Mdm10 which is not present in the human mitochondria but is also detected in the forms of the TOB/SAM complex present in *N. crassa* (Lackey *et al*., 2011; Klein *et al*., 2012) and *S. cerevisiae* (Waizenegger *et al*., 2004; Yamano *et al*., 2010; Qiu *et al*., 2013) mitochondria, although data concerning the size of the resulting complexes are not consistent.

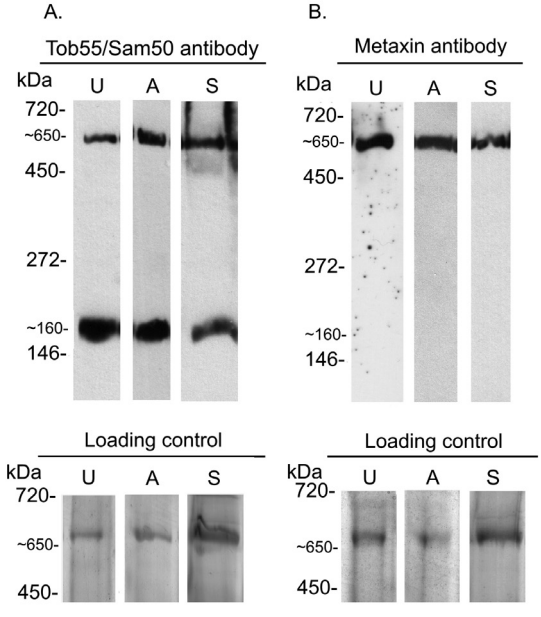

Figure 4. Estimation of the *D. discoideum* TOB/SAM complex forms in mitochondria of single cells, as well as cells from the early multicellular stages.
Mitochondria solubilized in the presence of 1.25% digitonin were separated by BN-PAGE and the obtained Western blots were immunodecorated by Tob55/Sam50 and metaxin antibody. The data presented are typical for 3 independent experiments. (**U**) unicellular; (**A**) aggregation; (**S**) streams. Loading control – a 650 kDa complex band shown on part of a Coomassie stained BN gel.

The 600 kDa form of the TOB/SAM complex corresponds to the 600–700 kDa supercomplex detected for *S. cerevisiae* (Qiu *et al*., 2013; Wenz *et al*., 2015) and human cells (Kozjak-Pavlovic *et al*., 2007; Ott *et al*., 2012). In the case of *S. cerevisiae* mitochondria, the 650-700 kDa supercomplex has been shown to contain the TOM complex interacting with the TOB/SAM complex and to promote substrate channeling in the β-barrel pathway (Qiu *et al*., 2013; Wenz *et al*., 2015) (Table 3). Thus, the presence of Tom40 in the 600 kDa *D. discoideum* form could be considered in two aspects. Firstly, Tom40 is the most abundant subunit of the TOM complex (Sirrenberg *et al*., 1997). As the molecular weight of the *D. discoideum* TOM complex has been estimated to be about 430 kDa (Wojtkowska *et al*., 2015), it can be assumed that the 600 kDa form may represent the supercomplex consisting of the TOB/SAM (160 kDa) and the TOM complex. Secondly, Tom40 being the β-barrel protein itself is imported by the TOB/SAM complex. Thus, its presence in the form of the TOB/SAM complex may also reflect its import process. However,Tom40 has not been detected in the 600–700 kDa complexes in human mitochondria.

The presence of mitofilin/Mic60, a key component of the MICOS complex (Harner *et al*., 2011; Malsburg *et al*., 2011; Eydt *et al*., 2017), in the 600 kDa form of the *D. discoideum* TOB/SAM complex at the U stage, appears to confirm the interaction between the protein and the main subunits of the TOB/SAM complex. This interaction has been shown for *S. cerevisiae* and human mitochondria (e.g. Ott *et al*., 2012; Rampelt *et al*., 2017) and is regarded to be mediated by Tob55/Sam50 (Ott *et al*., 2012; Xie *et al*.,2007; Ding *et al*., 2015) and/or metaxin (Xie *et al*., 2007). Accordingly, the yeast homologue of mitofilin/Mic60, termed Fcj1, has been shown to be important for association of the TOB/SAM complex with mitochondrial contact sites, resulting in stabilization of crista junctions in close proximity to the outer membrane (Korner *et al*., 2012). In addition, the TOB/SAM complex is also described as an anchor for the MICOS complex subunits (Harner *et al*., 2011). Moreover, the presence of mitofilin/Mic60 in the 600 kDa vari-

ant of the *D. discoideum* TOB/SAM complex, may result from the protein interaction with the TOM complex, as proposed for *S. cerevisiae* (Qiu *et al.*, 2013; Rampelt *at al.*, 2017), but not observed for human mitochondria. Thus, it can be assumed that the interaction of the TOB/SAM complex with the MICOS complex may occur at the U stage mitochondria and may include the TOB/SAM complex interaction with the TOM complex.

In summary, the detected forms of the *D. discoideum* TOB/SAM complex, i.e. the 160 and 600 kDa forms, appear to be similar to the forms found in *S. cerevisiae*, *N. crassa* and human mitochondria. The 600 kDa form seems to differentiate between unicellular and early multicellular stages by putative interaction with the MICOS complex subunit, although the next stages of the *D. discoideum* life cycle should be studied to observe more spectacular differences in the TOB/SAM complex forms.

Other acknowledgement

We would like to thank Arkadiusz Urbański, Ph.D. from the Department of Animal Physiology and Development, Faculty of Biology, AMU Poznań for technical support in preparing *D. discoideum* photos from light microscope. The equipment used was sponsored in part by the Centre for Preclinical Research and Technology (CePT), a project co-sponsored by European Regional Development Fund and Innovative Economy, The National Cohesion Strategy of Poland.

REFERENCES

Bradford MM (1976) A rapid and sensitive method for the quantitation of microgram quantities of protein utilizing the principle of protein-dye binding. *Anal Biochem* **72**: 248–254. https://doi.org/10.1016/0003-2697(76)90527-3

Buczek D, Wojtkowska M, Suzuki Y, Sonobe S, Nishigami Y, Antoniewicz M, Kmita H, Makałowski W (2016) Protein import complexes in the mitochondrial outer membrane of Amoebozoa representatives. *BMC Genomics* **17**: 99. https://doi.org/10.1186/s12864-016-2402-2

Chan NC, Lithgow T (2008) The peripheral membrane subunits of the SAM complex function codependently in mitochondrial outer membrane biogenesis. *Mol Biol Cell* **19**: 126–136. https://doi.org/10.1091/mbc.e07-08-0796

Czarna M, Mathy G, Mac'Cord A, Dobson R, Jarmuszkiewicz W, Sluse-Goffart CM, Leprince P, De Pauw E, Sluse FE (2010) Dynamics of the *Dictyostelium discoideum* mitochondrial proteome during vegetative growth, starvation and early stages of development. *Proteomics* **10**: 6–22. https://doi.org/10.1002/pmic.200900352

Ding C, Wu Z, Huang L, Wang Y, Xue J, Chen S, Deng Z, Wang L, Song Z, Chen S (2015) Mitofilin and CHCHD6 physically interact with Sam50 to sustain cristae structure. *Sci Rep* **5**: 16064. https://doi.org/10.1038/srep16064

Dukanovic J, Dimmer KS, Bonnefoy N, Krumpe K, Rapaport D (2009) Genetic and functional interactions between the mitochondrial outer membrane proteins Tom6 and Sam37. *Mol Cell Biol* **29**: 5975–5988. https://doi.org/10.1128/MCB.00069-09

Eichinger L, Pachebat JA, Glöckner G, Rajandream MA, Sucgang R, Berriman M, Song J, Olsen R, Szafranski K, Xu Q, Tunggal B, Kummerfeld S, Madera M, Konfortov BA, Rivero F, Bankier AT, Lehmann R, Hamlin N, Davies R, Gaudet P, Fey P, Pilcher K, Chen G, Saunders D, Sodergren E, Davis P, Kerhornou A, Nie X, Hall N, Anjard C, Hemphill L, Bason N, Farbrother P, Desany B, Just E, Morio T, Rost R, Churcher C, Cooper J, Haydock S, van Driessche N, Cronin A, Goodhead I, Muzny D, Mourier T, Pain A, Lu M, Harper D, Lindsay R, Hauser H, James K, Quiles M, Madan Babu M, Saito T, Buchrieser C, Wardroper A, Felder M, Thangavelu M, Johnson D, Knights A, Loulseged H, Mungall K, Oliver K, Price C, Quail MA, Urushihara H, Hernandez J, Rabbinowitsch E, Steffen D, Sanders M, Ma J, Kohara Y Sharp S, Simmonds M, Spiegler S, Tivey A, Sugano S, White B, Walker D, Woodward J, Winckler T, Tanaka Y, Shaulsky G, Schleicher M, Weinstock G, Rosenthal A, Cox EC, Chisholm RL, Gibbs R, Loomis WF, Platzer M, Kay RR, Williams J, Dear PH, Noegel AA, Barrell B, Kuspa A (2005) The genome of the social amoeba *Dictyostelium discoideum*. *Nature* **435**: 43–57. https://doi.org/10.1038/nature03481

Endo T, Yamano K (2010) Transport of proteins across or into the mitochondrial outer membrane. *Biochim Biophys Acta* **1803**: 706–704. https://doi.org/10.1016/j.bbamcr.2009.11.007

Eydt, K, Davies KM, Behrendt C, Wittig I, Reichert AS (2017) Cristae architecture is determined by an interplay of the MICOS complex and the F_1F_0 ATP synthase via Mic27 and Mic10. *Microb Cell* **4**: 259–272. https://doi.org/10.15698/mic2017.08.585

Fey P, Kowal AS, Gaudet P, Pilcher KE, Chisholm RL (2007) Protocols for growth and development of *Dictyostelium discoideum*. *Nat Protoc* **2**: 1307–1316. https://doi.org/10.1038/nprot.2007.178

Flinner N, Ellenrieder L, Stiller SB, Becker T, Schleiff E, Mirus O (2013) Mdm10 is an ancient eukaryotic porin co-occurring with the ERMES complex. *Biochim Biophys Acta* **1833**: 3314–3325. https://doi.org/10.1016/j.bbamcr.2013.10.006

Flowers JM, Li SI, Stathos A, Saxer G, Ostrowski EA, Queller DC, Strassmann JE, Purugganan MD (2010) Variation, Sex, and Social Cooperation: Molecular Population Genetics of the social amoeba *Dictyostelium discoideum*. *PLoS Genet* **6**: e1001013. https://doi.org/10.1371/journal.pgen.1001013

Harner M, Körner C, Walther D, Mokranjac D, Kaesmacher J, Welsch U, Griffith J, Mann M, Reggiori F, Neupert W (2011) The mitochondrial contact site complex, a determinant of mitochondrial architecture. *EMBO J* **30**: 4356–4370. https://doi.org/doi:10.1038/emboj.2011.379

Höhr AIC, Lindau C, Wirth C, Qiu J, Stroud DA, Kutik S, Guiard B, Hunte C, Becker T, Pfanner N, Wiedemann N (2018) Membrane protein insertion through a mitochondrial β-barrel gate. *Science* **359**: eaah6834. https://doi.org/10.1126/science.aah6834

Klein A, Israel L, Lackey SWK, Nargang FE, Imhof A, Baumeister W, Neupert W, Thomas DR (2012) Characterization of the insertase for β-barrel proteins of the outer mitochondrial membrane. *J Cell Biol* **199**: 599–611. https://doi.org/10.1083/jcb.201207161

Körner C, Barrera M, Dukanovic J, Eydt K, Harner M, Rabl R, Vogel F, Rapaport D, Neupert W, Reichert AS (2012) The C-terminal domain of Fcj1 is required for formation of crista junctions and interacts with the TOB/SAM complex in mitochondria. *Mol Biol Cell* **23**: 2143–2155. https://doi.org/10.1091/mbc.E11-10-0831

Kornmann B, Currie E, Collins SR, Schuldiner M, Nunnari J, Weissman JS, Walter P (2009) An ER-mitochondria tethering complex revealed by a synthetic biology screen. *Science* **325**: 477–481. https://doi.org/10.1126/science.1175088

Kozjak-Pavlovic V, Ross K, Benlasfer N, Kimming S, Karlas A, Rudel T (2007) Conserved roles of Sam50 and metaxins in VDAC biogenesis. *EMBO Rep* **8**: 576–582. https://doi.org/10.1038/sj.embor.7400982

Lackey SW, Wideman JG, Kennedy EK, Go NE, Nargang FE (2011) The *Neurospora crassa* TOB complex: analysis of the topology and function of Tob38 and Tob37. *PLoS One* **6**: e25650. https://doi.org/10.1371/journal.pone.0025650

Laemmli UK (1970) Cleavage of structural proteins during the assembly of the head of bacteriophage T4. *Nature* **227**: 680–685. https://doi.org/10.1038/227680a0

von der Malsburg K, Müller JM, Bohnert M, Oeljeklaus S, Kwiatkowska P, Becker T, Loniewska-Lwowska A, Wiese S, Rao S, Milenkovic D, Hutu DP, Zerbes RM, Schulze-Specking A, Meyer HE, Martinou JC, Rospert S, Rehling P, Meisinger C, Veenhuis M, Warscheid B, van der Klei IJ, Pfanner N, Chacinska A, van der Laan M (2011) Dual role of mitofilin in mitochondrial membrane organization and protein biogenesis. *Dev Cell* **21**: 694–707. https://doi.org/10.1016/j.devcel.2011.08.026

Neupert W (2015) A perspective on transport of proteins into mitochondria: a myriad of open questions. *J Mol Biol* **427**: 1135–1158. https://doi.org/10.1016/j.jmb.2015.02.001

Ott C, Ross K, Straub S, Thiede B, Götz M, Goosmann C, Krischke M, Mueller MJ, Krohne G, Rudel T, Kozjak-Pavlovic V (2012) Sam50 functions in mitochondrial intermembrane space bridging and biogenesis of respiratory complexes. *Mol Cell Biol* **32**: 1173–1188. https://doi.org/10.1128/MCB.06388-11

Ott C, Dorsch E, Fraunholz M, Straub S, Kozjak-Pavlovic V (2015) Detailed analysis of the human mitochondrial contact site complex indicate a hierarchy of subunits. *PLoS One* **10**: e0120213. https://doi.org/10.1371/journal.pone.0120213

Pfanner N, Warscheid B, Wiedemann N (2019) Mitochondrial proteins: from biogenesis to functional networks. *Nat Rev Mol Cell Biol* **20**: 267–284. https://doi.org/10.1038/s41580-018-0092-0

Qiu J, Wenz LS, Zerbes RM, Oeljeklaus S, Bohnert M, Stroud DA, Wirth C, Ellenrieder L, Thornton N, Kutik S, Wiese S, Schulze-Specking A, Zufall N, Chacinska A, Guiard B, Hunte C, Warscheid B, van der Laan M, Pfanner N, Wiedemann N, Becker T (2013) Coupling of mitochondrial import and export translocases by receptor-mediated supercomplex formation. *Cell* **154**: 596–608. https://doi.org/10.1016/j.cell.2013.06.033

Rampelt H, Bohnert M, Zerbes RM, Horvath SE, Warscheid B, Pfanner N, van der Laan M (2017) Mic10, a core subunit of the mitochondrial contact site and cristae organizing system, interacts with

the dimeric F_1F_0-ATP synthase. *J Mol Biol* **429**: 1162–1170. https://doi.org/10.1016/j.jmb.2017.03.006

Sirrenberg C, Endres M, Becker K, Bauer MF, Walther E, Neupert W, Brunner M (1997) Functional cooperation and stoichiometry of protein translocases of the outer and inner membranes of mitochondria. *J Biol Chem* **272**: 29963–29966. https://doi.org/10.1074/jbc.272.47.29963

Slocinska M, Antos-Krzeminska N, Rosinski G, Jarmuszkiewicz W (2011) Identification and characterization of uncoupling protein 4 in fat body and muscle mitochondria from the cockroach *Gromphadorhina cocquereliana*. *J Bioenerg Biomembr* **43**: 717–727. https://doi.org/10.1007/s10863-011-9385-0

Sokol AM, Sztolsztener ME, Wasilewski M, Heinz E, Chacinska A (2014) Mitochondrial protein translocases for survival and wellbeing. *FEBS Lett* **588**: 2484–2495. https://doi.org/10.1016/j.febslet.2014.05.028

Waizenegger T, Habib SJ, Lech M, Mokranjac M, Paschen SA, Hell K, Neupert W, Rapaport D (2004) Tob38, a novel essential component in the biogenesis of β-barrel proteins of mitochondria. *EMBO Rep* **5:** 704–709. https://doi.org/10.1038/sj.embor.7400183

Wenz LS, Ellenrieder L, Qiu J, Bohnert M, Zufall N, van der Laan M, Pfanner N, Wiedemann N, Becker T (2015) Sam37 is crucial for formation of the mitochondrial TOM–SAM supercomplex, thereby promoting β-barrel biogenesis. *J Cell Biol* **210**: 1047–1054. https://doi.org/10.1083/jcb.201504119

Witting I, Braun H, Schägger H (2006) Blue native PAGE. *Nat Protoc* **1**: 418–428. https://doi.org/10.1038/nprot.2006.62

Wojtkowska M, Jąkalski M, Pieńkowska JR, Stobienia O, Karachitos A, Przytycka TM, Weiner J, 3rd, Kmita H, Makałowski W (2012) Phylogenetic analysis of mitochondrial outer membrane β-barrel channels. *Genome Biol Evol* **4**: 110–125. https://doi.org/10.1093/gbe/evr130

Wojtkowska M, Buczek D, Stobienia O, Karachitos A, Antoniewicz M, Slocinska M, Makałowski W, Kmita H (2015) The TOM complex of amoebozoans: the cases of the amoeba *Acanthamoeba castellanii* and the slime mold *Dictyostelium discoideum*. *Protist* **166**: 349–362. https://doi.org/10.1016/j.protis.2015.05.005

Wojtkowska M, Buczek D, Suzuki Y, Shabardina V, Makałowski W, Kmita H (2017) The emerging picture of the mitochondrial protein import complexes of Amoebozoa supergroup. *BMC Genomics* **18**: 997. https://doi.org/10.1186/s12864-017-4383-1

Xie J, Marusich MF, Souda P, Whitelegge J, Capaldi RA (2007) The mitochondrial inner membrane protein Mitofilin exists as a complex with SAM50, metaxins 1 and 2, coiled-coil-helix coiled-coil-helix domain-containing protein 3 and 6 and DnaJC11. *FEBS Lett* **581**: 3545–3549. https://doi.org/10.1016/j.febslet.2007.06.052

Yamano K, Tanaka-Yamano S, Endo T (2010) Mdm10 as a dynamic constituent of the TOB/SAM complex directs coordinated assembly of Tom40. *EMBO Rep* **11**: 187–193. https://doi.org/10.1038/embor.2009.283

Yang RF, Zhao GW, Liang ST, Zhang Y, Sun LH, Chen HZ, Liu DP (2012) Mitofilin regulates cytochrome c release during apoptosis by controlling mitochondrial cristae remodeling. *Biochem Biophys Res Commun* **428**: 93–98. https://doi.org/10.1016/j.bbrc.2012.10.012

genes

MDPI

Article

Mitochondrial Processes during Early Development of *Dictyostelium discoideum*: From Bioenergetic to Proteomic Studies

Monika Mazur [1], Daria Wojciechowska [1,2], Ewa Sitkiewicz [3], Agata Malinowska [3], Bianka Świderska [3], Hanna Kmita [1] and Małgorzata Wojtkowska [1,*]

1 Institute of Molecular Biology and Biotechnology, Faculty of Biology, Adam Mickiewicz University, 61-614 Poznan, Poland; monika.antoniewicz@gmail.com (M.M.); grobys.d@amu.edu.pl (D.W.); kmita@amu.edu.pl (H.K.)
2 Department of Macromolecular Physics, Faculty of Physics, Adam Mickiewicz University, 61-614 Poznan, Poland
3 Institute of Biochemistry and Biophysics Polish Academy of Sciences, 02-106 Warszawa, Poland; ewa@ibb.waw.pl (E.S.); esme@ibb.waw.pl (A.M.); bianka.swiderska@gmail.com (B.Ś.)
* Correspondence: malgorzata.wojtkowska@amu.edu.pl; Tel.: +48-61929-59-02

Abstract: The slime mold *Dictyostelium discoideum's* life cycle includes different unicellular and multicellular stages that provide a convenient model for research concerning intracellular and intercellular mechanisms influencing mitochondria's structure and function. We aim to determine the differences between the mitochondria isolated from the slime mold regarding its early developmental stages induced by starvation, namely the unicellular (U), aggregation (A) and streams (S) stages, at the bioenergetic and proteome levels. We measured the oxygen consumption of intact cells using the Clarke electrode and observed a distinct decrease in mitochondrial coupling capacity for stage S cells and a decrease in mitochondrial coupling efficiency for stage A and S cells. We also found changes in spare respiratory capacity. We performed a wide comparative proteomic study. During the transition from the unicellular stage to the multicellular stage, important proteomic differences occurred in stages A and S relating to the proteins of the main mitochondrial functional groups, showing characteristic tendencies that could be associated with their ongoing adaptation to starvation following cell reprogramming during the switch to gluconeogenesis. We suggest that the main mitochondrial processes are downregulated during the early developmental stages, although this needs to be verified by extending analogous studies to the next slime mold life cycle stages.

Keywords: mitochondrial proteins; mass spectrometry; *Dictyostelium discoideum*; starvation; coupling efficiency; coupling capacity; spare respiratory capacity; qualitative and quantitative comparative studies

Citation: Mazur, M.; Wojciechowska, D.; Sitkiewicz, E.; Malinowska, A.; Świderska, B.; Kmita, H.; Wojtkowska, M. Mitochondrial Processes during Early Development of *Dictyostelium discoideum*: From Bioenergetic to Proteomic Studies. *Genes* **2021**, *12*, 638. https://doi.org/10.3390/genes12050638

Academic Editor: Chandrasekhar Natarajan

Received: 1 April 2021
Accepted: 20 April 2021
Published: 25 April 2021

1. Introduction

The unicellular slime mold *Dictyostelium discoideum*, one of the 150 species of *Dictyostelia* belonging to the Amoebozoa eukaryotic supergroup, displays the multicellularity form, namely aggregative or sorocarp multicellularity [1,2]. Due to starvation, the slime mold aggregates, which results in an intermediate migrating 'slug' stage and cells specializing into spores as well as three somatic cell types forming a stalk and structures to support the stalk and spore mass (Figure 1). This process is mainly based on chemical signals settled on cAMP and cAMP-dependent kinase (PkaC) [3], which induces the expression of the genes responsible for aggregation such as the receptor of cAMP (CarA), adenylate cyclase (AcaA), and cAMP phosphodiesterase (PdsA) [2,4]. cAMP pulses are initially secreted by a few starving cells, then cells move chemotactically toward the local cAMP and collect into molds, following which they form a slug and, finally, the fruiting body [5]. In addition, cAMP pulses upregulate the genes that are required during and after aggregation as tgrB and tgrC. These genes are responsible for cell adhesion and are known as the marker genes of post-aggregative cell differentiation [6].

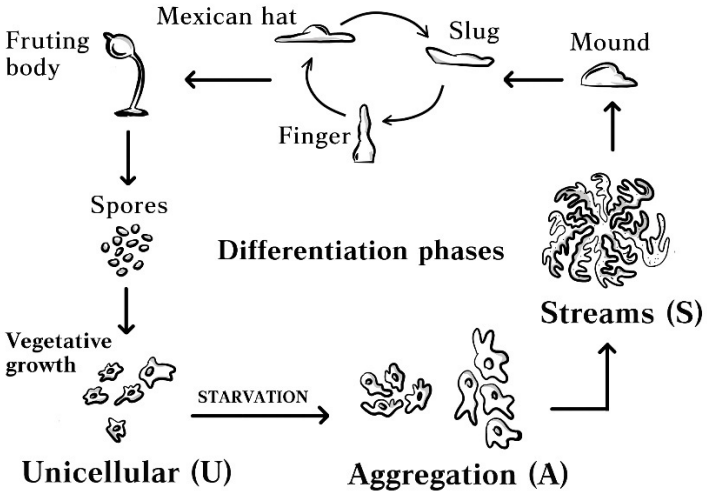

Figure 1. The life cycle of *D. discoideum.* The studied stages were marked by bold letters.

D. discoideum cells, during the early steps of aggregation when unicellular cells start to move and form waves, are referred to as early developmental stages induced by starvation (Figure 1) [1]. These early developmental stages have been studied previously [7,8]. Accordingly, transcriptomic and cell proteomic data on mutant strains lacking genes that are crucial for cell aggregation are available [7]. The data revealed the downregulation of mitochondria proteins of the Krebs cycle and oxidative phosphorylation (OXPHOS). Another application of comparative MitoProteome studies for mitochondria isolated from different developmental stages including the early ones, is the general downregulation of crucial mitochondrial proteins and the upregulation of alternative oxidation (AOX) [8] during the early stages. The results of these studies were related to the mitochondrial energy status that was detected in vivo with a MitoTracker. However, these studies were not functionally based, which could have provided more precise answers to the question regarding mitochondrial functionality during starvation-induced aggregation.

Undoubtedly, *D. discoideum* is a popular model organism for studying cellular processes such as cell signaling, cell differentiation, and morphogenesis [9], the evolution of sociality and prey–predator relationships [3]. Due to the wide range of human orthologue genes, slime mold can be used to study human diseases, particularly neurodegeneration [10]. Moreover, *D. discoideum* is also a perfect model for research concerning intracellular and intercellular mechanisms such as early and late aggregation from unicellularity to multicellularity, in which mitochondria seem to have a crucial function [4].

It has been shown that cell differentiation is under the control of the nutrient glucose [11–13]. In our study, we performed an estimation of mitochondria's functional state in intact cells representing the unicellular (U), aggregation (A), and streams (S) stages and combined the data with comparative proteomic analysis. The obtained results indicate that the observed differences among the studied stages may be associated with ongoing adaptation to starvation following the cell reprogramming that is supported by the metabolic background of starving cells. To our knowledge, this is the first report presenting combined *D. discoideum* mitochondrial proteomics and bioenergetic studies.

2. Methods

2.1. Cell Culture and Mitochondria Isolation

D. discoideum AX2 cell cultures were performed according to [14]. For the measurement of oxygen uptake using the Clarke electrode (Section 2.3), cells were cultured exponentially until they reached a density of 2.0–3.0 $\times$ 10^6 cells/mL (the doubling time of 10–11 h) in an axenic growth medium (1% *w/v* protease peptone, 0.5% *w/v* yeast extract, 0.45% *w/v* D-glucose, 0.09% *w/v* Na_2HPO_4, and 0.23% *w/v* KH_2PO_4). Cells were then cultured in 100 mL at 19 °C using a Certomat MO rotary shaker at 90 rpm. The cells of stage U

were transferred to sterile 24-well plates at 1 million cells per well and left for 1 h for cell adhesion. Cells at stages A and S were obtained by washing the cell culture twice in the developmental buffer (DB) starvation medium containing 5 mM of Na_2HPO_4, 5 mM of KH_2PO_4, 1 mM of $CaCl_2$, and 2 mM of $MgCl_2$, with a pH of 6.5 [15]. The cells were then transferred to the sterile 24-well plates for 23 h for the A stage and 25 h for the S stage cells. The presence of the U, A, and S stages was confirmed by using a Nikon Eclipse TE 2000-U microscope. For mitochondria isolation, cell cultures (850 mL)at a given stage were centrifuged at 600× *g* for 5 min and then washed twice in phosphate medium A (14.5 mM KH_2PO_4, 5 mM Na_2HPO_4, pH 6) by centrifugation at 600× *g* for 5 min. Next, the cells were homogenized in medium B (0.38 M sucrose, 20 mM Tris-Cl, 0.5 mM EDTA, 1% defatted bovine serum albumin [BSA], pH 7.5) using a glass/teflon homogenizer and centrifuged at 860× *g* for 5 min. After this step, the supernatant was centrifuged at 10,000× *g* for 15 min and the obtained pellet was suspended in medium C (0.38 M sucrose, 20 mM TrisCl, 0.5 mM EDTA, 0.6% defatted BSA, pH 7.2), and centrifuged at 860× *g* for 5 min to remove debris. The supernatant was centrifuged at 10,000× *g* for 10 min, the mitochondrial pellet was suspended in medium D (0.38 M sucrose; 20 mM, Tris-Cl, pH 7.2), and centrifuged at 10,000× *g* for 15 min. The mitochondrial pellet was suspended in medium D and used for further analysis. All centrifugation procedures were carried out at 4 °C and media used for mitochondria isolation were ice cold. The calculated mean values of the yield of mitochondria for 1 g of cells were 5 mg, 1.4 mg, and 1.7 mg for stage U, A, and S, respectively.

2.2. The Measurements of Cell Respiration and the Status of Mitochondrial Coupling in Intact D. discoideum Cells

To measure the oxygen consumption rates of *D. discoideum*, cells from the U, A, and S stages collected from the 24-well plates were centrifuged (11,000× *g*, 3 min) and resuspended in the DB containing 5 mM of Na_2HPO_4, 5 mM of KH_2PO_4, 1 mM of $CaCl_2$, and 2 mM of $MgCl_2$ at a pH of 6.5 [15]. The rate of the cells' oxygen uptake (2×10^6) was measured in 0.5 mL of the DB in a water-thermostated incubation chamber with a computer-controlled Clark-type O_2 electrode at 18 °C (Oxygraph, Hansatech, UK). To estimate the functional states of the mitochondria at the studied stages, mitochondrial coupling capacity and mitochondrial coupling efficiency were calculated based on basal (actual) respiration, state 4 (the resting state), state 3 (the phosphorylating state), and maximal respiration. Basal cell respiration was measured in the DB with supplementation of pyruvate at a final concentration of 10 mM. State 4 was enforced through the addition of 0.5–1.5 µM of tributyltin (TBT), which is an inhibitor of mitochondrial ATP synthase, whereas maximal respiration was induced by using 0.1–0.24 µM of carbonyl cyanide-p-trifluoromethoxyphenylhydrazone, an uncoupler (FCCP). State 3 was calculated by subtracting state 4 from basal respiration. The contribution of state 3 to the basal respiration corresponded to mitochondrial coupling efficiency, while the mitochondrial coupling capacity that corresponded to FCCP uncoupling capacity was estimated as the maximal respiration to state 4 ratio. The TBT and FCCP concentrations were titrated for each stage [16–18]. To estimate the ability of the substrate supply and electron transport to respond to an increase in energy demand, mitochondrial spare respiratory capacity was estimated through the determination of the difference between maximal respiration and basal respiration [19].

2.3. Sample Preparation for Mass Spectrometry Analysis

Mass spectrometry experiments were performed at the Mass Spectrometry Laboratory at the Institute of Biochemistry and Biophysics, PAS. A total of 5 µg of isolated mitochondria was suspended in a dissolution buffer (8 M of urea, 2% CHAPS, 10 mM of HEPES, with a pH of 8.5). Samples were processed using the modified single-pot solid-phase-enhanced sample preparation (SP3) method [20]. The exact sample preparation protocol was as follows. Cysteines were reduced through 1 h of incubation with 20 mM of tris (2-carboxyethyl)phosphine (TCEP) at 37 °C, followed by 10 min of incubation at

room temperature with 50 mM of methyl methanethiosulfonate (MMTS). The magnetic bead mix was prepared by combining equal parts of Sera-Mag Carboxyl hydrophilic and hydrophobic particles (09-981-121 and 09-981-123, GE Healthcare Lifesciences, Upsala, Sweden). The bead mix was washed three times with MS-grade water and resuspended in a working concentration of 10 µg/µL. Furthermore, 8 µL of the prepared bead mix, along with 5 µL of 10% formic acid and 500 µL of acetonitrile, was added to each sample. The proteins that bound to the beads were washed with 75% ethanol, isopropanol, and acetonitrile, followed by overnight digestion with 1 µg of trypsin/Lys-C mix (Promega). After digestion, the peptides were washed with acetonitrile and eluted from the beads by subsequent incubation with MS-grade water and 2% DMSO, with sonication during each step. The pulled aliquots were dried in a SpeedVac and resuspended in 60 µL of 2% acetonitrile and 0.1% formic acid. Peptide concentrations were measured using the Pierce Quantitative Colorimetric Peptide assay (Thermo Scientific, Rockford, IL, USA).

2.4. Mass Spectrometry

Three µg of digested samples were analyzed using the LC–MS system comprising a high-performance liquid chromatography (UPLC) chromatograph (nanoAcquity, Waters) and a Q Exactive mass spectrometer (Thermo). Peptides were trapped on a C18 pre-column (180 µm × 20 mm, Waters) using a 0.1% water solution of FA as a mobile phase then transferred to a BEH C18 column (75 µm × 250 mm, 1.7 µm, Waters) using an ACN gradient (0–35% ACN in 160 min) in the presence of 0.1% FA at a flow rate of 250 nL/min. The spectrometer was working in a data-dependent mode. To prevent cross-contamination, blank runs were performed between the sample runs.

2.5. Data Analysis

The obtained data were pre-processed with Mascot Distiller software (Matrixscience), and protein identification was performed using Mascot Server 2.5 (Matrixscience) against the *D. discoideum* protein sequences (13921 sequences) deposited in the NCBInr database (20180903, 167148673 sequences; 60963227986 residues). The parameters were set as follows: enzyme—trypsin, missed cleavages—1, fixed modifications—methylthio (C), variable modifications—GlyGly (K), oxidation (M), and instrument—HCD. To reduce mass errors, peptide and fragment mass tolerance settings were established separately for each file after an off-line mass recalibration [21]. The assessment of confidence was based on the target/decoy database search strategy [22], which provided *q*-value estimates for each peptide spectrum match. All queries with a *q*-value of >0.01, subset proteins, and proteins identified with one peptide were discarded from further analysis. The mass recalibration, false discovery rate (FDR) computations, and data filtering were done with Mscan software that was developed in-house (MScan 2.0.3 (accessed on 26 June 2018)).

The lists of identified peptides were merged and overlaid onto 2-D heatmaps generated from the LC-MS spectra, and the volumes were obtained from the assigned peaks (a more detailed description of data extraction procedures can be found in [23]). Quantitative values were then exported into text files for statistical analysis with Diffprot [21] software. The calculated *p*-values were adjusted for multiple testing using a procedure that controlled for a FDR. Diffprot was run with the following parameters: the number of random peptide sets = 10^6, clustering of peptide sets—only when 90% were identical, normalization through LOWESS, and quantification based on unique peptides. Only proteins with a *q*-value below 0.05 or those present in only one of the two compared analytical groups were taken into consideration during further analysis. The tendency in comparative studies as down in A and up in S was calculated from the ratio values of comparative qualitative studies for phase to phase ratio quotient U/A and A/S (Table 1). The expression profile was calculated against the U state as a basal of expression level (1). The ratio value (>1) and (<1) was regarded as upregulated and downregulated, respectively. The phase to phase ratio quotient "[S/U]" was taken for the proteins isocitrate dehydrogenase (NAD+), cytochrome c oxidase subunit IV, and heat shock protein Hsp70 family protein. For other proteins, the

[S/U] was calculated from the equation [A/U]/[A/S], where [A/U] and [A/S] are given as the ratio in Section for "Phase to phase ratio quotient [A/U]" and Section for "Phase to phase ratio quotient [A/S]".

3. Results and Discussion

3.1. The Functional Status of Intact D. discoideum Cells' Mitochondria at the Early Developmental Stages

The respiratory state of mitochondria is a dynamic state resulting from crosstalk between the two bioenergetic states termed state 3 and state 4 [16,19]. State 4, also referred to as the proton-selective leak, is characterized by low oxygen uptake and higher inner membrane potential, while state 3, also referred to as the phosphorylating state due to resulting ADP phosphorylation to ATP, reflects high oxygen uptake and lower inner membrane potential. Maximal respiration is triggered in the presence of an uncoupler and represents the respiratory chain's ability to support additional energetic demands [16,19]. All of the states are crucial for the estimation and comparison of the functional status of different intact cells' mitochondria, as they allow for the calculation of the following parameters: mitochondrial coupling efficiency, mitochondrial coupling capacity, and mitochondrial spare respiratory capacity, as described in the Methods (Section 2.2). The parameter calculation allows for the comparison of cells containing different amounts of mitochondria, which was observed herein (Methods, Section 2.5) and has already been reported for cell in stages U, A, and S [8]. The representative traces registered for cells in stages U, A, and S are presented in the Figure 2A whereas raw data used for the calculation of all bioenergetic parameters are presented in Supplementary file S1. As shown in Figure 2B, intact *D. discoideum* cells in stages U, A, and S displayed the same rate of state 4 respiration (i.e., the proton leak), but differed in their basal, state 3, and maximal respiration rates. The values of the parameters were higher for cells in the U stage than for cells in the A and S stages, while the cells in stages A and S did not differ in the values of their parameters, except for maximal respiration, which was lower for cells in the S stage. However, according to the yield of mitochondria isolation, it could be assumed that cells in stages A and S contained the comparable mitochondria mass that was lower than in cells in the U stage.

Table 1. Results of the comparative mitoproteomes of the U (unicellular), A (aggregation), and S (streams) stages. *D. discoideum* stages regarding the distinguished functional groups: A/U, S/U, and A/S.

RefSeq Database	Protein Name	Phase to Phase Ratio Quotient A/U				Phase to Phase Ratio Quotient S/U				Phase to Phase Ratio Quotient A/S			
		q Value	Ratio	Fold Change	Peptides	*q* Value	Ratio	Fold Change	Peptides	*q* Value	Ratio	Fold Change	Peptides
	Krebs												
XP_643860.1	citrate synthase, mitochondrial	0.00073	0.56	1.78	46					0.00023	0.63	1.6	45
XP_628920.1	isocitrate dehydrogenase (NAD+) (IdhB)	0.04842	0.66	1.52	25	0.01253	0.61	1.64	25				
XP_636263.1	succinate-CoA ligase (scsA)	0.00858	0.48	2.1	16					0.00599	0.42	2.37	16
XP_629516.1	malate dehydrogenase (mdhB)	0.00027	0.58	1.71	45					0.00006	0.58	1.73	45
	-												
XP_636911.1	3-oxoacid CoA-transferase	0.00569	0.55	1.82	29					0.04059	0.58	1.73	29
XP_645396.1	phosphoenolpyruvate carboxykinase (PCK2)	0.04045	0.54	1.86	30					0.00055	0.41	2.43	32
	OXPHOS												
XP_640649.1	cytochrome c oxidase subunit IV					0.03247	0.49	2.06	19				
	Protein biosynthesis												
XP_643155.1	heat shock protein Hsp70 family protein	0.00015	3.76	3.76	32	0.00007	3.47	3.47	33				
XP_637813.1	acetylglutamate kinase	0.00886	0.61	1.65	37					0.00061	0.54	1.86	37
XP_638096.1	branched-chain amino acid aminotransferase	0.00015	0.45	2.21	22					0.01041	0.57	1.75	21
XP_647552.1	4-aminobutyrate transaminase	0.00512	0.58	1.73	43					0.00368	0.57	1.74	43
	Protein import												
XP_629204.1	Stress-70 protein, mitochondrial (mtHsp70)	0.0004	0.6	1.67	62					0.00006	0.53	1.88	62
XP_645160.1	mitochondrial substrate carrier family protein Q	0.00739	3.11	3.11	10					0.00191	2.25	2.25	10
	Other known processes												
	FA metabolism												
XP_645587.1	acetyl-CoA C-acetyltransferase	0.00015	0.42	2.41	37					0.00549	0.61	1.65	35
XP_643323.1	acyl-CoA oxidase A	0.01325	2.16	2.16	25					0.00006	5.54	5.54	25
XP_635485.1	electron transfer flavoprotein alpha subunit	0.01932	0.51	1.97	24					0.00615	0.42	2.36	23
XP_642058.1	electron transfer flavoprotein beta subunit	0.03524	0.6	1.65	21					0.022	0.54	1.86	21
	Redox												
XP_645815.1	superoxide dismutase/SOD	0.01603	0.46	2.18	10					0.00404	0.4	2.52	12
	Uncharacterized proteins												
XP_639996.1	putative mitochondrial transferase caf17	0.00542	0.41	2.41	24					0.00006	0.28	3.59	24
XP_639145.1	putative delta-1-pyrroline-5-carboxylate dehydrogenase	0.04023	0.63	1.59	38					0.00006	0.49	2.04	37

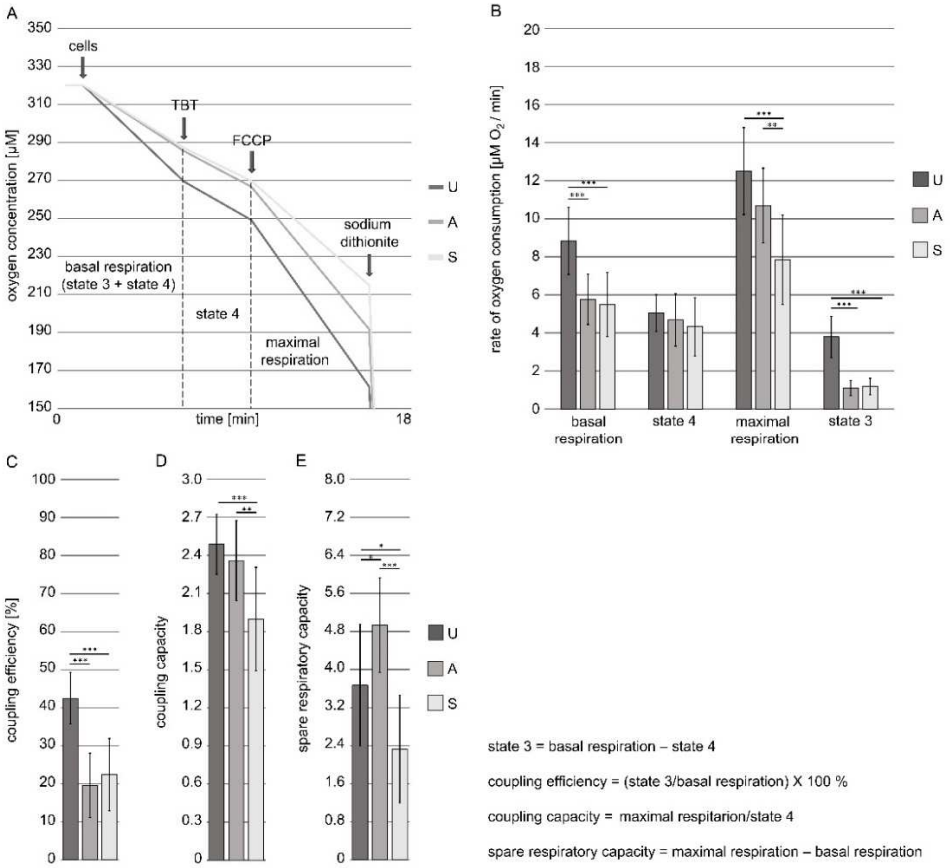

Figure 2. The functional state of mitochondria in intact *D. discoideum* cells in the studied stages. (**A**) Representative traces for cells in studied stages applied for calculations as well as explanation of the calculated parameters; (**B**) oxygen consumption rates under the applied oxygen uptake rate measurement condition; (**C**) coupling efficiency (contribution of state 3 to basal respiration); (**D**) coupling capacity (maximal respiration to state 4 ratio); (**E**) spare respiratory capacity (the difference between maximal respiration and basal respiration). The rate of oxygen uptake by cells (2×10^6) was measured in 0.5 mL of DB in a water-thermostated incubation chamber with a computer-controlled Clark-type O_2 electrode at 18 °C (Oxygraph, Hansatech, UK). Tributyltin (TBT) was added in a concentration (0.5–1.5 µM) to enforce state 4. The maximal respiration was induced by using 0.1–0.24 µM of carbonyl cyanidep-trifluoromethoxyphenylhydrazone (FCCP); sodium dithionite is a zero oxygen solution powder used for calibration of oxygen sensors at zero oxygen. The data are presented as mean values ± SD of three independent experiments. * $p < 0.05$; ** $p < 0.005$, *** $p < 0.001$. Calculated original data are presented in Supplementary file S1.

Basal respiration is usually strongly controlled by ATP turnover; hence, it alters in response to ATP demand [19]. The observed differences in basal respiration rates co-occurred with a decrease in the rate of state 3, suggesting that the cells in stages A and S displayed a lower demand for ATP (Figure 2B). Accordingly, mitochondrial coupling efficiency corresponding to state 3 respiration contribution to basal respiration decreased to the same level for the cells in stages A and S when compared to the cells in stage U (Figure 2C). Thus, the cells in stages A and S displayed lower levels of ATP synthesis than those in stage U. However, the cells in stages A and S differed in the uncoupling capacity of FCCP (Figure 2B), which resulted in differences in mitochondrial coupling capacity (Figure 2D), defined as the ratio of maximal respiration to state 4 respiration. The value of the parameter is sensitive to changes in substrate oxidation and proton leakage [19]. Accordingly, FCCP-imposed uncoupling should reflect the maximum activity of electron transport and substrate oxidation, which are achievable by cells under the given conditions. Therefore, we compared the mitochondrial spare respiratory capacity of the studied cells. The param-

eter corresponds to the difference between maximal respiration and basal respiration and reflects how close to its bioenergetic limit a cell is operating [19]. One of the known factors that influence the extent of mitochondrial spare respiratory capacity is substrate availability, which is based on substrate entry into the Krebs cycle that is synchronized with the electron transport of the respiratory chain. As shown in Figure 2E, the cells in stage S displayed a distinct decrease in mitochondrial spare respiratory capacity when compared to the cells in stages U and A, but the value of the parameter increased for the cells in stage A when compared to the cells in stage U. Interestingly, it has been shown that mitochondrial spare respiratory capacity increases in starvation-resistant cells [24], which may permit rapid adaptation to metabolic changes [25]. On the other hand, cell reprogramming may correlate with a decrease in mitochondrial spare respiratory capacity [26], which could explain the distinct decrease in the parameter value of the cells in stage S [27]. Overall, the analysis of bioenergetic parameters indicated decreased ATP synthesis during stages A and S, which co-occurred in the case of the latter, with the limited access of substrates to the respiratory chain. These changes may be associated with an ongoing adaptation to starvation, followed by cell reprogramming. Therefore, we decided to study the changes in mitochondrial proteome differences among the cells in stages U, A, and S.

3.2. Quantitative Comparative Analysis of the Mitochondrial Proteomes of the Early Developmental Stages

In mitochondria isolated from the cells in stages U, A, and S, and due to the mass spectrometry analysis, we detected 294 proteins overall (Supplementary file S2 and segregated them into nine functional groups of proteins: protein synthesis and degradation, signaling, protein import, substrate transport, mitochondrial gene expression, the Krebs cycle, OXPHOS, other known processes (fatty acid metabolism, redox), and uncharacterized proteins (Figure 3).

The numbers of proteins assigned to the mentioned functional groups were comparable for the studied mitochondria. As presented in Figure 3, the most abundant groups were protein biosynthesis and degradation, OXPHOS, and other known processes. The less-abundant groups were transport, protein import, the Krebs cycle, and uncharacterized proteins. The least-numerous groups of proteins were the signaling and gene expression functional groups. Thus, the mitochondrial proteomes obtained for the studied early developmental stages were comparable. Therefore, we decided to perform a qualitative comparative analysis of the obtained mitochondrial proteome data.

3.3. Qualitative Comparative Analysis of the Mitochondrial Proteomes of the Early Developmental Stages

Comparative qualitative analyses of the detected proteins were performed for the following pairs of stages: A/U, S/U, and A/S regarding the previously described functional groups of proteins. Analyses were done according to the procedure described in the Methods section (Sections 2.3–2.5).

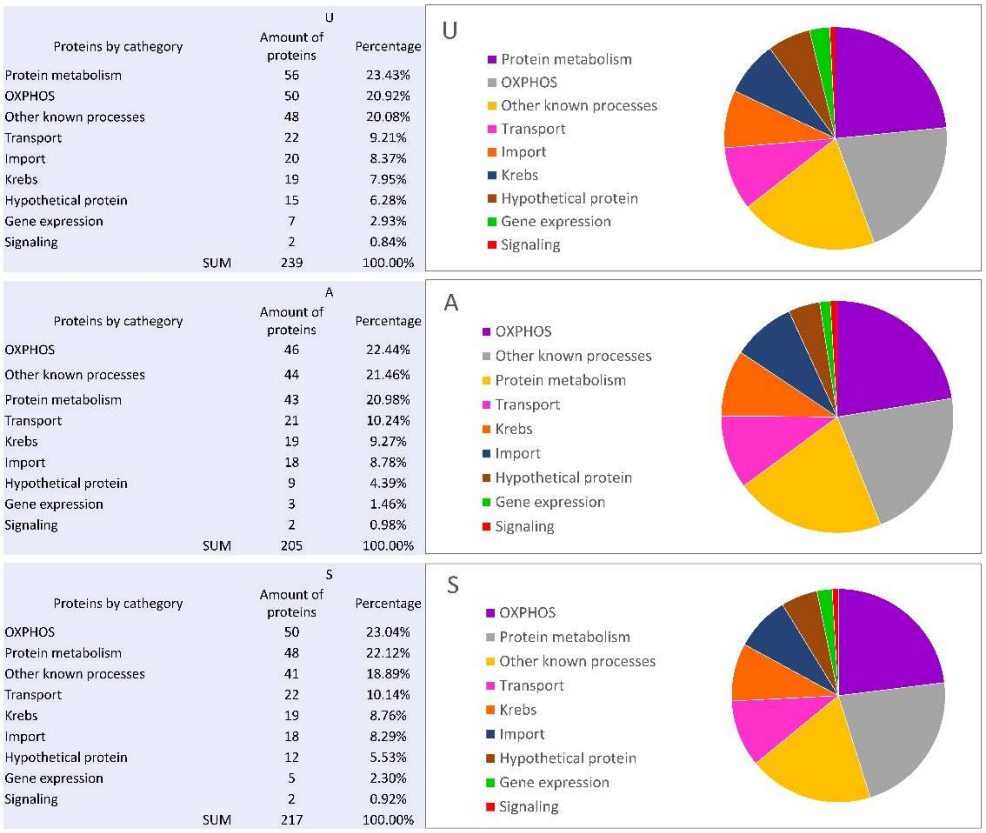

U			
Proteins by cathegory		Amount of proteins	Percentage
Protein metabolism		56	23.43%
OXPHOS		50	20.92%
Other known processes		48	20.08%
Transport		22	9.21%
Import		20	8.37%
Krebs		19	7.95%
Hypothetical protein		15	6.28%
Gene expression		7	2.93%
Signaling		2	0.84%
	SUM	239	100.00%

A			
Proteins by cathegory		Amount of proteins	Percentage
OXPHOS		46	22.44%
Other known processes		44	21.46%
Protein metabolism		43	20.98%
Transport		21	10.24%
Krebs		19	9.27%
Import		18	8.78%
Hypothetical protein		9	4.39%
Gene expression		3	1.46%
Signaling		2	0.98%
	SUM	205	100.00%

S			
Proteins by cathegory		Amount of proteins	Percentage
OXPHOS		50	23.04%
Protein metabolism		48	22.12%
Other known processes		41	18.89%
Transport		22	10.14%
Krebs		19	8.76%
Import		18	8.29%
Hypothetical protein		12	5.53%
Gene expression		5	2.30%
Signaling		2	0.92%
	SUM	217	100.00%

Figure 3. The numbers of *D. discoideum* mitochondrial proteins assigned to the nine functional groups. The classification of identified proteins was performed at the base of the dictybase.org and proteins belonging to the same functional groups were counted in order to assess the size of the classes for details (see Methods Section 2.5 and Supplementary file S2).

3.3.1. The Krebs Cycle and OXPHOS

The Krebs cycle and OXPHOS are well-known, crucial mitochondrial processes of energy transformation. The comparative analysis revealed the presence of four proteins of the Krebs cycle (citrate synthase (XP_643860.1), isocitrate dehydrogenase (NAD^+) (XP_628920.1), succinate-CoA ligase (XP_636263.1), and malate dehydrogenase (XP_629516.1) and two proteins functionally linked to this cycle (3-oxoacid CoA-transferase and phosphoenolpyruvate carboxykinase) (XP_636911.1) (Table 1). We observed decreased levels in the majority of the mentioned proteins in stage A and increased levels in stage S, termed the 'down in A and up in S tendency' (Table 1), which often resulted in down- or upregulation in stage S when compared to stage U (Figure 4A,B).

As shown in Figure 4A, when the detected Krebs cycle proteins were compared between stages S and U, succinate-CoA ligase was upregulated, citrate synthase and isocitrate dehydrogenase (NAD^+) were downregulated and malate dehydrogenase returned to stage U level, which denoted no change in its expression profile. The mitochondrial malate dehydrogenase catalyzed the reaction of the malate-to-oxaloacetate conversion with the use of NAD^+ reduction to NADH [28,29]. It has been shown that enzyme activity is inhibited by differentiation-inducing-factor 1 (DIF-1), which affects cell energy transformation and leads to the inhibition of cell proliferation. These data suggest that the described inhibition of malate dehydrogenase by DIF-1 could be one of the mechanisms that induce the anti-proliferative effects that remain in agreement with the differentiation processes that start to occur at stage A. However, the steady state of its expression profile seemed not to influence the Krebs cycle.

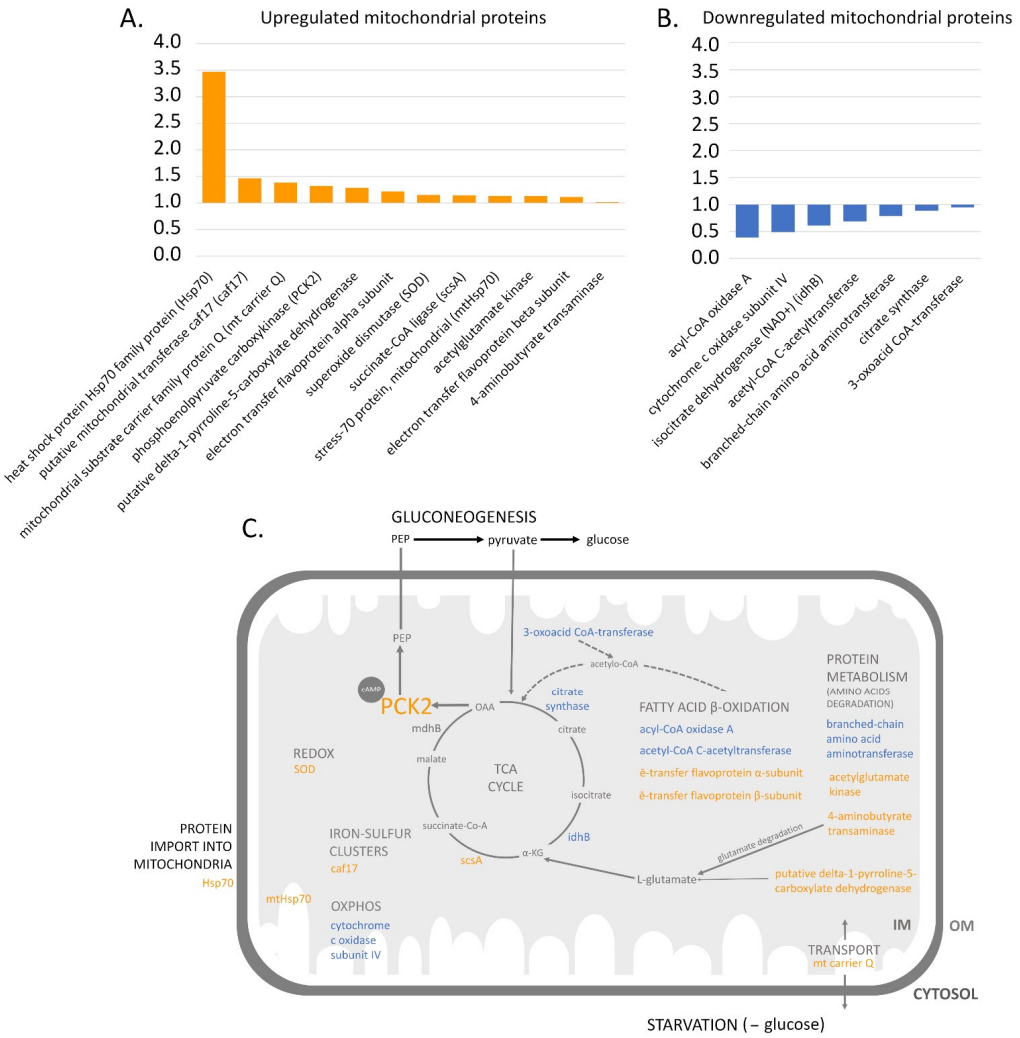

Figure 4. The mitochondrial proteins upregulated and downregulated in stage S when compared to stage U during *D. discoideum* starvation. (**A**) Upregulated mitochondrial proteins; (**B**) downregulated mitochondrial proteins. The protein upregulation and downregulation were estimated using qualitative comparative analysis between stages U and S (see Methods Section 2.5). (**C**) Diagram of downregulated (blue) and upregulated (orange) mitochondrial proteins assigned to cellular processes. The cell metabolic adaptation under glucose depletion includes attenuation of the Krebs cycle, fatty acid β oxidation, and oxidative phosphorylation, and enhancement of the amino acids' metabolism, being known as a fuel for gluconeogenesis. The early steps of gluconeogenesis is regulated by mitochondrial phosphoenolpyruvate carboxykinase (PCK2), which allows for alternative glucose/biosynthesis intermediates required for cell aggregation. TCA (tricarboxylic acid cycle, Krebs cycle); PEP (phosphoenolopyruvate); SOD (superoxide dismutase); caf17 (putative mitochondrial transferase); scsA (succinate-CoA ligase); mdhB (mitochondrial malate dehydrogenase); idhB (isocitrate dehydrogenase (NAD+)); α-KG (α-ketoglutarate); OM (mitochondrial outer membrane); IM (mitochondrial inner membrane).

The tendency of 'down in A and up in S' was also observed for the two enzymes functionally linked to the Krebs cycle. The cycle 3-oxoacid CoA-transferase was finally downregulated in stage S when compared to stage U (Figure 4B). Interestingly, the product of the human 3-oxoacid CoA-transferase (OXCT1) was converted to acetyl-CoA and finally fed into the Krebs cycle [30]. Mitochondrial phosphoenolpyruvate carboxykinase (PCK2) (XP_645396.1) [31] is a gluconeogenesis enzyme that catalyzes the phosphorylation reaction of oxaloacetate. PCK2 was the enzyme that was finally upregulated in stage S when compared to stage U (Figure 4A). We assumed that starving *D. discoideum* cells in stages A and S caused glucose deficiency that could trigger gluconeogenesis [32]. Interestingly, in our study, we observed an increase in phosphoenolpyruvate carboxykinase (PCK2) in stage S. The decrease in Krebs-cycle enzyme expression in stage A may coincide with enhanced

gluconeogenesis, which is used to produce glucose during starvation. Unexpectedly, in our comparative analysis, we did not observe a significant change in proteins in the OXPHOS functional group, except for the cytochrome c-oxidase, which was downregulated (Figure 4C).

Our obtained data coincided with the low state 3 contributions to basal respiration in stages A and S, reflecting decreased OXPHOS, decreased spare respiratory capacity in stage S, and possibly enhanced gluconeogenesis. Nevertheless, the obtained data did not reveal an upregulation of any glycolytic enzymes that could have explained the aerobic glycolysis that is regarded as typical for proliferative cells, similar to cancer [33]. This is because the study was focused on mitochondrial proteins. However, glycolytic enzymes could interact with mitochondria, as glycolysis occurs in the cytosol.

The data indicating the downregulation of the Krebs cycle enzymes coincide with the results that were obtained in [7,8]. We concluded that the main function of the mitochondria in the early developmental stages emerged temporarily, rewriting the mitochondrial metabolism from the Krebs cycle into gluconeogenesis. We showed, for the first time, the presence of PCK2 upregulation during *D. discoideum* starvation. The regulation of PCK2 at the level of the transcription of the encoding gene is under the positive control of cAMP and is crucial for cell aggregation. Indeed, the deficiency of glucose during starvation activates adenylate cyclase, which actives CREB and, finally, PCK2. This could take place when phosphoenolpyruvate (PEP) cannot be converted into pyruvate, which is used in the gluconeogenesis pathway (Figure 4C) [31].

3.3.2. Protein Metabolism

In the case of the protein biosynthesis and degradation group, the obtained data revealed three enzymes that were responsible for the metabolism of mitochondrial amino acids (Table 1). The general tendency concerning their expression level remained 'down in A and up in S' and was observed for acetyl glutamate kinase (XP_637813.1), 4-aminobutyrate transaminase (XP_647552.1) (Figure 4A), and branched-chain amino acid aminotransferase (XP_638096.1). The latter did not return to the level of stage U, so the enzyme was classified as downregulated in stage S when compared to stage U (Figure 4B). Acetyl glutamate kinase is a NAD^+ binding enzyme engaged in arginine biosynthesis [28]. In *D. discoideum*, the ArgC enzyme is similar to the bifunctional acetyl glutamate kinase and N-acetyl-γ-glutamyl-phosphate reductase from yeast, which catalyze the second and third steps in the biosynthesis of the arginine precursor ornithine. The detection of this protein revealed the known connection between the urea and Krebs cycles. However, we did not observe any changes in protein expression in the case of the urea cycle. The 4-aminobutyrate transaminase catalyzed the conversion of 4-aminobutanoate and 2-oxoglutarate into succinate semialdehyde and L-glutamate [33]. This process is dedicated to glutamate degradation and is also correlated with the urea and Krebs cycles. The expression profile of these proteins included downregulation in A and an increase in S, resulting in upregulation (Figure 4A). In the case of the branched-chain amino acid aminotransferase, another example of aminotransferase, the transamination of branch-amino acids as leucine, isoleucine, and valine as well as their respective alfa-ketoacids, was reported [28]. For this protein, an opposite decreasing tendency was observed, so we classified the protein as downregulated in stage S compared to stage U (Figure 4B). We speculate that the amino acids' biosynthesis protein expression profile revealed the metabolic flexibility of *D. discoideum* cells determined by their ability to reprogram anabolic and catabolic pathways, presumably through altering gene expression programs and intercellular interactions within the glucose-free microenvironment during starvation [34]. This reprogramming could be based on the temporary shift from the Krebs cycle to gluconeogenesis, with amino acids as the fuel for gluconeogenesis (Figure 4C).

The comparative study on the discussed groups of proteins also revealed that the presence of cytosolic chaperone Hsp70 (XP_643155.1) significantly increased in stage A when compared to stage U and slightly decreased in stage S when compared to stage U

(Figure 4A). Hsp70 is a chaperone that plays a crucial role in protein folding, disaggregation, and degradation [35]. It was also shown that ribosomes stay in close proximity to mitochondria [36], which implies their co-translational import into mitochondria [37]. Therefore, the presence of the mentioned chaperone could ensure sufficient protein refolding, which is essential for the successful import of protein into mitochondria.

To summarize, the detected changes in the expression levels of the functional protein group suggest that at the early developmental stages, the processes of mitochondrial amino acid metabolism are upregulated, which we showed here for the first time.

3.3.3. The Import of Proteins into Mitochondria and the Transport of Other Molecules

Most mitochondrial proteins are synthesized in the cytosol and have to be delivered to the various mitochondrial sub-locations. This process is regulated by the presence and activity of import apparatus consisting of proteins that, in general, recognize and translocate proteins across mitochondrial membranes (for details, see [37]). In this comparative study, we detected mtHsp70 (XP_629204.1) [38], which showed the 'down in A and up in S' expression profile tendency. We estimated that mtHsp70 was upregulated in stage S when compared to stage U (Figure 4A). This mitochondrial chaperone is responsible for the protein assembly of proteins delivered into the mitochondrial matrix and acts as a subunit of the PAM import machinery that is crucial for the proper unidirectional transfer of precursor proteins across the inner mitochondrial membrane. It seems that this process could be upregulated in stage S. The elevated level of cytosolic Hsp70 could be arranged in the same processes as those involved when the chaperone assists in the partial refolding of precursor proteins for import across the protein channel [8]. Moreover, mtHp70 is a chaperone that plays an important role in iron–sulfur cluster (IS) biogenesis [39]. Studies on yeast and human ISC involve gene mutations to show genome instability and the induction of the DNA damage repair pathway [40]. This, in turn, indicates that pathways related to ISC biosynthesis are strongly conserved—more so than for ATP production, for example—among diverse mitochondrial homologues [41]. This also explains ISC's presence (as only one common module to mitochondria) in mitosomes. This suggests that the essential process of ISC biosynthesis occurs in stage S.

In the case of the functional transport protein group, we detected an uncharacterized mitochondria substrate carrier protein named mt carrier Q (XP_645160.1). Its level significantly increased in stage A when compared to stage U and decreased in stage S when compared to stage U, although its level was higher when in stage U (Figure 4A). We conclude that the organization of the mitochondrial import machineries do not undergo major changes during the early developmental stages. We identified a new, uncharacterized transport protein, which was significantly upregulated in stage S (Figure 4A) and is worth further study to discern its exact function in the process of aggregation.

3.3.4. Other Known Processes

The functional group, termed 'other known processes', included enzymes engaged in fatty acid metabolism and redox processes. The oxidation of fatty acids may provide another source for biosynthetic growth under glucose limitation during *D. discoideum* starvation [42]. Our comparative study provided four enzymes of the fatty acid metabolism acetyl-CoA C-acetyltransferase (XP_645587.1), which showed the 'down in A and up in S' tendency, but its level in stage S was lower than in stage U, denoting a final downregulation (Table 1 and Figure 4B). The 'down in A and up in S' tendency was also observed for the electron transfer of flavoprotein α and β subunits (XP_635485.1 and XP_642058.1). However, the comparison of the proteins' levels between stages U and S indicate their upregulation (Figure 4A). Interestingly, acyl-CoA oxidase A (XP_643323.1) engaged in β-oxidation that was elevated in stage A when compared to stage U and strongly decreased in stage S when compared to stage U (Figure 4B). This profile was distinctly different from that observed for the previous groups of proteins. Therefore, we can assume the diminution of β-oxidation.

During β-oxidation, acetyl-CoA is produced, then enters the Krebs cycle and consequently stimulates ATP synthesis. However, during starvation, acetyl-CoA could activate the first enzyme of gluconeogenesis—the pyruvate carboxykinase that converts pyruvate into oxaloacetate. As shown, the detected β-oxidation proteins were mostly downregulated in stage S when compared to stage U. Therefore, *D. discoideum* cells probably do not use acetyl-CoA during starvation to stimulate gluconeogenesis (the first enzyme of this pathway). Consequently, glycerol is not used as a carbon source for *D. discoideum's* gluconeogenesis. Thus, as described, during starvation, gluconeogenesis may start due to PCK2, which has been proven to upregulate in stage S when compared to stage U and uses amino acids as fuel. Thus, amino acids are metabolized into the oxaloacetate, then converted into PEP by mitochondrial PCK2 (Figure 4C) [43].

Within the described group of other known processes, proteins engaged in the redox reaction were also enclosed. For this group, we detected mitochondrial superoxidase dismutase (SOD2) (XP_645815.1). SOD2 followed the 'down in A and up in S' pattern. It was finally upregulated in stage S when compared to stage U, which coincides with the available data [8]. This upregulation was not very significant (Figure 4A) but remained in agreement with the data concerning the role of ROSs as signaling molecules during aggregation, where SOD control signaling molecules are essential for proper development [44]. The ROS production could increase as a response of mitochondrial metabolism reprogramming. Thus, additional studies in this field are needed.

3.3.5. Uncharacterized Proteins

Two uncharacterized mitochondrial proteins were detected in the comparative analysis (Table 1). The putative mitochondrial transferase caf17 (XP_639996.1) and an uncharacterized protein (XP_639145.1), named in the *D.discoideum* database (dictybase) 'as putative delta-1-pyrroline-5-carboxylate dehydrogenase', were discovered. Both followed the 'down in A and up in S' tendency. The putative mitochondrial transferase caf17 was presumably involved in the incorporation of iron–sulfur clusters (ISC) into mitochondrial aconitase-type proteins. ISC was previously mentioned as being a common but crucial molecule present in mitochondria and related to organelles [45], which is thought to reflect its basic mitochondrial function. The 'putative delta-1-pyrroline-5-carboxylate dehydrogenase' is probably involved in synthesis of L-glutamate from L-proline, suggesting its function in the amino acid degradation process (Figure 4C). Both uncharacterized proteins were upregulated in stage S when compared to stage U (Figure 4A) and warrant a deeper investigation.

4. Conclusions

Our study on *D. discoideum* cells in early developmental stages revealed differences in their mitochondria functional state. The differences correspond to the comparative proteomic analysis results and may be associated with diminution of β oxidation, Krebs cycle, and oxidative phosphorylation, and enhancement of the metabolism of amino acids, being a known fuel for gluconeogenesis during starvation. This in turn may support metabolically ongoing adaptation to starvation and following cell reprogramming.

Supplementary Materials: The following are available online at https://www.mdpi.com/article/10.3390/genes12050638/s1, Supplementary file S1 show raw data obtained from oxygraphic measurements and Supplementary file S2 show proteins and peptides identified in LC-MS analysis.

Author Contributions: Conceptualization, M.W. and H.K.; Methodology, M.W., E.S. and M.M.; Software, E.S.; Validation, E.S., D.W., M.M. and A.M.; Formal analysis, M.W., D.W., E.S. and A.M.; Investigation, M.M., E.S., D.W. and B.Ś.; Resources, M.M.; Data curation, M.W., D.W. and M.M.; Writing—original draft preparation M.W. and H.K.; Writing—review and editing, M.W. and H.K.; Visualization, M.M., D.W., A.M. and E.S.; Supervision, H.K.; Project administration, M.W.; Funding acquisition, M.W., M.M. and H.K. All authors have read and agreed to the published version of the manuscript.

Funding: This project was supported by the National Science Center (Poland) project (grant no. 2012/05/N/NZ3/00293) and the "KNOW RNA Research Center in Poznan" (grant no. 01/KNOW2/2014). Special Support was provided by the Dean of Faculty of Biology UAM Poznań, P. Wojtaszek.

Institutional Review Board Statement: Not applicable.

Informed Consent Statement: Not applicable.

Data Availability Statement: LC-MS data are available on request at the Mass Spectrometry Laboratory IBB PAS.

Acknowledgments: Not applicable.

Conflicts of Interest: The authors declare no conflict of interest.

References

1. Schilde, C.; Schaap, P. The Amoebozoa. *Methods Mol. Biol.* **2013**, *983*, 1–15. [PubMed]
2. Kawabe, Y.; Du, Q.; Schilde, C.; Schaap, P. Evolution of multicellularity in Dictyostelia. *Int. J. Dev. Biol.* **2019**, *63*, 359–369. [CrossRef] [PubMed]
3. Du, Q.; Kawabe, Y.; Schilde, C.; Zhi-Hui, C.; Schaap, P. The evolution of aggregative multicellularity and cell-cell commu-nication in the Dictyostelia. *J. Mol. Biol.* **2015**, *427*, 3722–3733. [CrossRef] [PubMed]
4. Maeda, Y. Cell-cycle checkpoint for transition from cell division to differentiation. *Dev. Growth Differ.* **2011**, *53*, 463–481. [CrossRef]
5. Dormann, D.; Kim, J.Y.; Devreotes, P.N.; Weijer, C.J. cAMP receptor affinity controls wave dynamics, geometry and morphogenesis in *Dictyostelium*. *J. Cell Sci.* **2001**, *114*, 2513–2523.
6. Hirose, S.; Chen, G.; Kuspa, A.; Shaulsky, G. The polymorphic proteins TgrB1 and TgrC1 function as a ligand-receptor pair in *Dictyostelium allorecognition*. *J. Cell Sci.* **2017**, *130*, 4002–4012. [CrossRef]
7. González-Velasco, Ó.; De Las Rivas, J.; Lacal, J. Proteomic and transcriptomic profiling identifies early developmentally reg-ulated proteins in *Dictyostelium discoideum*. *Cells* **2019**, *8*, 1187. [CrossRef]
8. Czarna, M.; Mathy, G.; Mac'Cord, A.; Dobson, R.; Jarmuszkiewicz, W.; Sluse-Goffart, C.M.; Leprince, P.; De Pauw, E.; Sluse, F.E. Dynamics of the *Dictyostelium discoideum* mitochondrial proteome during vegetative growth, starvation and early stages of development. *Proteomics* **2009**, *10*, 6–22. [CrossRef]
9. Mathavarajah, S.; Flores, A.; Huber, R.J. *Dictyostelium discoideum*: A Model System for Cell and Developmental Biology. *Curr. Protoc. Essent. Lab. Tech.* **2017**, *15*, 14.1.1–14.1.19. [CrossRef]
10. Pearce, X.G.; Annesley, S.J.; Fisher, P.R. The Dictyostelium model for mitochondrial biology and disease. *Int. J. Dev. Biol.* **2019**, *63*, 497–508. [CrossRef]
11. Leach, C.K.; Ashworth, J.M.; Garrod, D.R. Cell sorting out during the differentiation of mixtures of metabolically distinct populations of *Dictyostelium discoideum*. *J. Embryol. Exp. Morphol.* **1973**, *29*, 647–661. [PubMed]
12. Tasaka, M.; Takeuchi, I. Role of Cell Sorting in Pattern Formation in *Dictyostelium discoideum*. *Differentiation* **1981**, *18*, 191–196. [CrossRef]
13. Thompson, C.R.; Kay, R.R. Cell-Fate Choice in *Dictyostelium*: Intrinsic Biases Modulate Sensitivity to DIF Signaling. *Dev. Biol.* **2000**, *227*, 56–64. [CrossRef]
14. Mazur, M.; Wojtkowska, M.; Skalski, M.; Słocińska, M.; Kmita, H. The The TOB/SAM complex composition in mitochondria of *Dictyostelium discoideum* during progression from unicellularity to multicellularity. *Acta Biochim. Pol.* **2019**, *66*, 551–557. [CrossRef]
15. Fey, P.; Kowal, A.S.; Gaudet, P.; Pilcher, K.E.; Chisholm, R.L. Protocols for growth and development of *Dictyostelium dis-coideum*. *Nat. Protoc.* **2007**, *2*, 1307–1316. [CrossRef]
16. Michejda, J.; Guo, X.J.; Lauquin, G.J.-M. The respiration of cells and mitochondria of porin deficient yeast mutants is coupled. *Biochem. Biophys. Res. Commun.* **1990**, *171*, 354–361. [CrossRef]
17. Karachitos, A.; Jordán, J.; Kmita, H. Cytoprotective activity of minocycline includes improvement of mitochondrial coupling: The importance of minocycline concentration and the presence of VDAC. *J. Bioenerg. Biomembr.* **2012**, *44*, 297–307. [CrossRef]
18. Karachitos, A.; Grobys, D.; Antoniewicz, M.; Jedut, S.; Jordan, J.; Kmita, H. Human VDAC isoforms differ in their capability to interact with minocycline and to contribute to its cytoprotective activity. *Mitochondrion* **2016**, *28*, 38–48. [CrossRef]
19. Brand, M.D.; Nicholls, D.G. Assessing mitochondrial dysfunction in cells. *Biochem. J.* **2011**, *435*, 297–312. [CrossRef]
20. Hughes, C.S.; Foehr, S.; Garfield, D.A.; Furlong, E.E.; Steinmetz, L.M.; Krijgsveld, J. Ultrasensitive proteome analysis using paramagnetic bead technology. *Mol. Syst. Biol.* **2014**, *10*, 757. [CrossRef] [PubMed]
21. Malinowska, A.; Kistowski, M.; Bakun, M.; Rubel, T.; Tkaczyk, M.; Mierzejewska, J.; Dadlez, M. Diffprot—Software for non-parametric statistical analysis of differential proteomics data. *J. Proteom.* **2012**, *75*, 4062–4073. [CrossRef]
22. Elias, J.; Haas, W.; Faherty, B.; Gygi, S.P. Comparative evaluation of mass spectrometry platforms used in large scale prote-omics investigations. *Nat. Methods* **2005**, *2*, 667–675. [CrossRef] [PubMed]
23. Bakun, M.; Karczmarski, J.; Poznanski, J.; Rubel, T.; Rozga, M.; Malinowska, A.; Sands, D.; Hennig, E.; Oledzki, J.; Ostrowski, J.; et al. An integrated LC-ESI-MS platform for quantitation of serum peptide ladders. Application for colon carcinoma study. *Proteom. Clin. Appl.* **2009**, *3*, 932–946. [CrossRef] [PubMed]

24. Isono, T.; Chano, T.; Yonese, J.; Yuasa, T. Therapeutic inhibition of mitochondrial function induces cell death in starva-tion-resistant renal cell carcinomas. *Sci. Rep.* **2016**, *9*, 25669. [CrossRef]
25. Keuper, M.; Jastroch, M.; Yi, C.; Fischer-Posovszky, P.; Wabitsch, M.; Tschöp, M.H.; Hofmann, S.M. Spare mitochondrial respiratory capacity permits human adipocytes to maintain ATP homeostasis under hypoglycemic conditions. *FASEB J.* **2014**, *28*, 761–770. [CrossRef]
26. Zhou, Y.; Al-Saaidi, R.A.; Fernandez-Guerra, P.; Freude, K.K.; Olsen, R.K.J.; Jensen, U.B.; Gregersen, N.; Hyttel, P.; Bolund, L.; Aagaard, L.; et al. Mitochondrial Spare Respiratory Capacity Is Negatively Correlated with Nuclear Reprogramming Efficiency. *Stem Cells Dev.* **2017**, *26*, 166–176. [CrossRef] [PubMed]
27. Pfleger, J.M.; He, M.; Abdellatif, M.M.M. Mitochondrial complex II is a source of the reserve respiratory capacity that is regulated by metabolic sensors and promotes cell survival. *Cell Death Dis.* **2015**, *6*, e1835. [CrossRef]
28. Journet, A.; Klein, G.; Brugière, S.; Vandenbrouck, Y.; Chapel, A.; Kieffer, S.; Bruley, C.; Masselon, C.; Aubry, L. Investigating the macropinocytic proteome of Dictyostelium amoebae by high-resolution mass spectrometry. *Proteomics* **2012**, *12*, 241–245. [CrossRef]
29. Matsuda, T.; Takahashi-Yanaga, F.; Yoshihara, T.; Maenaka, K.; Watanabe, Y.; Miwa, Y.; Morimoto, S.; Kubohara, Y.; Hirata, M.; Sasaguri, T. Dictyostelium differentiation-inducing factor-1 binds to mitochondrial malate dehydrogenase and inhibits its activity. *J. Pharmacol. Sci.* **2010**, *112*, 320–326. [CrossRef]
30. Zhang, S.; Xie, C. The role of OXCT1 in the pathogenesis of cancer as a rate-limiting enzyme of ketone body metabolism. *Life Sci.* **2017**, *183*, 110–115. [CrossRef]
31. Li, C.-L.F.; Santhanam, B.; Webb, A.N.; Zupan, B.; Shaulsky, G. Gene discovery by chemical mutagenesis and whole-genome sequencing in *Dictyostelium*. *Genome Res.* **2016**, *26*, 1268–1276. [CrossRef]
32. Vincent, E.E.; Sergushichev, A.; Griss, T.; Gingras, M.-C.; Samborska, B.; Ntimbane, T.; Coelho, P.P.; Blagih, J.; Raissi, T.C.; Choinière, L.; et al. Mitochondrial Phosphoenolpyruvate Carboxykinase Regulates Metabolic Adaptation and Enables Glucose-Independent Tumor Growth. *Mol. Cell* **2015**, *60*, 195–207. [CrossRef]
33. Wu, Y.; Janetopoulos, C. Systematic Analysis of γ-Aminobutyric Acid (GABA) Metabolism and Function in the Social Amoeba *Dictyostelium discoideum*. *J. Biol. Chem.* **2013**, *288*, 15280–15290. [CrossRef]
34. Pavlova, N.N.; Thompson, C.B. The Emerging Hallmarks of Cancer Metabolism. *Cell Metab.* **2016**, *23*, 27–47. [CrossRef]
35. Fernández-Fernández, M.R.; Valpuesta, J.M. Hsp70 chaperone: A master player in protein homeostasis. *F1000Research* **2018**, *7*, 1497. [CrossRef] [PubMed]
36. Vardi-Oknin, D.; Arava, Y. Characterization of factors involved in localized translation near mitochondria by ribosome-proximity labeling. *Front. Cell Dev. Biol.* **2019**, *7*, 305. [CrossRef] [PubMed]
37. Hansen, K.G.; Herrmann, J.M. Transport of Proteins into Mitochondria. *Protein J.* **2019**, *38*, 330–342. [CrossRef]
38. Wojtkowska, M.; Buczek, D.; Suzuki, Y.; Shabardina, V.; Makałowski, W.; Kmita, H. The emerging picture of the mitochon-drial protein import complexes of Amoebozoa supergroup. *BMC Genom.* **2017**, *18*, 997.
39. Shan, Y.; Cortopassi, G. Mitochondrial Hspa9/Mortalin regulates erythroid differentiation via iron-sulfur cluster assembly. *Mitochondrion* **2016**, *26*, 94–103. [CrossRef]
40. Stehling, O.; Wilbrecht, C.; Lill, R. Mitochondrial iron–sulfur protein biogenesis and human disease. *Biochimie* **2014**, *100*, 61–77. [CrossRef]
41. Embley, T.M.; Martin, W. Eukaryotic evolution, changes and challenges. *Nat. Cell Biol.* **2006**, *440*, 623–630. [CrossRef] [PubMed]
42. Vacanti, N.M.; Divakaruni, A.S.; Green, C.R.; Parker, S.J.; Henry, R.R.; Ciaraldi, T.P.; Murphy, A.N.; Metallo, C.M. Regula-tion of substrate utilization by the mitochondrial pyruvate carrier. *Mol. Cell* **2014**, *56*, 425–435. [CrossRef] [PubMed]
43. Satre, M.; Mattei, S.; Aubry, L.; Gaudet, P.; Pelosi, L.; Brandolin, G.; Klein, G. Mitochondrial carrier family: Repertoire and peculiarities of the cellular slime mould *Dictyostelium discoideum*. *Biochimie* **2007**, *89*, 1058–1069. [CrossRef] [PubMed]
44. Bloomfield, G.; Pears, C. Superoxide signalling required for multicellular development of *Dictyostelium*. *J. Cell Sci.* **2003**, *116*, 3387–3397. [CrossRef]
45. Roger, A.J.; Muñoz-Gómez, S.A.; Kamikawa, R. The Origin and Diversification of Mitochondria. *Curr. Biol.* **2017**, *27*, R1177–R1192. [CrossRef] [PubMed]

molecules

MDPI

Review

The Diversity of the Mitochondrial Outer Membrane Protein Import Channels: Emerging Targets for Modulation

Monika Mazur, Hanna Kmita and Małgorzata Wojtkowska *

Institute of Molecular Biology and Biotechnology, Faculty of Biology, Adam Mickiewicz University, 61-614 Poznan, Poland; monika.antoniewicz@gmail.com (M.M.); kmita@amu.edu.pl (H.K.)
* Correspondence: malgorzata.wojtkowska@amu.edu.pl; Tel.: +48-61929-59-02

Abstract: The functioning of mitochondria and their biogenesis are largely based on the proper function of the mitochondrial outer membrane channels, which selectively recognise and import proteins but also transport a wide range of other molecules, including metabolites, inorganic ions and nucleic acids. To date, nine channels have been identified in the mitochondrial outer membrane of which at least half represent the mitochondrial protein import apparatus. When compared to the mitochondrial inner membrane, the presented channels are mostly constitutively open and consequently may participate in transport of different molecules and contribute to relevant changes in the outer membrane permeability based on the channel conductance. In this review, we focus on the channel structure, properties and transported molecules as well as aspects important to their modulation. This information could be used for future studies of the cellular processes mediated by these channels, mitochondrial functioning and therapies for mitochondria-linked diseases.

Keywords: mitochondria; import channel; TOM; TOB/SAM; Tom40; Tob55/Sam50; Mdm10; MIM; MAC

Citation: Mazur, M.; Kmita, H.; Wojtkowska, M. The Diversity of the Mitochondrial Outer Membrane Protein Import Channels: Emerging Targets for Modulation. *Molecules* **2021**, *26*, 4087. https://doi.org/10.3390/molecules26134087

Academic Editor: Yukio Yoneda

Received: 4 June 2021
Accepted: 1 July 2021
Published: 4 July 2021

1. Introduction

According to the endosymbiotic theory, mitochondria arose from prokaryotes through (endo)symbiosis. These double-membrane organelles have retained the oxidative phosphorylation system to synthesize ATP. This is the best-known function of mitochondria, which makes them unique and crucial for cells. However, in the course of evolution, nearly all ancestral genes were transferred into the nucleus. As a result, most mitochondrial proteins are synthesized in the cytosol and must be delivered to their correct mitochondrial destination [1,2]. Thus, protein import into the mitochondria seems to be additional evidence for the single origin of these organelles.

Since the last years, studies of protein import into mitochondria have revealed many aspects concerning the composition and function of the protein import machinery, which consists of protein import complexes with the main module working as an import channel that allows protein transfer across and into both mitochondrial membranes. The first barrier for incoming proteins is the mitochondrial outer membrane, which has approximately 200 proteins, of which some display channel activity [3]. To date, nine different channel-forming proteins responsible for the transport of metabolites, inorganic ions and proteins have been distinguished in the outer membrane [4]. Some of these proteins have a β-barrel structure and include Tom40, Tob55/Sam50, the voltage-dependent anion-selective channel (VDAC) and Mdm10, mitochondrial apoptosis channel (MAC) while those with other types of structure include Mim1, Ayr1, OMC7 and OMC8 [5]. The protein channels described in this review, except of the MAC, are constitutively open and do not need activators to regulate its opening. This phenomenon makes them different than channels located within the inner mitochondria membrane.

In this review, we focus on the outer membrane protein import channels characterized as single modules and as subunits of the native complexes. We present current data about their structure, regulation and variety of transported molecules. Such knowledge is crucial

for development of the channels' modulators which could prove effective in correcting mitochondrial processes that in turn may constitute an important therapeutic approach in disease treatment.

2. Overview of the Mitochondrial Protein Import Machinery

The successful import of precursor proteins into their destinations in mitochondria primarily depends on the mitochondrial membrane complexes and specific signals localised within the incoming precursor proteins. The membrane import complexes—known as translocases—are composed of receptor subunits that recognise incoming precursor proteins, proteins that form channels for transport across membranes or insertion into membranes and protein subunits that modulate the activity and stability of complexes. In the mitochondrial outer membrane, four complexes have been identified (Figure 1): translocase of the outer mitochondrial membrane (TOM) [6,7], topogenesis of the mitochondrial outer membrane β-barrel proteins/sorting and assembly machinery (TOB/SAM) [8–11], mitochondrial import complex (MIM) [12,13] and endoplasmic reticulum-mitochondria encounter structure (ERMES) [14]. The TOM complex recognises, translocates and segregates most of the precursor proteins delivered to different mitochondrial locations. The TOB/SAM complex inserts into the outer membrane proteins of the β-barrel structure displayed by proteins forming channels, such as Tom40, Tob55/Sam50, mitochondrial distribution and morphology protein 10 (Mdm10; part of the ERMES complex) and mitochondrial porin (a VDAC responsible for metabolite and inorganic ion transport in and out of the mitochondria) [2]. The MIM complex inserts the α helical outer membrane proteins, which are imported independently of the TOM complex [12].

Precursor proteins destined for the intermembrane space (IMS) are assisted by the mitochondrial intermembrane space and assembly (MIA) complex [15]. Other precursors are transported or inserted into the inner membrane by two complexes (i.e., TIM23 [15,16] and TIM22 [17,18]). The TIM23 complex primarily performs import into the mitochondrial matrix, whereas the TIM22 complex performs insertion into the inner membranes of carrier proteins (for more details on the import across and into the inner membrane, see the following reviews: [19,20]) (Figure 1).

Protein Import across and into the Mitochondrial Outer Membrane

The most widely used model organism in studies on mitochondria protein import machinery is the yeast *Saccharomyces cerevisiae*, which is also used as a reference for comparative studies on other eukaryotic organisms, including plants and animals [2,21]. As previously mentioned, the TOM complex receptors specifically recognise the incoming precursor proteins. Tom20 binds to the hydrophobic surface of the cleavable amphipathic presequence and initiates contact with the next receptor (i.e., Tom22 protein via its positively charged surface). In the case of non-cleavable hydrophobic precursors serving as carrier proteins with the inner membrane as the destination, the Tom70 receptor is engaged. Crossing of the outer membrane is performed by channel-forming Tom40 protein and small Tom subunits (e.g., Tom5, Tom6 and Tom7) that stabilize the complex and contribute to the proper assembly of its subunits [22]. From this entry point, import pathways diverge into different directions depending on the final destination of the protein [2] (Figure 1). After crossing through the channel formed by Tom40, proteins that adopted a β-barrel structure are bound to small TIM proteins in the IMS (i.e., Tim9 and Tim10) [23,24] and delivered to the TOB/SAM complex. The TOB/SAM complex consists of two peripheral membrane proteins exposed to the cytosol, namely Tob38 (also known as Sam35) and Tob37 (also known as Sam37/Mas37), as well as the channel-forming protein Tob55/Sam50 [25–29]. Thus, the TOB/SAM complex recognises β-barrel proteins and assists their membrane insertion and assembly [3,30]. Available data concerning the mammalian TOB/SAM complex indicate the presence of weakly conserved homologues of Tob37 and Tob38, known as metaxin 1 (Mtx1) and metaxin 2 (Mtx2), respectively [30–32]. The TOB/SAM complex of the slime mould *Dictyostelium discoideum* includes Tob55/Sam50 and one metaxin homolog [33–35].

It has also been proven that β-barrel proteins interact with the mitochondrial contact site and cristae organising system (MICOS) complex, which maintains the characteristic pleated structure of the mitochondrial inner membrane [36,37]. One of the MICOS complex subunits, Mic60/mitofilin, stimulates β-barrel protein transfer from the TOM complex to the TOB/SAM complex [38]. The outer membrane proteins anchored by one or more α-helical transmembrane segments are mostly inserted by the MIM complex, which consists of Mim1 and Mim2 protein subunits [4]. Additionally, the MIM complex cooperates with the protein Mdm10, which is part of the ERMES complex [14].

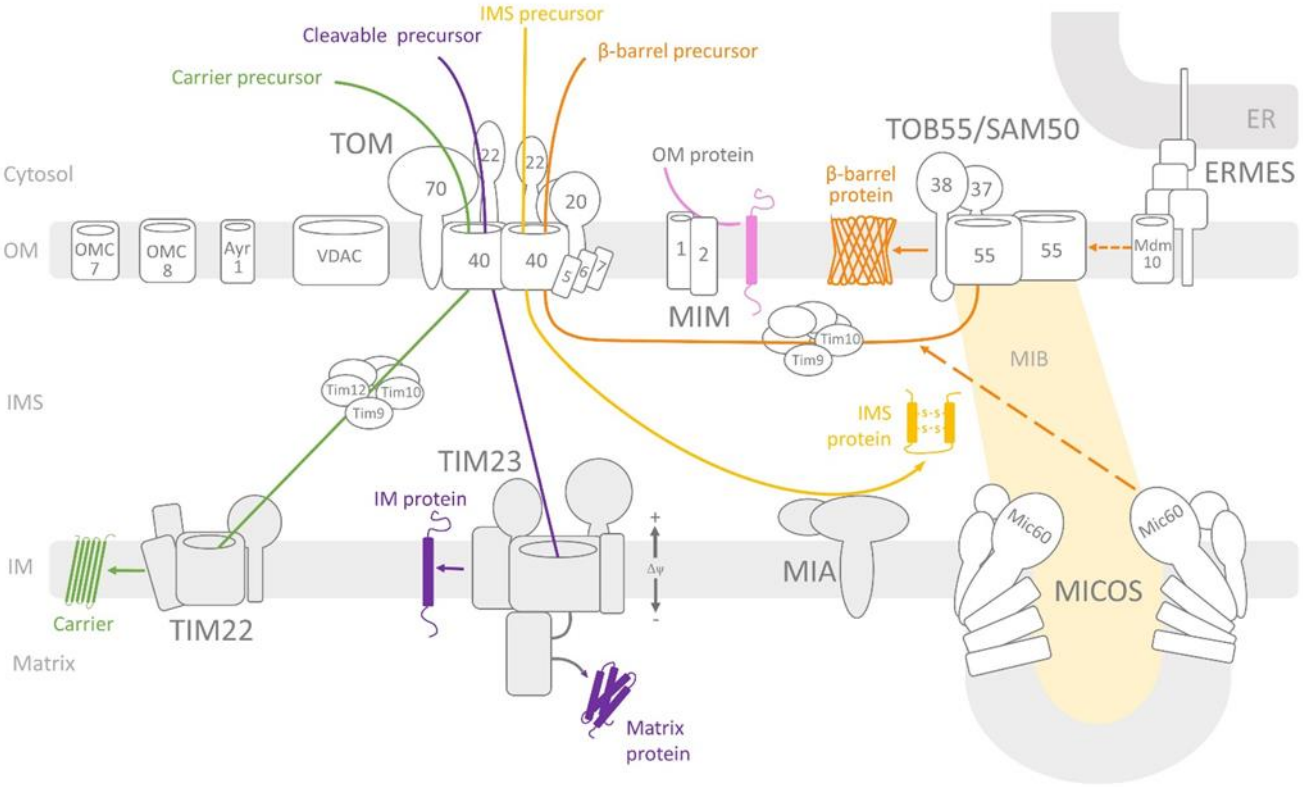

Figure 1. Overview of protein import into mitochondria. The TOM complex recognises most of the mitochondrial preproteins via its receptors (i.e., Tom20, Tom22 and Tom70) and imports across the outer membrane through the Tom40 channel (dimer). Small TOM subunits (i.e., Tom5, Tom6 and Tom7) stabilise the TOM complex. β-barrel precursors (i.e., Tom40, Tob55/Sam50, VDAC and Mdm10) are inserted into the outer membrane by the TOB/SAM complex, which consists of the protein channel Tob55/Sam50 (dimer) and receptors Tob38 and Tob37. The mitochondrial contact site and cristae organising system (MICOS) complex supports the insertion of the β-barrel proteins into the OM. The dynamic structure of TOB/SAM and MICOS is called mitochondrial intermembrane space bridging (MIB). α-helical precursors are inserted into the OM by the MIM complex (Mim1 and Mim2). The ERMES complex links the mitochondria and endoplasmic reticulum (ER) and supports the topogenesis of the mitochondrial outer membrane β-barrel proteins/sorting and assembly machinery (TOB/SAM) complex. The precursor targeted into the intermembrane space engages the MIA complex. TIM23 is responsible for import across the IM or into the mitochondrial matrix. TIM22 inserts carrier proteins into the IM. Voltage-dependent anion-selective channel (VDAC) is responsible for metabolite transport. Ayr1, OMC7 and OMC8 are the channels of unknown substrates. OM—outer membrane; IM—inner membrane; IMS—intermembrane space; ER—endoplasmic reticulum.

3. Structure and Properties of the Outer Membrane Protein Import Channels

3.1. Tom40 Channel

Tom40 is the central and channel-forming subunit of the TOM complex [3,21]. A wide range of important studies on protein import into mitochondria have shown that Tom40 is not only the entry gate for most mitochondrial precursor proteins delivered from the

cytosol to various sub-mitochondrial locations [39–41] since it also works as a decisive general selectivity filter in the uptake of newly synthesized mitochondrial proteins [42,43]. Moreover, it was also proposed that the TOM complex can act as an insertase mediating lateral release of the membrane imported proteins into the outer membrane [44].

As a protein with a β-barrel structure, Tom40 [45] contains 19 antiparallel β-strands that enable channel formation [10]. The copy number of Tom40 proteins in yeasts cells was estimated at ~45,000 copies per cell [46]. The structure of the TOM complex and its electrophysiological properties has been studied for the last three decades. In the previous study [47,48], two kinds of the TOM complex were observed: three-channel complex representing trimeric form of Tom40 and two-channel complex representing dimeric form of Tom40. It was showed that the two-channel complex consisted of two Tom40 and small Tom subunits but did not contain Tom22. It was concluded that the two-channel complex dimmer functioned as a premature complex [49] whereas the mature TOM complex dynamically exchanges with the two channel one providing an assembly platform for the integration of new subunits. Recent years have brought the intensive development of microscopy techniques that have facilitated the study of specifically labelled active membrane protein complexes in the native membrane. The structure of the studied complexes is based on electron cryo-tomography (cryo-ET) presenting the surface and internal conformation at nanometre resolution [50]. The higher resolution of cryo-EM microscopy revealed a stable dimeric form of the TOM complex for *Neurospora crassa* at a resolution of 0.68 nm [51], with resolutions of 0.38 nm for *S. cerevisiae* [52] and 0.34 nm for humans [53] and a resolution of 0.41 nm for its tetrameric form [50,54]. According to the obtained TOM complex model, two Tom40 subunits form two pores for protein translocation across the membrane. Each Tom40 is connected by two Tom22 receptors and one phosphatidylcholine (PC) molecule. The latter is the most abundant phospholipid in the mitochondrial outer membranes and functions as a player in protein import into mitochondria [55]. Each Tom40 is surrounded by small Tom subunits (i.e., Tom5, Tom6 and Tom7), with Tom5 being situated at the distal end of the Tom40 dimer and Tom6 and Tom7 being located on opposite sides across the channel pore. A study on the human TOM complex [53] revealed a negative interior of the pore and positive regions at its periphery. Notably, the dimeric form of the TOM complex may associate to form a tetramer. The molecular weight of the human TOM complex was estimated at 150 kD, which is comparable to the size of the TOM complexes of *S. cerevisiae* [52,54] and *N. crassa* [51,56]. This is congruent with a previous study on the monomeric forms of the *N. crassa* [47] and *S. cerevisiae* TOM complexes [40], which were obtained via the circular dichroism method. These TOM complexes were estimated at a resolution of 0.68 nm and showed two pores in the dimer, each with a shortest diameter of 1.1 nm and longest diameter of 3.2 nm.

The structure of the Tom40 pore has been reported by various groups [52,54] and resulted in similar models with some differences. In contrast to the Tom40 structure of yeast, the human Tom40 structure does not contain an α-helical segment preceding the internal helix at the N terminus and also lacks an additional C-terminal α-helix at the end of 19th β-strand. Studies of the purified Tom40 of *Candida glabrata* [57] revealed that the conserved 51 amino acids at the N terminus of the Tom40 sequence, the 15 amino acids at its C terminus and the interaction with a pre-sequence of the precursor protein were not crucial for channel formation. These results demonstrated that all studied Tom40 constructs formed channels of different conductance. Each of the expressed proteins interacted with a pre-sequence peptide in the concentration dependent manner although the interaction with the conserved N-terminal Tom40 domain was not required. This study showed that Tom40 dimers were functional and their distinct conformations were regulated by binding of the substrate. For yeast and human Tom40, the α-helical domain that traverses the channel pore and extends into IMS plays a crucial function in import across the Tom40 channel. It was noted that residues T82, N79, P80, H87 and Q97 in the internal portion of Tom40 form hydrogen bonds with R195, T200, K253, T264 and Q353 in β-strands 7, 8, 11, 12 and 19 of

Tom40, respectively. Despite it being partially unfolded, the presence of the internal helix limits the diameter of Tom40 enough for the translocation of the precursor protein.

As previously mentioned, the activity of the Tom40 channel could be stimulated by PC, which contains the positively charged choline group extending into the IMS. This was suggested to have a possible function in the translocation process [55]. Electrophysiological studies were performed on purified TOM complex and purified Tom40. The Tom40 channel shows a preference for cations: P_{K^+}/P_{Cl^-} = 8:1 with a reversal potential of 40 mV (planar lipid bilayer technique performed on *S. cerevisiae* Tom40, according to [40]) (Table 1). In an experiment performed by [58], *S. cerevisiae* and *N. crassa* Tom40 were expressed in *Escherichia coli* cells and renatured. The electrophysiology measurements in planar lipid bilayers at a symmetrical concentration of 250 mM KCl were indistinguishable at 370 and 390 pS, respectively.

Tom40 is the voltage dependent channel. In the absence of membrane potential, the reconstituted channel is completely open but closes symmetrically at positive or negative potentials. The studies on the reconstituted *S. cerevisiae* Tom40 showed that in the presence of low membrane potential the pre-sequence peptide selectively bound to Tom40 and thereby altered the gating of the channel but was rapidly translocated through the channel when driven by higher voltage [40]. For purified and reconstituted *S. cerevisiae* TOM complex, the maximal conductance was estimated at 740 ± 18 pS, whereas the same estimate in the outer membrane vesicles was 760 ± 12 pS. In general, the maximal conductance of the *S. cerevisiae* or *N. crassa* TOM complexes were 2-fold higher than the total conductance of renatured Tom40 alone. The maximal conductance channel was 370 ± 8 pS for *S. cerevisiae* Tom40 and 390 ± 10 pS for *N. crassa* Tom40 at 250 mM KCl. Thus, the channel properties of purified Tom40 are lower than those of the TOM complex [58]. Interestingly, in the case of the *A. castellanii* and *D. discoideum* TOM complexes, channel conductance activities were estimated at 2.5 and 2.3 nS, respectively, in 1M KCl [59]. After extrapolation (625 pS and 575 nS respectively in 250 mM KCl), this result is in agreement with the data obtained for *S. cerevisiae* and *N. crassa*. The data for *N. crassa* [60] correspond well to the conductance states for *C. glabrata*, where different truncated forms of purified Tom40 were studied in planar lipid bilayers (~125–500 pS in 250 mM KCl, described by [57] (Table 1). The reconstituted version of *C.glabrata* Tom40 forms provided a better understanding of the channel flickering phenomena observed during a study of *S. cerevisiae*, *N. crassa*, *A. castellanii* and *D. discoideum* TOM complex [58,59]. This data indicated flickering which is typical for this kind of the outer membrane channels.

The channel conductance was measured using the specific signal peptides known to be recognised by the TOM complex receptors [61]. The presence of signal peptides resulted in the channel flickering, i.e., rapid transitions from the fully open state to substates of lower conductance resulting from the channel blockade. This is a consequence of signal peptides interaction with TOM complex subunits. In a study by [58], it was shown that for the purified Tom40 of *S. cerevisiae*, the signal peptide of CoxIV had to be used in a much higher concentration than in the case of the TOM complex to obtain a 50% reduction in open channel probability (3 μM vs. 50–80 nM). This implies that the sensitivity of the Tom40 channel pore is enhanced by the presence of the TOM complex subunits. The channel properties were also measured in the presence of the other recognised signal peptide. The pre-sequence peptide of the F1-ATP synthase subunit β also induced the blockage of Tom40 conductance in a concentration-dependent manner, which indicates a direct interaction of this peptide with the Tom40 channel pore. Similarly, in a study of the *A. castellanii* and *D. discoideum* TOM complexes, a signal peptide of subunit 9 of ATP synthase also blocked the purified TOM complex in a concentration-dependent manner [59]. Additionally, the results obtained for the TOM complex revealed that the binding sites for the incoming precursor proteins had a presequence recognised by the TOM complex subunits, which was not present in purified Tom40. Notably, data on the individual TOM complex receptors revealed relatively low affinities (high KD) for the pre-sequences [40,62], while high-affinity binding of the pre-sequences was observed for the TOM complex [61]. Thus, data on the

TOM complex and purified Tom40 alone uncovered the roles of the TOM complex subunits in the regulation of Tom40 channel activity.

It should be mentioned that the means of protein preparation for the studies on Tom40 and other described in this review protein channels, as well as the applied methods as planar lipid bilayer membranes and patch clump could greatly influence the determined channel properties. Thus, combining electrophysiological data with structural data provide reasonable background for putative modulation. However, this always would need verification under cellular conditions.

Table 1. Characteristics of the mitochondrial outer membrane channels based on reconstitution studies *.

Protein Name	Conductance **	Reversal Potential (mV) ***	P_{K^+}/P_{Cl^-}	Studied Organism	Constitutively Open	Molecules Transported across Channel	Channel Activity Modulators	References
Tom40	370 ± 8 pS [a]	40 [a]	8 [a]	*S. cerevisiae* [a]	Yes	Mitochondria proteins [c] RNA [d] Pink 1 [e] Aβ [f]	PC [i] α-Syn [j]	[58] [a] [59] [b] [6] [c] [63] [d] [64] [e] [65] [f] [66,67] [g] [68] [h] [69] [h] [58] [i] [70] [j]
	390 ± 10 pS [a]			*N. crassa* [a]				
	TOM complex: 740 ± 18 pS (purified complex) [a] 760 ± 12 pS (complex in OMVs) [a]			*S. cerevisiae* [a]	Yes	TOM complex: RNA [g] Metabolites [h]	signal peptides of: CoxIV [a] preSu9 [a,b]	
	625 npS (purified complex) [b]			*A. castellanii* [b]				
	575 pS (purified complex) [b]			*D. discoideum* [b]				
Tob55/ Sam50	640 pS [k]	30 [k]	4 [k]	*S. cerevisiae* [k]	Yes	β barrel proteins [l] Granzymes (a and b) [m] Caspase-3 [m] Suggested: metabolites [n]	Unknown	[71] [k] [30] [l] [72] [m] [73,74] [n]
Mdm10	480 pS [o]	21.5 [o]	2.8 [o]	*S. cerevisiae* [o]	Yes	Unknown	Tom22 [o]	[14] [o]
Mim1	580 pS [p]	53 [p]	23.5 [p]	*S. cerevisiae* [p]	N/D	α helical outer membrane proteins [r]	Mim2 [p]	[4] [p] [12] [r]
MAC	1500–5000 pS [s]	voltage-independent [s]	3 [t]	Mammalian [s]	No	apoptotic cofactors e.g.,: Cyt c [s] Smac/DIABLO [s] AIF [s]	Bcl-2 [s] Bcl-xL [s] Dibucaine [s] Trifluoperazine [s] Propranolol (and its derivatives) [s]	[75] [s] [76] [t]
OMC7	570 pS [p]	−12.5 [p]	0.55 [p]	*S. cerevisiae* [p]	N/D	Suggested: RNA and/or metabolites	Unknown	[4] [p]
OMC8	550 pS [p]	−15.5 [p]	0.48 [p]	*S. cerevisiae* [p]	N/D	Suggested: RNA and/or metabolites	Unknown	[4] [p]
Ayr1	1470 pS [p]	30 [p]	4.5 [p]	*S. cerevisiae* [p]	N/D	Suggested: proteins	NADPH [r]	[4] [p]

* Channels are listed in the order in which they appear in the text. Abbreviations: PC—Phosphatidylcholine; α-Syn—α-synuclein; Aβ—amyloid β peptide; Pink 1—PTEN-induced kinase 1, cyt c—cytochrome c, AIF—Apoptosis Inducing Factor. References are listed using letter designations (a–t), with each letter also being assigned to the data contained in a given publication. ** Study performed in 250 mM KCl (by planar lipid bilayer membranes), with exception of MAC channel: 150 mM KCl (study performed by patch clump). *** Study performed in 250 mM/20 mM KCl (cis/trans) gradient.

3.2. Tob55/Sam50 Channel

Tob55/Sam50 protein (also known as Omp85) is a member of the Omp85 family of β-barrel-channels typical of the outer membranes of Gram-negative bacteria, mitochondria and chloroplasts [25,45,77]. The copy number of Tob55/Sam50 proteins in yeasts is estimated at ~1500 copies per cell [3,46]. The Tob55/Sam50 channel is composed of a 16-stranded transmembrane β-barrel with a single polypeptide-transport-associated (POTRA) domain extending into the IMS. The POTRA domain is an N-terminal domain consisting of

~100 amino acids involved in the recognition and transfer of β-barrel forming precursors from the IMS via small Tim9 and Tim10 to the TOB/SAM complex [8–11].

The TOB/SAM complex was also suggested to be involved in apoptosis [72]. An important study on yeast and human cells conducted by [72] revealed that Tob55/Sam50 was required for the transport of granzymes (a and b) and caspase-3 to cross the outer membrane. Granzymes are serine proteases that trigger cell death in a caspase-dependent and independent manner [78,79]. It was also shown that Tob55/Sam50 was sufficient for active caspase-3 to enter the mitochondria to induce cell death. Moreover, the depletion of Tob55/Sam50 caused cells to become more resistant to cell death. Thus, Tob55/Sam50 is engaged in a wider range of imported substrates than previously thought (Table 1).

The TOB/SAM complex remains in dynamic interactions with other complexes, including TOM [80,81], MICOS (e.g., [82]) and ERMES (shared Mdm10 subunit) [83]. The TOM complex binding site is based on the interaction between Tom22 and Tob37 [29,81] and on the interaction between Tom5 and Tom22. It was found that a small fraction of Tom5 being associated with a TOB/SAM complex promotes the folding of Tom40 during its import to the outer membrane [80,84]. The interaction of the TOB/SAM complex with the MICOS complex is based on Mic60/mitofilin [36,85,86] and results in the regulation of cristae morphology, mitochondrial shape and respiratory chain complexes' assembly [85–87]. It has been shown that the TOB/SAM complex subunits exist in a large protein complex with Mic60/mitofilin, other Mic proteins (i.e., Mic10, Mic12, Mic19, Mic23, Mic25 and Mic 27) and CHCHD3 to create the so-called large mitochondrial IMS bridging (MIB) complex [85,86,88]. The MIB complex also likely contains the homolog metaxin-3 the DnaJC11 protein [89]. The depletion of Tob55/Sam50 in human cells resulted in the loss of the crista junction, which highlights its crucial function in crista formation [89]. The interaction of TOB/SAM with ERMES is mediated by Mdm10, which is considered a subunit of both of these complexes [82,90,91].

The Tob55/Sam50 channel has an inner diameter of approximately 7–8 nm (outer diameter: ~15 nm, central cavity: ~4–5 nm) [3,11]. A recent study on the *S. cerevisiae* TOB/SAM complex performed by electron microscopy at a resolution of 0.28–0.32 nm resulted in the description of two different forms of the TOB/SAM complex [92]. The TOB/SAM complex forms a dimer based on two different Tob55/Sam50 isoforms: Tob55/Sam50a and Tob55/Sam50b. Tob55/Sam50a is responsible for channel formation, while isoform b is responsible for releasing incoming precursor proteins from the channel [92]. The *S. cerevisiae* Tob55/Sam50 channel was studied in planar lipid bilayers, which revealed that it displayed a conductance of 640 pS at 250 mM KCl [71]. This result is in agreement with data obtained by [8] where Tob55/Sam50 showed a channel activity level of 3.75 nS in 1M KCl what after extrapolation correspond to 925 pS in 250 mM KCl Tob55/Sam50 has a preference for cations (P_{K^+}/P_{Cl^-} = 4:1) and a reversal potential of 30 mV [8,71]. At voltages greater than ±70 mV, the channel formed by Tob55/Sam50 is partially closed, which clearly distinguishes this channel from the VDAC channel measured by the same technique as planar lipid bilayers [93]. It has also been shown that the channel is mediated by a precursor protein β-signal that causes the displacement of the endogenous carboxy-terminal β-signal of the Tob55/Sam50 channel [94]. β-signal is localised at the C-terminal part of β-barrel precursor proteins and is highly conservative among bacteria, mitochondria and chloroplasts [71,94]. β-signal was shown to interact with Tob55/Sam50 channel and bind precisely at its β-strand 1. In doing so, it replaces β-strand 16 (endogenous Tob55/Sam50 β-signal). This opens the channel's lateral gate between β-strand 1 and β-strand 16 [94]. From this point, the remaining precursor proteins are inserted to gradually gain β structures. At the end of this process, matured protein is released into the outer membrane of the mitochondria [29,94,95] (Table 1).

3.3. Mdm10 Channel

Mdm10 has no sequence homologs in bacteria and is not present in higher eukaryotes [10]. In *S. cerevisiae*, its molecular weight is 56 kDa and the copy number is estimated at ~500

copies per cell [46]. Mdm10 was found together with Mdm12, Mdm34 and Mmm1 as a part of a complex responsible for the maintenance of mitochondrial morphology and distribution [96]. Mdm10 is involved in lipid biosynthesis and the tethering of the endoplasmic reticulum (ER) with mitochondria [83]. The resulting connection between these organelles is called the ERMES complex [97]. In addition, being a part of the ERMES complex, Mdm10 protein was reported to bind to the TOB/SAM complex and influence β-barrel protein import into the mitochondrial outer membrane [83,90,91]. After being trans-ported through the TOB/SAM complex into the TOM, Mdm10 is involved in the late assembly of the TOM complex by interacting with the TOB/SAM complex in the process of proper Tom40 protein assembly [83,90,98]. This step involves the association of Tom40 with Tom22 and small Tom proteins. This interaction between Mdm10 and TOB/SAM is regulated by Tom7 protein, which stimulates the release of Mdm10 from the TOB/SAM complex [3,28,98,99].

After incorporation into liposomes and planar lipid bilayers, the expressed and purified *S. cerevisiae* Mdm10 exhibits channel activity with a main conductance of 480 pS at 250 mM KCl and has a preference for cation selectivity (P_{K^+}/P_{Cl^-} = 2.8:1; reversal potential: 21.5 mV). Moreover, three independently gated pores have been reported [14]. Additionally, the presence of Tom22 precursor increases Mdm10 conductance to 550 pS at 250 mM KCl while also increasing the number of independently gated pores from three to four. This indicates the possible function of Mdm10 in the import of Tom22 protein [4,14].

3.4. Mim1 Channel

Mim1, also known as Tom13, plays a role in the import of α-helical outer membrane proteins such as Tom70 and Tom20 [12]. This protein forms a channel composed of the N-terminal domain exposed to the cytosol, central putative transmembrane segment (TMS) and C-terminal domain exposed to the IMS [12,13]. Mim1 is involved in the import of small Tom proteins and indirectly influences proper Tom40 membrane insertion [100,101] because the N-terminal domain of Mim1 and Tob37/Sam37 combined regulate the release of Tom40 protein from TOB/SAM [13,100]. Mim1 is also crucial for the proper insertion of Tom70 and Tom20, which, in the case of the latter, requires the homo-oligomerisation of Mim1 proteins via its transmembrane domain (TMS) [12]. It has also been shown that the precursors of multi-spanning α-helical proteins directly interact with Mim1, which cooperates with the Tom70 receptor for protein insertion into the outer mitochondrial membrane [101]. Moreover, Mim1 regulates the binding and insertion of mitochondrial fusion and the transport protein Ugo1 [102] while promoting the import of UBX domain-containing protein 2 (Ubx2), which is the TOM complex-associated protein suspected to remove mitochondrial precursor proteins that become stuck in the import channel [103].

The *S. cerevisiae* Mim1, expressed in *E. coli* and then purified and renatured, was studied in planar lipid bilayer. A channel conductance of 580 pS was calculated at 250 mM KCl and a closing tendency due to high positive and negative voltage was observed. This study showed cation selectivity (P_{K^+}/P_{Cl^-} = 23.5:1) and a reversal potential of 53 mV [4]. The channel activity was modulated by specific anti-Mim1 antibodies. The same channel properties were obtained for *S. cerevisiae* Mim1 expressed in wheat germ lysate [4]. Modulation of the Mim1 channel was also observed after adding purified Mim2, which did not reveal channel activity. The channel properties of Mim1 determined in the presence of Mim2 included a reduced maximal current, decreased reversal potential of 48 mV and reduced cation selectivity P_{K^+}/P_{Cl^-} of 11:1. Thus, Mim1 is a channel of cation preference for the positively charged precursor proteins modulated by the Mim2 protein [4].

3.5. Mitochondrial Apoptosis-Induced Channel (MAC)

MAC is the outer membrane large channel known as an early marker of the onset of apoptosis. It participates in release of proteins normally constrained within the intermembrane space, such as cytochrome c, second mitochondria-derived activator of caspases (Smac)/Direct inhibitor of apoptosis-binding protein with low pI (DIABLO) or apoptosis

induced factor (AIF) [75,104]. MAC is formed by Bax and/or Bak proteins and at least one of the proteins must be present. Bax protein is cytosolic whereas Bak is an integral protein of the outer membrane and they both stay in an inactive form until MAC formation [75,104]. The activity of MAC is significantly different from the TOM and TOB/SAM complexes. Moreover, the former are constitutive channels of the outer membrane whereas MAC activity co-occur only with apoptosis [75,76,104]. MAC activity is regulated by other Bcl-2 family proteins. Bcl-2 and Bcl-xL inhibit apoptosis by separating Bax and Bak. Moreover, MAC can be block by dibucaine, trifluoperazine and propranolol in a dose-dependent manner) as well as 3.6 dibromocarbazole piperazine derivatives of 2-propanol (that blocked cytochrome c release induced in isolated mitochondria by tBid).

By application of patch-clump, the reconstituted MAC conductance was estimated as heterogenous; i.e between 1.5–5 nS (1500–5000 pS in 150 mM KCl). MAC frequently fluctuates between the fully open state and fully closed state, with a maximal single transition size of 2000 pS in 150 mM KCl and at least three substates [75]. MAC is a voltage-independent channel and is slightly cation-selective. As it has been shown for mammalian apoptotic FL5.12 cells after interleukin 3 (IL-3) withdrawal, P_{K^+}/P_{Cl^-} = 3:1. The cation selectivity is consistent with its putative role in releasing cationic proteins such as cytochrome *c* [75]. At high conductance state MAC is permeable dextran of molecular weight in the range of 10 to 17 kDa, but not in the range of 45 to 71 kDa. Based on the polymer exclusion method, MAC pore diameters were estimated in the range of 2.9 to 7.6 nm [75,76].

4. Non-Proteinaceous Molecules Transported by Protein Import Channels

4.1. Transport of RNA

RNA import into mitochondria has been shown for many different groups of eukaryotic organisms, including plants, mammals, yeast *S. cerevisiae* and protozoans. Notably, it is assumed that this phenomenon is universal for all eukaryotes. It has also been shown that mitochondria can import diverse types of RNA molecules, which suggests the existence of an extrinsic RNA importome [105]. The latter includes transfer RNAs (tRNAs), ribosomal RNAs (rRNAs), microRNAs (miRNAs) and long non-coding RNAs (lncRNAs) (for a review on this topic, see [105–107]). RNA import and the imported RNA molecules' contribution to gene expression are considered essential for mitochondrial function (e.g., [108]). The majority of the studied imported RNA molecules are tRNAs (e.g., [109,110]) since their import can be clearly explained as a compensation for tRNA encoding genes not being present in the mitochondrial genome (mtDNA). This applies to plants lacking a few tRNA encoding genes in mtDNA (e.g., [111]) as well as protozoans lacking a distinct part or complete set of tRNA coding genes in mtDNA (e.g., *Tetrahymena thermophila*, *Trypanosoma brucei* and *Leishmania tarentolae* [112–114]). Moreover, tRNA import from the cytosol can be observed in the presence of all necessary tRNA genes in mtDNA and is regarded as an important mechanism in stress response [105,115].

Available data indicates that routes for RNA import into the mitochondria may overlap with mitochondrial protein import channels since some components of the TOM and TIM complexes may contribute to translocation across mitochondrial membranes. In the case of the mitochondrial outer membrane, translocation is purportedly mediated by Tom40; however, an important role is also assigned to relevant VDAC paralogs. In plant mitochondria, Tom40 and Tom20 likely participate in the fixation of RNA molecules at the surface of mitochondria [63,64], while Tom40 is also suggested to partially contribute to translocation in yeast and mammalian mitochondria [105,109,110,116,117]. In the case of African trypanosomes (represented by *T. brucei*), the Tom40 orthologue ATOM40 (atypical TOM, e.g., [118]), as well as Tom22 orthologues ATOM14 and two additional ATOM subunits (ATOM11 and 12), have been shown to perform RNA molecule translocation across the mitochondrial outer membrane [63,119]. While the proteins involved in RNA molecule translocation across the inner mitochondrial membrane remain largely unknown, data available for yeast and *T. brucei* point to the important contribution of TIM complexes.

In the case of yeast mitochondria, TIM23 is suggested as the translocation pathway due to the putative involvement of Tim44 (subunits of the TiM23 complex) [105,116,120]. For *T. brucei*, the Tim22 orthologue TbTim17 (subunit of the TIM22 complex) has been shown to participate in translocation [120]. For translocation, the latter requires some of the other subunits of the non-canonical, singular TIM complex [121] (i.e., TbTim42, Tb-Tim62 and putative acyl-CoA dehydrogenase homologue (ACAD) [122].

The mechanisms involved in the import of RNA molecules into mitochondria are still not completely understood and seem to differ between organisms with different phylogenetic lineages and RNA molecule types. Although the transport of molecules across mitochondrial membranes is ATP-dependent and requires the presence of the inner membrane potential and relevant translocating proteins, differences exist in terms of selective import signals and the interacting proteins participating in redirection to the mitochondrial surface (e.g., [105,107,110]). In the case of imported tRNA molecules, the participating proteins may involve aminoacyl-tRNA synthetases in plants and yeast (e.g., [115,123], respectively), cytosolic translation elongation factor eEF1α in *T. brucei* [124] and glycolytic enzyme enolase in yeast [125]. It is also suggested that mitochondria-targeted proteins may be common elements participating in the redirection of different RNA molecules to mitochondria and their translocation across membranes (e.g., [105]). However, it is also suggested that RNA molecules may be translocated by Tom40 without protein assistance [63]. There is also the possible contribution of mitochondrial IMS proteins, which could function as intramitochondrial RNA import factors, as proposed for polynucleotide phosphorylase (PNPase) in human mitochondria (e.g., [105]).

4.2. Transport of Metabolites

It is well known that the universal pathway for metabolite transport across the outer mitochondrial membrane is formed by the VDAC, which may be formed by different VDAC paralogs (e.g., [126–130]). The molecular mass cut-off for the transported molecules is assumed to be about 4 kDa although the limit could be decreased when VDAC switches to lower conducting substates featuring less anion selectivity [131]. Nevertheless, VDAC is considered to be the major transport pathway for compounds as diverse as inorganic ions (e.g., K^+, Na^+ and Cl^-), metabolites of different size and charge (e.g., big anions as ATP, AMP and glutamate and small anions as superoxide anion as well as big cations as NADH and acetylocholine) and large macromolecules such as tRNA (e.g., [128,132,133]). However, for yeast *S. cerevisiae* mitochondria under the condition of the dominant VDAC paralog(yVDAC1) limited permeability or encoding gene deletion, metabolite transport across the mitochondrial outer membrane may be supported by the TOM complex [68,69,134]. This assumption was initially based on observation that in the absence of yVDAC1, NADH, ADP and CATR (carboxyatractylate) displayed limited access into the mitochondrial intermembrane space and the observed limitations depended on charge and size of these molecules (the highest for CATR being big anion of molecular weight higher than ADP and the lowest for NADH being big cation of molecular weight slightly smaller than CATR). Moreover, the limitations were weakened by the presence of Mg^{2+} that together implies involvement of cation selective channel of lower conductance that yVDAC1 [134]. This in turn correlates with the electrophysiological characteristic of the TOM complex channel (see Section 3.1 for details).

Later, it has been proven that blockage of the TOM complex by an imported protein decreases external reduced nicotinamide adenine dinucleoide (NADH) access to the inner membrane, which limits imported protein translocation by the TOM complex and increases competition in the absence of functional yVDAC1. Moreover, it has been observed that blocking the TOM complex with an imported protein decreased superoxide anion ($O_2^{\bullet -}$) release from mitochondria, particularly in the absence of functional yVDAC1 [135]. Notably, yeast mitochondria contain two VDAC paralogs (i.e., yVDAC1 and yVDAC2 [136,137]), both of which can form channels of comparable electrophysiological characteristics [130], but differ in their expression levels and (likely) substrate selectivity [138]. These postu-

lated differences coincide with a yVDAC2 contribution to the global permeability of the mitochondrial outer membrane that has remained undetected to date [4,139]. While yVDAC2 encoding gene deletion also results in competition between imported proteins and external NADH for access to the yeast mitochondria inner membrane, this competition is distinctly less pronounced than in the absence of functional yVDAC1 [68]. This observation contributes to solving the unresolved issue of yVDAC2 function.

One of the regulatory aspects concerning TOM complex involvement in metabolite transport is the expression level of its subunits. It has been reported that the expression level increases in the absence of yVDAC1 or yVDAC2, with the latter increase being less pronounced [68,73]. The upregulation of TOM complex subunits may result from increased transcription as well as the stability and/or translation of proper mRNAs [140]. Interestingly, this upregulation appears to be mediated by the cytosol reduction-oxidation (redox) state change in the absence of yVDAC1 or yVDAC2 and during yeast cell growth [73,74]. Moreover, redox state-dependent upregulation was also observed for Tob55/Sam50, which implicates TOB/SAM complex involvement in metabolite transport [73,74,139]; however, functional data to support this involvement remain missing.

4.3. Ayr1 and OMC7 and OMC8: Mitochondrial Outer Membrane Channels for Unknown Molecules

In the mitochondrial outer membrane, three channels of unknown function have been identified. These include a cation-selective channel formed by Ayr1 and two channels of anion selectivity formed by OMC7 and OMC8 [4]. *S. cerevisiae* Ayr1 (1-acyldihydroxyacetone-phosphate reductase) is a 33kD protein containing a conserved nucleotide-binding motif (TGX3GXG) that is localised in the ER [141,142]. It was suggested that this could be part of the contact sites between the ER and mitochondria [143]. This protein has also been suggested to participate in cell wall biogenesis and lipid metabolism [144]; however, its true function remains unexplained.

Ayr1 reconstituted in liposomes in planar lipid bilayer membrane revealed a main conductance of 1.47 nS in 1 M KCl (367 pS at 250 m M KCl after extrapolation) in the fully open state. Additionally, three partially open states with a lower conductance of ≅490 pS at 250 mM KCl and a reversal potential of 30 mV were observed. It has also been shown that the channel, as a monomer, displays cation selectivity (P_{K^+}/P_{Cl^-} = 4.5:1) that can be modulated by NADPH, which increases the reversal potential to 43 mV and cation selectivity ratio P_{K^+}/P_{Cl^-} to 10:1 [4]. The observed cation selectivity of the Ayr1 channel might suggests its contribution to protein import. The presented parameters of the Ayr1 could be consistent with a localization of Ayr1 in mitochondrial outer membrane and ER fractions, as being arranged in contact sites between ER and mitochondria.

In contrast, OMC7 and OMC8 were described as anion-selective channels of similar conductance (550 and 570 pS, respectively, at 250 mM KCl) (Table 1). In light of its anion selectivity, these channels could not be suggested as being engaged in the interaction with positively charged precursor protein; however, its contribution to nucleic acid and metabolite transport within and outside of the mitochondria are worthy of further study.

5. Conclusions and Perspectives

The mitochondrial outer membrane selectively communicates with the cytosol environment via protein channels for a wide variety of molecules that must be delivered into the mitochondria and/or released from the mitochondria. Moreover, these channels display high flexibility in their specificity, as illustrated by their ability to transport different types of molecules. Undoubtedly, these results highlight many implications for the channel modulation that might affect mitochondrial protein turnover as well as transport of different small molecules including crucial metabolites as ATP, ADP, substrates of the respiratory chain and superoxide anion, as well as drugs as granzymes. This in turn might be beneficial for treatment of mitochondria-linked diseases mediated by the outer membrane permeability impairment as cancer [75] as well as by incorrect intramitochondrial processes as neurodegenerative disorders including Parkinson and Alzheimer diseases.

Author Contributions: Conceptualization: M.W.; Writing: M.M., H.K. and M.W.; Preparing Figure and Table: M.M. Editing: M.W.; formatting: M.M. All authors have read and agreed to the published version of the manuscript.

Funding: This research was funded by the National Science Center (Poland) project (grant no. 2012/05/N/NZ3/00293 and the "KNOW RNA Research Center in Poznan" (grant no. 01/KNOW2/2014).

Institutional Review Board Statement: Not applicable.

Informed Consent Statement: Not applicable.

Acknowledgments: We would like to thank the Dean of the Faculty of Biology for the financial support.

Conflicts of Interest: The authors declare no conflict of interest.

References

1. Kutik, S.; Guiard, B.; Meyer, H.E.; Wiedemann, N.; Pfanner, N. Cooperation of translocase complexes in mitochondrial protein import. *J. Cell Bio.* **2007**, *179*, 585–591. [CrossRef] [PubMed]
2. Wiedemann, N.; Pfanner, N. Mitochondrial machineries for protein import and assembly. *Annu. Rev. Biochem.* **2017**, *86*, 685–714. [CrossRef] [PubMed]
3. Pfanner, N.; Warscheid, B.; Wiedemann, N. Mitochondrial proteins: From biogenesis to functional networks. *Nat. Rev. Mol. Cell Biol.* **2019**, *20*, 267–284. [CrossRef] [PubMed]
4. Kruger, V.; Becker, T.; Becker, L.; Montilla-Martinez, M.; Ellenrieder, L.; Vögtle, F.N.; Meyer, H.E.; Ryan, M.T.; Wiedemann, N.; Warscheid, B.; et al. Identification of new channels by systematic analysis of the mitochondrial outer membrane. *J. Cell Biol.* **2017**, *216*, 3485–3495. [CrossRef] [PubMed]
5. Checchetto, V.; Szabo, I. Novel channels of the outer membrane of mitochondria: Recent discoveries change our view. *Bioessays* **2018**, *40*, e1700232. [CrossRef]
6. Endo, T.; Yamano, K. Multiple pathways for mitochondrial protein trafc. *Biol. Chem.* **2009**, *390*, 723–730. [CrossRef] [PubMed]
7. Kreimendahl, S.; Rassow, J. The mitochondrial outer membrane protein Tom70-mediator in protein traffic, membrane contact sites and innate immunity. *Int. J. Mol. Sci.* **2020**, *21*, 7262. [CrossRef]
8. Paschen, S.A.; Waizenegger, T.; Stan, T.; Preuss, M.; Cyrklaff, M.; Hell, K.; Rapaport, D.; Neupert, W. Evolutionary conservation of biogenesis of β-barrel membrane proteins. *Nature* **2003**, *426*, 862–866. [CrossRef] [PubMed]
9. Habib, S.J.; Waizenegger, T.; Niewienda, A.; Paschen, S.A.; Neupert, W.; Rapaport, D. The N-terminal domain of Tob55 has a receptor-like function in the biogenesis of mitochondrial β-barrel proteins. *J. Cell Biol.* **2007**, *176*, 77–88. [CrossRef] [PubMed]
10. Zeth, K. Structure and evolution of mitochondrial outer membrane proteins of β-barrel topology. *Biochim. Biophys. Acta* **2010**, *1797*, 1292–1299. [CrossRef]
11. Misra, R. Assembly of the *β*-barrel outer membrane proteins in Gram-negative bacteria, mitochondria, and chloroplasts. *ISRN Mol. Biol.* **2012**, *2012*, 708203. [CrossRef]
12. Popov-Celeketic, J.; Waizenegger, T.; Rapaport, D. Mim1 functions in an oligomeric form to facilitate the integration of Tom20 into the mitochondrial outer membrane. *J. Mol. Biol.* **2008**, *376*, 671–680. [CrossRef]
13. Lueder, F.; Lithgow, T. The three domains of the mitochondrial outer membrane protein Mim1 have discrete functions in assembly of the TOM complex. *FEBS Lett.* **2009**, *583*, 1475–1480. [CrossRef]
14. Ellenrieder, L.; Opalinski, L.; Becker, L.; Kruger, V.; Mirus, O.; Straub, S.P.; Ebell, K.; Flinner, N.; Stiller, S.B.; Guiard, B.; et al. Separating mitochondrial protein assembly and endoplasmic reticulum tethering by selective coupling of Mdm10. *Nat. Commun.* **2016**, *7*, 13021. [CrossRef]
15. Chacinska, A.; Koehler, C.M.; Milenkovic, D.; Lithgow, T.; Pfanner, N. Importing mitochondrial proteins: Machineries and mechanisms. *Cell* **2009**, *138*, 628–644. [CrossRef]
16. Truscott, K.N.; Kovermann, P.; Geissler, A.; Merlin, A.; Meijer, M.; Driessen, A.J.; Rassow, J.; Pfanner, N.; Wagner, R. A presequence- and voltage-sensitive channel of the mitochondrial preprotein translocase formed by Tim23. *Nat. Struct. Biol.* **2001**, *8*, 1074–1082. [CrossRef]
17. Sirrenberg, C.; Bauer, M.F.; Guiard, B.; Neupert, W.; Brunner, M. Import of carrier proteins into the mitochondrial inner membrane mediated by Tim22. *Nature* **1996**, *384*, 582–585. [CrossRef] [PubMed]
18. Callegari, S.; Richter, F.; Chojnacka, K.; Jans, D.C.; Lorenzi, I.; Pacheu-Grau, D.; Jakobs, S.; Lenz, C.; Urlaub, H.; Dudek, J.; et al. TIM29 is a subunit of the human carrier translocase required for protein transport. *FEBS Lett.* **2016**, *590*, 4147–4158. [CrossRef]
19. Callegari, S.; Cruz-Zaragoza, L.D.; Rehling, P. From TOM to the TIM23 complex-handing over of a precursor. *Biol. Chem.* **2020**, *401*, 709–721. [CrossRef] [PubMed]
20. Chaudhuri, M.; Darden, C.; Gonzalez, F.S.; Singha, U.K.; Quinones, L.; Tripathi, A. Tim17 updates: A comprehensive review of an ancient mitochondrial protein translocator. *Biomolecules* **2020**, *10*, 1643. [CrossRef] [PubMed]
21. Neupert, W. A perspective on transport of proteins into mitochondria: A myriad of open questions. *J. Mol. Biol.* **2015**, *427*, 1135–1158. [CrossRef] [PubMed]

22. Doan, K.N.; Ellenrieder, L.; Becker, T. Mitochondrial porin links protein biogenesis to metabolism. *Curr. Genet.* **2019**, *65*, 899–903. [CrossRef]
23. Sirrenberg, C.; Endres, M.; Folsch, H.; Stuart, R.A.; Neupert, W.; Brunner, M. Carrier protein import into mitochondria mediated by the intermembrane proteins Tim10/Mrs11 and Tim12/Mrs5. *Nature* **1998**, *391*, 912–915. [CrossRef]
24. Adam, A.; Endres, M.; Sirrenberg, C.; Lottspeich, F.; Neupert, W.; Brunner, M. Tim9, a new component of the TIM22.54 translocase in mitochondria. *EMBO J.* **1999**, *18*, 313–319. [CrossRef]
25. Kozjak, V.; Wiedemann, N.; Milenkovic, D.; Lohaus, C.; Meyer, H.E.; Guiard, B.; Meisinger, C.; Pfanner, N. An Essential role of Sam50 in the protein sorting and assembly machinery of the mitochondrial outer membrane. *J. Biol. Chem.* **2003**, *278*, 49. [CrossRef]
26. Wiedemann, N.; Kozjak, V.; Chacinska, A.; Schonfisch, B.; Rospert, S.; Ryan, M.T.; Pfanner, N.; Meisinger, C. Machinery for protein sorting and assembly in the mitochondrial outer membrane. *Nature* **2003**, *424*, 565–571. [CrossRef]
27. Waizenegger, T.; Habib, S.J.; Lech, M.; Mokranjac, D.; Paschen, S.A.; Hell, K.; Neupert, W.; Rapaport, D. Tob38, a novel essential component in the biogenesis of betabarrel proteins of mitochondria. *EMBO Rep.* **2004**, *5*, 704709. [CrossRef]
28. Klein, A.; Israel, L.; Lackey, S.W.K.; Nargang, F.E.; Imhof, A.; Baumeister, W.; Neupert, W.; Thomas, D.R. Characterization of the insertase for β-barrel proteins of the outer mitochondrial membrane. *J. Cell Biol.* **2012**, *99*, 599–611. [CrossRef] [PubMed]
29. Diederichs, K.A.; Ni, X.; Rollauer, S.E.; Botos, I.; Tan, X.; King, M.S.; Kunji, E.R.S.; Jiang, J.; Buchanan, S.K. Structural insight into mitochondrial β-barrel outer membrane protein biogenesis. *Nat. Commun.* **2020**, *11*, 3290. [CrossRef]
30. Kozjak-Pavlovic, V.; Ross, K.; Benlasfer, N.; Kimmig, S.; Karlas, A.; Rudel, T. Conserved roles of Sam50 and metaxins in VDAC biogenesis. *EMBO Rep.* **2007**, *8*, 576–582. [CrossRef] [PubMed]
31. Xiea, J.; Marusichb, M.F.; Soudac, P.; Whiteleggec, J.; Capaldi, R.A. The mitochondrial inner membrane protein Mitofilin exists as a complex with SAM50, metaxins 1 and 2, coiled-coil-helix domain-containing protein 3 and 6 and DnaJC11. *FEBS Lett.* **2007**, *581*, 3545–3549. [CrossRef]
32. Cartron, P.F.; Petit, E.; Bellot, G.; Oliver, L.; Vallette, F.M. Metaxins 1 and 2, two proteins of the mitochondrial protein sorting and assembly machinery, are essential for Bak activation during TNF alpha triggered apoptosis. *Cell. Signal.* **2014**, *26*, 1928–1934. [CrossRef]
33. Buczek, D.; Wojtkowska, M.; Suzuki, Y.; Sonobe, S.; Nishigami, Y.; Antoniewicz, M.; Kmita, H.; Makałowski, W. Protein import complexes in the mitochondrial outer membrane of Amoebozoa representatives. *BMC Genom.* **2016**, *17*, 99. [CrossRef]
34. Wojtkowska, M.; Buczek, D.; Suzuki, Y.; Shabardina, V.; Makałowski, W.; Kmita, H. The emerging picture of the mitochondrial protein import complexes of Amoebozoa supergroup. *BMC Genom.* **2017**, *18*, 997. [CrossRef]
35. Mazur, M.; Wojtkowska, M.; Skalski, M.; Słocińska, M.; Kmita, H. The TOB/SAM complex composition in mitochondria of *Dictyostelium discoideum* during progression from unicellularity to multicellularity. *Acta Biochim. Pol.* **2019**, *66*, 551–557. [CrossRef]
36. Kornera, C.; Barrerac, M.; Dukanovice, J.; Eydt, K.; Harner, M.; Rabla, R.; Vogelf, F.; Rapaporte, D.; Neupert, W.; Reichert, A.S. The C-terminal domain of Fcj1 is required for formation of crista junctions and interacts with the TOB/SAM complex in mitochondria. *Mol. Biol. Cell* **2012**, *23*, 2143–2155. [CrossRef]
37. Kozjak-Pavlovic, V. The MICOS complex of human mitochondria. *Cell Tissue Res.* **2017**, *367*, 83–93. [CrossRef] [PubMed]
38. Horvath, S.E.; Rampelt, H.; Oeljeklaus, S.; Warscheid, B.; van der Laan, M.; Pfanner, N. Role of membrane contact sites in protein import into mitochondria. *Protein Sci.* **2015**, *24*, 277–297. [CrossRef] [PubMed]
39. Dekker, P.J.; Martin, F.; Maarse, A.C.; Bömer, U.; Muller, H.; Guiard, B.; Meijer, M.; Rassow, J.; Pfanner, N. The Tim core complex defines the number of mitochondrial translocation contact sites and can hold arrested preproteins in the absence of matrix Hsp70-Tim44. *EMBO J.* **1997**, *16*, 5408–5419. [CrossRef] [PubMed]
40. Hill, K.; Model, K.; Ryan, M.T.; Dietmeier, K.; Martin, F.; Wagner, R.; Pfanner, N. Tom40 forms the hydrophilic channel of the mitochondrial import pore for preproteins. *Nature* **1998**, *395*, 516–521. [CrossRef] [PubMed]
41. Suzuki, H.; Okazawa, Y.; Komiya, T.; Saeki, K.; Mekada, E.; Kitada, S.; Ito, A.; Mihara, K. Characterization of rat TOM40, a central component of the preprotein translocase of the mitochondrial outer membrane. *J. Biol. Chem.* **2000**, *275*, 37930–37936. [CrossRef] [PubMed]
42. Meisinger, C.; Ryan, M.T.; Hill, K.; Model, K.; Lim, J.H.; Sickmann, A.; Müller, H.; Meyer, H.E.; Wagner, R.; Pfanner, N. Protein import channel of the outer mitochondrial membrane: A highly stable Tom40-Tom22 core structure differentially interacts with preproteins, small tom proteins, and import receptors. *Mol. Cell. Biol.* **2001**, *21*, 2337–2348. [CrossRef] [PubMed]
43. Kreimendahl, S.; Schwichtenberg, J.; Günnewig, K.; Brandherm, L.; Rassow, J. The selectivity filter of the mitochondrial protein import machinery. *BMC Biol.* **2020**, *18*, 156. [CrossRef] [PubMed]
44. Harner, M.; Neupert, W.; Deponteb, M. Lateral release of proteins from the TOM complex into the outer membrane of mitochondria. *EMBO J.* **2011**, *30*, 3232–3241. [CrossRef]
45. Wojtkowska, M.; Jakalski, M.; Pienkowska, J.R.; Stobienia, O.; Karachitos, A.; Przytycka, T.M.; Weiner, J., 3rd; Kmita, H.; Makalowski, W. Phylogenetic analysis of mitochondrial outer membrane β-barrel channels. *Genome Biol. Evol.* **2012**, *4*, 110–125. [CrossRef]
46. Morgenstern, M.; Stiller, S.B.; Lubbert, P.; Peikert, C.D.; Dannenmaier, S.; Drepper, F.; Weill, U.; Hoß, P.; Feuerstein, R.; Gebert, M.; et al. Definition of a high- confidence mitochondrial proteome at quantitative scale. *Cell Rep.* **2017**, *19*, 2836–2852. [CrossRef]
47. Ahting, U.; Thun, C.; Hegerl, R.; Typke, D.; Nargang, F.E.; Neupert, W.; Nussberger, S. The TOM core complex: The general protein import pore of the outer membrane of mitochondria. *J. Cell Biol.* **1999**, *147*, 959–968. [CrossRef]

48. Shiota, T.; Imai, K.; Qiu, J.; Hewitt, V.L.; Tan, K.; Shen, H.H.; Sakiyama, N.; Fukasawa, Y.; Hayat, S.; Kamiya, M.; et al. Molecular architecture of the active mitochondrial protein gate. *Science* **2015**, *349*, 1544–1548. [CrossRef]
49. Model, K.; Meisinger, C.; Prinz, T.; Wiedemann, N.; Truscott, K.N.; Pfanner, N.; Ryan, M.T. Multistep assembly of the protein import channel of the mitochondrial outer membrane. *Nat. Struct. Biol.* **2001**, *8*, 361–370. [CrossRef]
50. Gold, V.A.; Brandt, T.; Cavellini, L.; Cohen, M.M.; Ieva, R.; van der Laan, M. Analysis of mitochondrial membrane protein complexes by electron cryo-tomography. *Methods Mol. Biol.* **2017**, *1567*, 315–336. [PubMed]
51. Bausewein, T.; Naveed, H.; Liang, J.; Nussberger, S. The structure of the TOM core complex in the mitochondrial outer membrane. *Biol. Chem.* **2020**, *401*, 687–697. [CrossRef]
52. Araiso, Y.; Tsutsumi, A.; Qiu, J.; Imai, K.; Shiota, T.; Song, J.; Lindau, C.; Wenz, L.S.; Sakaue, H.; Yunoki, K.; et al. Structure of the mitochondrial import gate reveals distinct preprotein paths. *Nature* **2019**, *575*, 395–401. [CrossRef]
53. Wang, W.; Chen, X.; Zhang, L.; Yi, J.; Ma, Q.; Yin, J.; Zhuo, W.; Gu, J.; Yang, M. Atomic structure of human TOM core complex. *Cell Discov.* **2020**, *6*, 1–10. [CrossRef] [PubMed]
54. Tucker, K.; Park, E. Cryo-EM structure of the mitochondrial protein-import channel TOM complex at near-atomic resolution. *Nat. Struct. Mol. Biol.* **2019**, *26*, 1158–1166. [CrossRef] [PubMed]
55. Becker, T.; Horvath, S.E.; Bottinger, L.; Gebert, N.; Daum, G.; Pfanner, N. Role of phosphatidylethanolamine in the biogenesis of mitochondrial outer membrane proteins. *J. Biol. Chem.* **2013**, *288*, 16451–16459. [CrossRef] [PubMed]
56. Bausewein, T.; Mills, D.J.; Langer, J.D.; Nitschke, B.; Nussberger, S.; Kuhlbrandt, W. Cryo-EM structure of the TOM core complex from *Neurospora crassa*. *Cell* **2017**, *170*, 693–700. [CrossRef]
57. Kuszak, A.J.; Jacobs, D.; Gurnev, P.A.; Shiota, T.; Louis, J.M.; Lithgow, T.; Bezrukov, S.M.; Rostovtseva, T.K.; Buchanan, S.K. Evidence of distinct channel conformations and substrate binding affinities for the mitochondrial outer membrane protein translocase pore Tom40. *J. Biol. Chem.* **2015**, *290*, 26204–26217. [CrossRef]
58. Becker, L.; Bannwarth, M.; Meisinger, C.; Hill, K.; Model, K.; Krimmer, T.; Casadio, R.; Truscott, K.N.; Schulz, G.E.; Pfanner, N.; et al. Preprotein translocase of the outer mitochondrial membrane: Reconstituted Tom40 forms a characteristic TOM pore. *J. Mol. Biol.* **2005**, *353*, 1011–1020. [CrossRef]
59. Wojtkowska, M.; Buczek, D.; Stobienia, O.; Karachitos, A.; Antoniewicz, M.; Slocinska, M.; Makalowski, W.; Kmita, H. The TOM complex of amoebozoans: The cases of the amoeba *Acanthamoeba castellanii* and the slime mold *Dictyostelium discoideum*. *Protist* **2015**, *166*, 349–362. [CrossRef]
60. Poynor, M.; Eckert, R.; Nussberger, S. Dynamics of the preprotein translocation channel of the outer membrane of mitochondria. *Biophys. J.* **2008**, *95*, 1511–1522. [CrossRef] [PubMed]
61. Stan, T.; Ahting, U.; Dembowski, M.; Kunkele, K.P.; Nussberger, S.; Neupert, W.; Rapaport, D. Recognition of preproteins by the isolated TOM complex of mitochondria. *EMBO J.* **2000**, *19*, 4895–4902. [CrossRef]
62. Abe, Y.; Shodai, T.; Muto, T.; Mihara, K.; Torii, H.; Nishikawa, S.; Endo, T.; Kohda, D. Structural basis of presequence recognition by the mitochondrial protein import receptor Tom20. *Cell* **2000**, *100*, 551–560. [CrossRef]
63. Niemann, M.; Harsman, A.; Mani, J.; Peikert, C.D.; Oeljeklaus, S.; Warscheid, B.; Wagner, R.; Schneider, A. tRNAs and proteins use the same import channel for translocation across the mitochondrial outer membrane of trypanosomes. *Proc. Natl. Acad. Sci. USA* **2017**, *114*, E7679–E7687. [CrossRef]
64. Pickrell, A.M.; Youle, R.J. The roles of PINK1, parkin, and mitochondrial fidelity in Parkinson's disease. *Neuron* **2015**, *85*, 257–273. [CrossRef]
65. Hansson Petersen, C.A.; Alikhani, N.; Behbahani, H.; Wiehager, B.; Pavlov, P.F.; Alafuzoff, I.; Leinonen, V.; Ito, A.; Winblad, B.; Glaser, E.; et al. The amyloid beta-peptide is imported into mitochondria via the TOM import machinery and localized to mitochondrial cristae. *Proc. Natl. Acad. Sci. USA* **2008**, *105*, 13145–13150. [CrossRef]
66. Salinas, T.; Duchene, A.M.; Delage, L.; Nilsson, S.; Glaser, E.; Zaepfel, M.; Marechal-Drouard, L. The voltage-dependent anion channel, a major component of the tRNA import machinery in plant mitochondria. *Proc. Natl. Acad. Sci. USA* **2006**, *103*, 18362–18367. [CrossRef]
67. Salinas, T.; El Farouk-Ameqrane, S.; Ubrig, E.; Sauter, C.; Duchene, A.M.; Marechal-Drouard, L. Molecular basis for the differential interaction of plant mitochondrial VDAC proteins with tRNAs. *Nucleic Acids Res.* **2014**, *42*, 9937–9948. [CrossRef]
68. Antos, N.; Budzinska, M.; Kmita, H. An interplay between the TOM complex and porin isoforms in the yeast *Saccharomyces cerevisiae* mitochondria. *FEBS Lett.* **2001**, *500*, 12–16. [CrossRef]
69. Kmita, H.; Budzińska, M. Involvement of the TOM complex in external NADH transport into yeast mitochondria depleted of mitochondrial porin1. *Biochim. Biophys. Acta* **2000**, *1509*, 86–94. [CrossRef]
70. Di Maio, R.; Barrett, P.J.; Hoffman, E.K.; Barrett, C.W.; Zharikov, A.; Borah, A.; Hu, X.; McCoy, J.; Chu, C.T.; Burton, E.A.; et al. α-Synuclein binds to TOM20 and inhibits mitochondrial protein import in Parkinson's disease. *Sci. Transl. Med.* **2016**, *8*, 342ra78. [CrossRef] [PubMed]
71. Kutik, S.; Stojanovski, D.; Becker, L.; Becker, T.; Meinecke, M.; Kruger, V.; Prinz, C.; Meisinger, C.; Guiard, B.; Wagner, R.; et al. Dissecting membrane insertion of mitochondrial β-barrel proteins. *Cell* **2008**, *132*, 1011–1024. [CrossRef]
72. Chiusolo, V.; Jacquemin, G.; Bassoy, E.Y.; Vinet, L.; Liguori, L.; Walch, M.; Kozjak-Pavlovic, V.; Martinvalet, D. Granzyme B enters the mitochondria in a Sam50-, Tim22- and mtHsp70-dependent manner to induce apoptosis. *Cell Death Differ.* **2017**, *24*, 747–758. [CrossRef]

73. Galganska, H.; Budzinska, M.; Wojtkowska, M.; Kmita, H. Redox regulation of protein expression in *Saccharomyces cerevisiae* mitochondria: Possible role of VDAC. *Arch. Biochem. Biophys.* **2008**, *479*, 39–45. [CrossRef]
74. Galganska, H.; Karachitos, A.; Wojtkowska, M.; Stobienia, O.; Budzinska, M.; Kmita, H. Communication between mitochondria and nucleus: Putative role for VDAC in reduction/oxidation mechanism. *Biochim. Biophys. Acta* **2010**, *1797*, 1276–1280. [CrossRef] [PubMed]
75. Dejean, L.M.; Ryu, S.Y.; Martinez-Caballero, S.; Teijido, O.; Peixoto, P.M.; Kinnally, K.W. MAC and Bcl-2 family proteins conspire in a deadly plot. *Biochim. Biophys. Acta* **2010**, *1797*, 1231–1238. [CrossRef] [PubMed]
76. Pavlov, E.V.; Priault, M.; Pietkiewicz, D.; Cheng, E.H.Y.; Antonsson, B.; Manon, S.; Korsmeyer, S.J.; Mannella, C.A.; Kinnally, K.W. A novel, high conductance channel of mitochondria linked to apoptosis in mammalian cells and Bax expression in yeast. *J. Cell Biol.* **2001**, *155*, 725–732. [CrossRef]
77. Walther, D.M.; Rapaport, D. Biogenesis of mitochondrial outer membrane proteins. *Biochim. Biophys. Acta* **2009**, *1793*, 42–51. [CrossRef]
78. Sutton, V.R.; Davis, J.E.; Cancilla, M.; Johnstone, R.W.; Ruefli, A.A.; Sedelies, K.; Browne, K.A.; Trapani, J.A. Initiation of apoptosis by granzyme B requires direct cleavage of bid, but not direct granzyme B-mediated caspase activation. *J. Exp. Med.* **2000**, *192*, 1403–1414. [CrossRef] [PubMed]
79. Goping, I.S.; Barry, M.; Liston, P.; Sawchuk, T.; Constantinescu, G.; Michalak, K.M.; Shostak, I.; Roberts, D.L.; Hunter, A.M.; Korneluk, R.; et al. Granzyme B-induced apoptosis requires both direct caspase activation and relief of caspase inhibition. *Immunity* **2003**, *18*, 355–365. [CrossRef]
80. Qiu, J.; Wenz, L.S.; Zerbes, R.M.; Oeljeklaus, S.; Bohnert, M.; Stroud, D.A.; Wirth, C.; Ellenrieder, L.; Thornton, N.; Kutik, S.; et al. Coupling of mitochondrial import and export translocases by receptor-mediated supercomplex formation. *Cell* **2013**, *154*, 596–608. [CrossRef]
81. Wenz, L.S.; Ellenrieder, L.; Qiu, J.; Bohnert, M.; Zufall, N.; van der Laan, M.; Pfanner, N.; Wiedemann, N.; Becker, T. Sam37 is crucial for formation of the mitochondrial TOM–SAM supercomplex, thereby promoting β-barrel biogenesis. *J. Cell Biol.* **2015**, *210*, 1047–1054. [CrossRef] [PubMed]
82. Rampelt, H.; Bohnert, M.; Zerbes, R.M.; Horvath, S.E.; Warscheid, B.; Pfanner, N.; van der Laan, M. Mic10, a core subunit of the mitochondrial contact site and cristae organizing system, interacts with the dimeric F_1F_0-ATP synthase. *J. Mol. Biol.* **2017**, *429*, 1162–1170. [CrossRef] [PubMed]
83. Yamano, K.; Tanaka-Yamano, S.; Endo, T. Mdm10 as a dynamic constituent of the TOB/SAM complex directs coordinated assembly of Tom40. *EMBO Rep.* **2010**, *11*, 187–193. [CrossRef]
84. Becker, T.; Guiard, B.; Thornton, N.; Zufall, N.; Stroud, D.A.; Wiedemann, N.; Pfanner, N. Assembly of the mitochondrial protein import channel: Role of Tom5 in two-stage interaction of Tom40 with the SAM complex. *Mol. Biol. Cell.* **2010**, *21*, 3106–3113. [CrossRef]
85. Ott, C.; Ross, K.; Straub, S.; Thiede, B.; Gotz, M.; Goosmann, C.; Krischke, M.; Mueller, M.J.; Krohne, G.; Rudel, T.; et al. Sam50 functions in mitochondrial intermembrane space bridging and biogenesis of respiratory complexes. *Mol. Cell. Biol.* **2012**, *32*, 1173–1188. [CrossRef] [PubMed]
86. Ott, C.; Dorsch, E.; Fraunholz, M.; Straub, S.; Kozjak-Pavlovic, V. Detailed analysis of the human mitochondrial contact site complex indicate a hierarchy of subunits. *PLoS ONE* **2015**, *10*, e0120213. [CrossRef]
87. Ding, C.; Wu, Z.; Huang, L.; Wang, Y.; Xue, J.; Chen, S.; Deng, Z.; Wang, L.; Song, Z.; Chen, S. Mitofilin and CHCHD6 physically interact with Sam50 to sustain cristae structure. *Sci. Rep. Nov.* **2015**, *5*, 1–11. [CrossRef]
88. Huynen, M.A.; Mühlmeister, M.; Gotthardt, K.; Guerrero-Castillo, S.; Brandt, U. Evolution and structural organization of the mitochondrial contact site (MICOS) complex and the mitochondrial intermembrane space bridging (MIB) complex. *Biochim. Biophys. Acta* **2016**, *1863*, 91–101. [CrossRef]
89. Tang, J.; Zhang, K.; Dong, J.; Yan, C.; Hu, C.; Ji, H.; Chen, L.; Chen, S.; Zhao, H.; Song, Z. Sam50-Mic19-Mic60 axis determines mitochondrial cristae architecture by mediating mitochondrial outer and inner membrane contact. *Cell Death Differ.* **2020**, *27*, 146–160. [CrossRef] [PubMed]
90. Meisinger, C.; Rissler, M.; Chacinska, A.; Sanjua Szklarz, L.K.; Milenkovic, D.; Kozjak, V.; Schonfisch, B.; Lohaus, C.; Meyer, H.E.; Yaffe, M.P.; et al. The Mitochondrial Morphology Protein Mdm10 Functions in Assembly of the Preprotein Translocase of the Outer Membrane. *Dev. Cell* **2004**, *7*, 61–71. [CrossRef] [PubMed]
91. Thornton, N.; Stroud, D.A.; Milenkovic, D.; Guiard, B.; Pfanner, N.; Becker, T. Two modular forms of the mitochondrial sorting and assembly machinery are involved in biogenesis of a-helical outer membrane proteins. *J. Mol. Biol.* **2010**, *396*, 540–549. [CrossRef] [PubMed]
92. Takeda, H.; Tsutsumi, A.; Nishizawa, T.; Lindau, C.; Busto, J.V.; Wenz, L.S.; Ellenrieder, L.; Imai, K.; Straub, S.P.; Mossmann, W.; et al. Mitochondrial sorting and assembly machinery operates by β-barrel switching. *Nature* **2021**, *590*, 163–169. [CrossRef] [PubMed]
93. Blachly-Dyson, E.; Forte, M. VDAC channels. *IUBMB Life* **2001**, *52*, 113–118. [PubMed]
94. Hohr, A.I.C.; Lindau, C.; Wirth, C.; Qiu, J.; Stroud, D.A.; Kutik, S.; Guiard, B.; Hunte, C.; Becker, T.; Pfanner, N.; et al. Membrane protein insertion through a mitochondrial beta-barrel gate. *Science* **2018**, *359*, eaah6834. [CrossRef] [PubMed]
95. Lionello, S.; Marzaro, G.; Martinvalet, D. SAM50, a side door to the mitochondria: The case of cytotoxic proteases. *Pharmacol. Res.* **2020**, *160*, 105196. [CrossRef]

96. Boldogh, I.R.; Nowakowski, D.W.; Yang, H.C.; Chung, H.; Karmon, S.; Royes, P.; Pon, L.A. A Protein Complex Containing Mdm10p, Mdm12p, and Mmm1p Links Mitochondrial Membranes and DNA to the Cytoskeleton-based Segregation Machinery. *Mol. Biol. Cell* **2003**, *14*, 4618–4627. [CrossRef]
97. Kornmann, K.; Currie, E.; Collins, S.R.; Schuldiner, M.; Nunnari, J.; Weissman, J.S.; Walter, P. An ER-mitochondria tethering complex revealed by a synthetic biology screen. *Science* **2009**, *325*, 477–481. [CrossRef]
98. Flinner, N.; Ellenrieder, L.; Stiller, S.B.; Becker, T.; Schleiff, E.; Mirus, O. Mdm10 is an ancient eukaryotic porin co-occurring with theERMES complex. *Biochim. Biophys. Acta* **2013**, *1833*, 3314–3325. [CrossRef]
99. Meisinger, C.; Wiedemann, N.; Rissler, M.; Strub, A.; Milenkovic, D.; Schonfisch, B.; Muller, H.; Kozjak, V.; Pfanner, N. Mitochondrial Protein Sorting. Differentiation of β-barrel assembly by Tom7-mediated segregation of Mdm10. *J. Biol. Chem.* **2006**, *281*, 22819–22826. [CrossRef]
100. Becker, T.; Pfannschmidt, S.; Guiard, B.; Stojanovski, D.; Milenkovic, D.; Kutik, S.; Pfanner, N.; Meisinger, C.; Wiedemann, N. Biogenesis of the mitochondrial TOM complex. Mim1 promotes insertion and assembly of signal-anchored receptors. *J. Biol. Chem.* **2008**, *283*, 120–127. [CrossRef]
101. Becker, T.; Wenz, L.S.; Kruger, V.; Lehmann, W.; Müller, J.M.; Goroncy, L.; Zufall, N.; Lithgow, T.; Guiard, B.; Chacinska, A.; et al. The mitochondrial import protein Mim1 promotes biogenesis of multispanning outer membrane proteins. *J. Cell Biol.* **2011**, *194*, 387–395. [CrossRef]
102. Papic, D.; Krumpe, K.; Dukanovic, J.; Dimmer, K.S.; Rapaport, D. Multispan mitochondrial outer membrane protein Ugo1 follows a unique Mim1-dependent import pathway. *J. Cell Biol.* **2011**, *194*, 397–405. [CrossRef]
103. Martensson, C.U.; Priesnitz, C.; Song, J.; Ellenrieder, L.; Doan, K.N.; Boos, F.; Floerchinger, A.; Zufall, N.; Oeljeklaus, S.; Warscheid, B.; et al. Mitochondrial protein translocation associated degradation. *Nature* **2019**, *569*, 679–683. [CrossRef] [PubMed]
104. Peixoto, P.M.; Lue, J.K.; Ryu, S.Y.; Wroble, B.N.; Sible, J.C.; Kinnally, K.W. Mitochondrial apoptosis-induced channel (MAC) function triggers a Bax/Bak-dependent bystander effect. *Am. J. Pathol.* **2011**, *178*, 48–54. [CrossRef] [PubMed]
105. Jeandard, D.; Smirnova, A.; Tarassov, I.; Barrey, E.; Smirnov, A.; Entelis, N. Import of non-coding RNAs into human mitochondria: A critical review and emerging approaches. *Cells* **2019**, *8*, 286. [CrossRef] [PubMed]
106. Dietrich, A.; Wallet, C.; Iqbal, R.K.; Gualberto, J.M.; Lotfi, F. Organellar non-coding RNAs: Emerging regulation mechanisms. *Biochimie* **2015**, *117*, 48–62. [CrossRef]
107. Verechshagina, N.; Nikitchina, N.; Yamada, Y.; Harashima, H.; Tanaka, M.; Orishchenko, K.; Mazunin, I. Future of human mitochondrial DNA editing technologies. *Mitochondrial DNA Part A DNA Mapp. Seq. Anal.* **2019**, *30*, 214–221. [CrossRef]
108. Kim, K.M.; Noh, J.H.; Abdelmohsen, K.; Gorospe, M. Mitochondrial noncoding RNA transport. *BMB Rep.* **2017**, *50*, 164–174. [CrossRef] [PubMed]
109. Campo, S.; Gilbert, K.B.; Carrington, J.C. Small RNA-based antiviral defense in the phytopathogenic fungus colletotrichum higginsianum. *PLoS Pathog.* **2016**, *12*, e1005640. [CrossRef]
110. Kamenski, P.; Krasheninnikov, I.; Tarassov, I. 40 Years of Studying RNA Import into Mitochondria: From Basic Mechanisms to Gene Therapy Strategies. *Mol. Biol. (Mosk.)* **2019**, *53*, 924–932. [CrossRef]
111. Ramamonjisoa, D.; Kauffmann, S.; Choisne, N.; Marechal-Drouard, L.; Green, G.; Wintz, H.; Small, I.; Dietrich, A. Structure and expression of several bean (Phaseolus vulgaris) nuclear transfer RNA genes: Relevance to the process of tRNA import into plant mitochondria. *Plant Mol. Biol.* **1998**, *36*, 613–625. [CrossRef]
112. Rusconi, C.P.; Cech, T.R. The anticodon is the signal sequence for mitochondrial import of glutamine tRNA in Tetrahymena. *Genes Dev.* **1996**, *10*, 28702880. [CrossRef]
113. Hancock, K.; Hajduk, S.L. The mitochondrial tRNAs of *Trypanosoma brucei* are nuclear encoded. *J. Biol. Chem.* **1990**, *265*, 19208–19215. [CrossRef]
114. Shi, X.; Chen, D.H.; Suyama, Y. A nuclear tRNA gene cluster in the protozoan Leishmania tarentolae and differential distribution of nuclear encoded tRNAs between the cytosol and mitochondria. *Mol. Biochem. Parasitol.* **1994**, *65*, 2337. [CrossRef]
115. Kamenski, P.; Smirnova, E.; Kolesnikova, O.; Krasheninnikov, I.A.; Martin, R.P.; Entelis, N.; Tarassov, I. tRNA mitochondrial import in yeast: Mapping of the import determinants in the carrier protein, the precursor of mitochondrial lysyl-tRNA synthetase. *Mitochondrion* **2010**, *10*, 284–293. [CrossRef]
116. Tarassov, I.; Entelis, N.; Martin, R.P. An intact protein translocating machinery is required f or mitochondrial import of a yeast cytoplasmic tRNA. *J. Mol. Biol.* **1995**, *245*, 315–323. [CrossRef]
117. Vyssokikh, M.Y.; Schirtz, T.; Kolesnikova, O.; Entelis, N.; Antonenko, Y.N.; Rokitskaya, T.I.; Tarassov, I. Isoform porin 2 is involved in tRNA(Lys) transport from cytosol to mitochondria in yeast. *BBA Bioenerg.* **2012**, *1817*, 124–125. [CrossRef]
118. Harsman, A.; Schneider, A. Mitochondrial protein import in trypanosomes: Expect the unexpected. *Traffic* **2017**, *18*, 96–109. [CrossRef] [PubMed]
119. Shikha, S.; Huot, J.L.; Schneider, A.; Niemann, M. tRNA import across the mitochondrial inner membrane in *T. brucei* requires TIM subunits but is independent of protein import. *Nucleic Acids Res.* **2020**, *48*, 12269–12281. [CrossRef] [PubMed]
120. Cosma, M.P.; Panizza, S.; Nasmyth, K. Cdk1 Triggers association of RNA polymerase to cell cycle promoters only after recruitment of the mediator by SBF. *Mol. Cell* **2016**, *7*, 1213–1220. [CrossRef]
121. Singha, U.K.; Hamilton, V.; Chaudhuri, M. Tim62, a novel mitochondrial protein in *Trypanosoma brucei*, is essential for assembly and stability of the TbTim17 protein complex. *J. Biol. Chem.* **2015**, *290*, 23226–23239. [CrossRef] [PubMed]

122. Singha, U.K.; Tripathi, A.; Smith, J.T., Jr.; Quinones, L.; Saha, A.; Singha, T.; Chaudhuri, M. Novel IM-associated protein Tim54 plays a role in the mitochondrial import of internal signal-containing proteins in *Trypanosoma brucei*. *Biol. Cell* **2021**, *113*, 39–57. [CrossRef] [PubMed]
123. Salinas-Giege, T.; Giege, R.; Giege, P. tRNA biology in mitochondria. *Int. J. Mol. Sci.* **2015**, *16*, 4518–4559. [CrossRef] [PubMed]
124. Bouzaidi-Tiali, N.; Aeby, E.; Charriere, F.; Pusnik, M.; Schneider, A. Elongation factor 1a mediates the specificity of mitochondrial tRNA import in *T. brucei*. *EMBO J.* **2007**, *26*, 4302–4312. [CrossRef]
125. Entelis, N.; Brandina, I.; Kamenski, P.; Krasheninnikov, I.A.; Martin, R.P.; Tarassov, I. A glycolytic enzyme, enolase, is recruited as a cofactor of tRNA targeting toward mitochondria in *Saccharomyces cerevisiae*. *Genes Dev.* **2006**, *20*, 1609–1620. [CrossRef]
126. Benz, R. Permeation of hydrophilic solutes through mitochondrial outer membranes: Review on mitochondrial porins. *Biochim. Biophys. Acta* **1994**, *1197*, 167–196. [CrossRef]
127. Colombini, M. VDAC: The channel at the interface between mitochondria and the cytosol. *Mol. Cell. Biochem.* **2004**, *256-257*, 107–115. [CrossRef]
128. Shoshan-Barmatz, V.; De Pinto, V.; Zweckstetter, M.; Raviv, Z.; Keinan, N.; Arbel, N. VDAC, a multi-functional mitochondrial protein regulating cell life and death. *Mol. Aspects Med.* **2010**, *31*, 227–285. [CrossRef]
129. Mannella, C.A. VDAC-A primal perspective. *Int. J. Mol. Sci.* **2021**, *22*, 1685. [CrossRef]
130. De Pinto, V. Renaissance of VDAC: New insights on a protein family at the interface between mitochondria and cytosol biomolecules. *Biomolecules* **2021**, *11*, 107. [CrossRef]
131. Colombini, M. VDAC structure, selectivity, and dynamics. *Biochim. Biophys. Acta* **2012**, *1818*, 1457–1465. [CrossRef] [PubMed]
132. Han, D.; Antunes, F.; Canali, R.; Rettori, D.; Cadenas, E. Voltage-dependent anion channels control the release of the superoxide anion from mitochondria to cytosol. *J. Biol. Chem.* **2003**, *278*, 5557–5563. [CrossRef] [PubMed]
133. Homble, F.; Krammer, E.-M.; Prevost, M. Plant VDAC: Facts and speculations. *Biochim. Biophys. Acta Biomembr.* **2012**, *1818*, 1486–1501. [CrossRef] [PubMed]
134. Kmita, H.; Stobienia, O.; Michejda, J. The access of metabolites into yeast mitochondria in the presence and absence of the voltage dependent anion selective channel (YVDAC1). *Acta Biochim. Pol.* **1999**, *46*, 991–1000. [CrossRef]
135. Budzinska, M.; Gałgańska, H.; Karachitos, A.; Wojtkowska, M.; Kmita, H. The TOM complex is involved in the release of superoxide anion from mitochondria. *J. Bioenerg. Biomembr.* **2009**, *41*, 361–367. [CrossRef] [PubMed]
136. Blachly-Dyson, E.; Song, J.; Wolfgang, W.J.; Colombini, M.; Forte, M. Multicopy suppressors of phenotypes resulting from the absence of yeast VDAC encode a VDAC-like protein. *Mol. Cell. Biol.* **1997**, *17*, 5727–5738. [CrossRef]
137. Lee, A.C.; Xu, X.; Blachly-Dyson, E.; Forte, M.; Colombini, M. The role of yeast VDAC genes on the permeability of the mitochondrial outer membrane. *J. Membr. Biol.* **1998**, *161*, 173–181. [CrossRef]
138. Guardiani, C.; Magri, A.; Karachitos, A.; Di Rosa, M.C.; Reina, S.; Bodrenko, I.; Messina, A.; Kmita, H.; Ceccarelli, M.; De Pinto, V. yVDAC2, the second mitochondrial porin isoform of *Saccharomyces cerevisiae*. *Biochim. Biophys. Acta Bioenerg.* **2018**, *1859*, 270–279. [CrossRef]
139. Magri, A.; Di Rosa, M.C.; Orlandi, I.; Guarino, F.; Reina, S.; Guarnaccia, M.; Morello, G.; Spampinato, A.; Cavallaro, S.; Messina, A.; et al. Deletion of Voltage-Dependent Anion Channel 1 knocks mitochondria down triggering metabolic rewiring in yeast. *Cell. Mol. Life Sci.* **2020**, *77*, 3195–3213. [CrossRef]
140. Kmita, H.; Antos, N.; Wojtkowska, M.; Hryniewiecka, L. Processes underlying the upregulation of Tom proteins in *S. cerevisiae* mitochondria depleted of the VDAC channel. *J. Bioenerg. Biomembr.* **2004**, *36*, 187–193. [CrossRef]
141. Athenstaedt, K.; Daum, G. 1-Acyldihydroxyacetone-phosphate reductase (Ayr1p) of the yeast *Saccharomyces cerevisiae* encoded by the open reading frame YIL124w is a major component of lipid particles. *J. Biol. Chem.* **2000**, *275*, 235–240. [CrossRef] [PubMed]
142. Natter, K.; Leitner, P.; Faschinger, A.; Wolinski, H.; McCraith, S.; Fields, S.; Kohlwein, S.D. The spatial organization of lipid synthesis in the yeast *Saccharomyces cerevisiae* derived from large scale green fluorescent protein tagging and high resolution microscopy. *Mol. Cell. Proteom.* **2005**, *4*, 662–672. [CrossRef] [PubMed]
143. Herrera-Cruz, M.S.; Simmen, T. Over six decades of discovery and characterization of the architecture at mitochondria-associated membranes (MAMs). *Adv. Exp. Med. Biol.* **2017**, *997*, 13–31. [PubMed]
144. Ploier, B.; Scharwey, M.; Koch, B.; Schmidt, C.; Schatte, J.; Rechberger, G.; Kollroser, M.; Hermetter, A.; Daum, G. Screening for hydrolytic enzymes reveals Ayr1p as a novel triacylglycerol lipase in *Saccharomyces cerevisiae*. *J. Biol. Chem.* **2013**, *288*, 36061–36072. [CrossRef]